

VARIABILITY OF INDICATORS USED IN MOTOR FAULT DETECTION
BASED ON ELECTRICAL MEASUREMENTS

A Thesis

by

SHANTUR S. TAPAR

Submitted to the Office of Graduate Studies of
Texas A&M University
in partial fulfillment of the requirements for the degree of

MASTER OF SCIENCE

August 2005

Major Subject: Mechanical Engineering

VARIABILITY OF INDICATORS USED IN MOTOR FAULT DETECTION
BASED ON ELECTRICAL MEASUREMENTS

A Thesis

by

SHANTUR S. TAPAR

Submitted to the Office of Graduate Studies of
Texas A&M University
in partial fulfillment of the requirements for the degree of

MASTER OF SCIENCE

Approved by:

Chair of Committee, Alexander G. Parlos
Committee Members, Gholamreza Langari
Andrew Chan

Head of Department, Dennis L. O'Neal

August 2005

Major Subject: Mechanical Engineering

ABSTRACT

Variability of Indicators Used in Motor Fault Detection Based on Electrical Measurements. (August 2005)

Shantur S. Tapar, B.E., Amravati University, Amravati, India

Chair of Advisory Committee: Dr. Alexander G. Parlos

Online condition assessment, product quality assurance and improved operational efficiency of engineering systems, such as induction motors, has increased in significance due to the advantages it offers in terms of productivity. Early detection of faults would not only allow for extensive trending but also provide advanced warnings regarding the health of the machinery. The implementation of on-line fault detection systems must not only exhibit high level of detection accuracy, but also discriminate between actual incipient faults and false alarms caused by temporal variations in operating conditions.

The objective of this research is to develop the elements of a fault detection system suitable for continuous, on-line condition monitoring and assessment of 3- ϕ induction motors. The use of only voltage and current sensors, already present in the motor control centers, for assessing the overall health of the motor, provides for a cost-effective and non-intrusive method for condition monitoring. The algorithms developed in SIMULINK are applicable for near steady-state operating conditions. To detect the quasi-stationary regions of motor operation, a signal segmentation technique is used. To calculate the indicators, the pertinent information is extracted from the spectra of the voltage and current signals for healthy and faulty data sets. The reciprocal of signal-to-noise ratio of current signal is proposed as a fault indicator for detecting mechanical faults. The negative-sequence component and imbalance of

the three phases of current signals are proposed as fault indicators for detecting electrical faults.

The variability of the developed fault indicators are investigated on 1 hp, 3 hp, 150 hp, 500 hp, 700 hp, and 800 hp motors at different loading conditions and the indicators are shown to be effective for detecting a variety of mechanical and electrical faults for motors of different ratings. Moreover, the algorithms are shown effective for distinguishing actual faults from false alarms resulting from temporal variations in motor operating conditions.

To my loving parents.

ACKNOWLEDGMENTS

I would like to express my sincere gratitude to my advisor, Dr. Alexander Parlos; without his guidance this thesis would not have been accomplished. I appreciate his time and effort throughout the duration of my research.

I wish to extend my thanks to Dr. Reza Langari and Dr. Andrew Chan for serving on my thesis committee. I am grateful to them for their time and interest in my research.

I am fortunate to have the company of a talented and motivated bunch of colleagues in the Networked Intelligent Machine Lab, Texas A&M University. I am thankful to Parashuram Harihara for his valuable suggestions during the course of my research. I would also like to thank Rajesh Bade, Lin Wang, Aninda Bhattacharya, Ajit Ambike, and Yash Shukla for their time and constructive suggestions.

My wholehearted gratitude to my parents, Sheela and Suresh Tapar, for their immeasurable support throughout my life. Without their unconditional love, encouragement and support, I could have never come so far.

TABLE OF CONTENTS

CHAPTER		Page
I	AN INTRODUCTION TO INDUCTION MOTOR FAULT DETECTION	1
	A. Introduction	1
	B. Types of Induction Motor Faults	2
	C. Literature Review	3
	D. Research Objectives and Proposed Approach	5
	1. Objectives	5
	2. Proposed Approach	5
	E. Contributions of the Research	6
	F. Organization of the Thesis	7
II	PROPOSED FAULT DETECTION SCHEME	8
	A. Fault Detection Methods	8
	B. Signal Processing and Development of Fault Indicators	9
	1. Re-sampling and Scaling	10
	2. Signal Segmentation	10
	3. Operating Parameters	11
	4. Development of Fault Indicators	13
	C. Chapter Summary	15
III	EXPERIMENT DESCRIPTION AND EXPERIMENTAL RE- SULTS	16
	A. Experimental Setup and Data Collection	16
	1. Small Machine Set-up	16
	2. Large Machine Set-up	16
	B. Description of Experiments Conducted	17
	1. Small Machines	17
	2. Large Machines	19
	C. Detection of Mechanical Faults	19
	1. Eccentric Loading	22
	2. Bad Bearings	22
	a. Single Deteriorating Bearing	22
	b. Double Deteriorating Bearing	25

CHAPTER	Page
3. Broken Rotor Bars - Case A	31
a. Half Broken Rotor Bar	31
b. One Broken Rotor Bar	31
c. Two Broken Rotor Bars	40
d. Four Broken Rotor Bars	42
4. Broken Rotor Bars - Case B	44
5. Air-Gap Eccentricity - Case A	46
a. Air-gap Eccentricity - Case A1	46
b. Air-gap Eccentricity - Case A2	47
6. Air-Gap Eccentricity - Case B	52
7. Mechanical Imbalance	55
D. Detection of Electrical Faults	56
1. Stator Imbalance - Case A	60
a. Stator Imbalance - Case A1	60
b. Stator Imbalance - Case A2	61
2. Stator Imbalance - Case B	63
3. Stator Winding Shorts	65
a. Stator Winding Shorts - Case 1	65
b. Stator Winding Shorts - Case 2	67
4. Ground Wall Insulation	73
5. Interlaminar Insulation Short	74
E. Chapter Summary	74
IV COMPARISON OF FAULT SIGNATURES	81
A. Comparison of Mechanical Fault Based on Load Levels	81
B. Comparison of Electrical Fault Based on Load Levels	91
C. Chapter Summary	105
V SUMMARY AND CONCLUSIONS	110
A. Summary of the Research	110
B. Conclusions from the Research	112
C. Future Research Work	113
REFERENCES	114
VITA	117

LIST OF TABLES

TABLE		Page
I	List of staged mechanical fault experiments.	20
II	List of staged electrical fault experiments.	21
III	Fault I: 1 hp motor at 0% load (healthy).	23
IV	Fault I: 1 hp motor at 0% load (eccentric loading).	24
V	Fault II: 3 hp motor at 0% load (healthy).	25
VI	Fault II: 3 hp motor at 25% load (healthy).	26
VII	Fault II: 3 hp motor at 0% load (single bearing fault).	27
VIII	Fault II: 3 hp motor at 25% load (single bearing fault).	28
IX	Fault II: 3 hp motor at 0% load (double bearing fault).	29
X	Fault II: 3 hp motor at 25% load (double bearing fault).	30
XI	Fault III: 800 hp motor at 0% load (healthy).	32
XII	Fault III: 800 hp motor at 50% load (healthy).	33
XIII	Fault III: 800 hp motor at 100% load (healthy).	34
XIV	Fault III: 800 hp motor at 0% load (half broken rotor bar).	35
XV	Fault III: 800 hp motor at 50% load (half broken rotor bar).	36
XVI	Fault III: 800 hp motor at 100% load (half broken rotor bar).	37
XVII	Fault III: 800 hp motor at 0% load (one broken rotor bar).	37
XVIII	Fault III: 800 hp motor at 50% load (one broken rotor bar).	38
XIX	Fault III: 800 hp motor at 100% load (one broken rotor bar).	39

TABLE	Page
XX	Fault III: 800 hp motor at 0% load (two broken rotor bars). 40
XXI	Fault III: 800 hp motor at 50% load (two broken rotor bars). 41
XXII	Fault III: 800 hp motor at 100% load (two broken rotor bars). 41
XXIII	Fault III: 800 hp motor at 0% load (four broken rotor bars). 42
XXIV	Fault III: 800 hp motor at 50% load (four broken rotor bars). 44
XXV	Fault III: 800 hp motor at 100% load (four broken rotor bars). 45
XXVI	Fault III: 700 hp motor at 50% load (healthy). 46
XXVII	Fault III: 700 hp motor at 100% load (healthy). 47
XXVIII	Fault III: 700 hp motor at 50% load (grease on winding and two broken rotor bars). 48
XXIX	Fault III: 700 hp motor at 100% load (grease on winding and two broken rotor bars). 49
XXX	Fault IV: 800 hp motor at 50% load (air-gap eccentricity - case A1). 50
XXXI	Fault IV: 800 hp motor at 100% load (air-gap eccentricity - case A1). 51
XXXII	Fault IV: 800 hp motor at 0% load (air-gap eccentricity - case A2). . 52
XXXIII	Fault IV: 800 hp motor at 50% load (air-gap eccentricity - case A2). 54
XXXIV	Fault IV: 800 hp motor at 100% load (air-gap eccentricity - case A2). 54
XXXV	Fault IV: 700 hp motor at 50% load (air-gap eccentricity - case B). . 55
XXXVI	Fault IV: 700 hp motor at 100% load (air-gap eccentricity - case B).. 56
XXXVII	Fault V: 500 hp motor at 0% load (healthy). 57
XXXVIII	Fault V: 500 hp motor at 50% load (healthy). 57
XXXIX	Fault V: 500 hp motor at 100% load (healthy). 58
XL	Fault V: 500 hp motor at 0% load (mechanical imbalance). 58

TABLE	Page
XLI	Fault V: 500 hp motor at 50% load (mechanical imbalance). 59
XLII	Fault V: 500 hp motor at 100% load (mechanical imbalance). 59
XLIII	Fault I: 150 hp motor at 50% load (healthy). 60
XLIV	Fault I: 150 hp motor at 100% load (healthy). 61
XLV	Fault I: 150 hp motor at 50% load (stator imbalance - case A1). . . . 62
XLVI	Fault I: 150 hp motor at 100% load (stator imbalance - case A1). . . 63
XLVII	Fault I: 150 hp motor at 50% load (stator imbalance - case A2). . . . 64
XLVIII	Fault I: 150 hp motor at 100% load (stator imbalance - case A2). . . 65
XLIX	Fault I: 800 hp motor at 0% load (healthy). 66
L	Fault I: 800 hp motor at 50% load (healthy). 67
LI	Fault I: 800 hp motor at 100% load (healthy). 68
LII	Fault I: 800 hp motor at 0% load (stator imbalance - case B). 69
LIII	Fault I: 800 hp motor at 50% load (stator imbalance - case B). 70
LIV	Fault I: 800 hp motor at 100% load (stator imbalance - case B). . . . 70
LV	Fault II: 500 hp motor at 0% load (stator winding shorts - case 1). . . 71
LVI	Fault II: 500 hp motor at 50% load (stator winding shorts - case 1). . 72
LVII	Fault II: 500 hp motor at 100% load (stator winding shorts - case 1). 73
LVIII	Fault II: 500 hp motor at 0% load (stator winding shorts - case 2). . . 74
LIX	Fault II: 500 hp motor at 50% load (stator winding shorts - case 2). . 75
LX	Fault II: 500 hp motor at 100% load (stator winding shorts - case 2). 76
LXI	Fault III: 500 hp motor at 0% load (ground wall insulation). 76
LXII	Fault III: 500 hp motor at 50% load (ground wall insulation). 77

	TABLE	Page
LXIII	Fault III: 500 hp motor at 100% load (ground wall insulation).	77
LXIV	Fault IV: 500 hp motor at 0% load (interlaminar insulation short).	78
LXV	Fault IV: 500 hp motor at 100% load (interlaminar insulation short).	79

LIST OF FIGURES

FIGURE	Page
1	Block diagram of signal processing approach. 10
2	Block diagram of the experimental set-up for small machines. 17
3	Block diagram of the experimental set-up for first set of large machines. 18
4	Block diagram of the experimental set-up for second set of large machines. 18
5	Four rotor broken bar test for 800 hp motor; raw motor current (top), motor current spectra (bottom). 43
6	Air-gap eccentricity test for 800 hp motor; raw motor current (top), motor current spectra (bottom). 53
7	Load dependence of Indicator-1 and Fault Indicator-1 Change for 3 hp motor; single bad bearing. 82
8	Load dependence of Indicator-1 and Fault Indicator-1 Change for 3 hp motor; double bad bearing. 83
9	Load dependence of Indicator-1 and Fault Indicator-1 Change for 800 hp motor; half broken rotor bar. 85
10	Load dependence of Indicator-1 and Fault Indicator-1 Change for 800 hp motor; one broken rotor bar. 86
11	Load dependence of Indicator-1 and Fault Indicator-1 Change for 800 hp motor; two broken rotor bars. 87
12	Load dependence of Indicator-1 and Fault Indicator-1 Change for 800 hp motor; four broken rotor bars. 88
13	Load dependence of Indicator-1 and Fault Indicator-1 Change for 700 hp motor; grease on winding and two broken rotor bars - case B. 89

FIGURE	Page
14	Load dependence of Indicator-1 and Fault Indicator-1 Change for 800 hp motor; air-gap eccentricity - case A2. 90
15	Load dependence of Indicator-1 and Fault Indicator-1 Change for 700 hp motor; air-gap eccentricity - case B. 92
16	Load dependence of Indicator-1 and Fault Indicator-1 Change for 500 hp motor; mechanical imbalance. 93
17	Load dependence of Indicator-2 and Fault Indicator-2 Change for 150 hp motor; stator imbalance - case A1 (resistance of 0.012Ω in series with phase A). 95
18	Load dependence of Indicator-3 and Fault Indicator-3 Change for 150 hp motor; stator imbalance - case A1 (resistance of 0.012Ω in series with phase A). 96
19	Load dependence of Indicator-2 and Fault Indicator-2 Change for 150 hp motor; stator imbalance - case A2 (resistance of 0.633Ω in series with phase A). 97
20	Load dependence of Indicator-3 and Fault Indicator-3 Change for 150 hp motor; stator imbalance - case A2 (resistance of 0.633Ω in series with phase A). 98
21	Load dependence of Indicator-2 and Fault Indicator-2 Change for 800 hp motor; stator imbalance - case B (2.7Ω resistor in phase A). 99
22	Load dependence of Indicator-3 and Fault Indicator-3 Change for 800 hp motor; stator imbalance - case B (2.7Ω resistor in phase A). 100
23	Load dependence of Indicator-2 and Fault Indicator-2 Change for 500 hp motor; stator winding shorts - case 1 (2.7Ω turn-turn resistance in series with phase C). 101
24	Load dependence of Indicator-3 and Fault Indicator-3 Change for 500 hp motor; stator winding shorts - case 1 (2.7Ω turn-turn resistance in series with phase C). 102

FIGURE	Page
25	Load dependence of Indicator-2 and Fault Indicator-2 Change for 500 hp motor; stator winding shorts - case 2 (1.35Ω turn-turn resistance in series with phase C). 103
26	Load dependence of Indicator-3 and Fault Indicator-3 Change for 500 hp motor; stator winding shorts - case 2 (1.35Ω turn-turn resistance in series with phase C). 104
27	Load dependence of Indicator-2 and Fault Indicator-2 Change for 500 hp motor; ground wall insulation ($10 \text{ M}\Omega$ resistance in phase C). 106
28	Load dependence of Indicator-3 and Fault Indicator-3 Change for 500 hp motor; ground wall insulation ($10 \text{ M}\Omega$ resistance in phase C). 107
29	Load dependence of Indicator-2 and Fault Indicator-2 Change for 500 hp motor; interlaminar insulation short (damaged stator core). . 108
30	Load dependence of Indicator-3 and Fault Indicator-3 Change for 500 hp motor; interlaminar insulation short (damaged stator core). . 109

CHAPTER I

AN INTRODUCTION TO INDUCTION MOTOR FAULT DETECTION

A. Introduction

Induction motors are crucial for many industrial processes and play a critical role in efficient and successful operation of industrial plants and many other real-world applications. Despite of their high reliability, electric machine components are susceptible to failures. In order to prevent productivity losses and achieve minimum machinery downtime, it is extremely important that such motors are constantly monitored and diagnosed early for potential faults. Different parts of machines are subjected to different failure conditions. For example, the stator windings are subjected to insulation breakdowns caused by mechanical vibration, heat, damage during installation, and contamination of oil [1]. Inadequate lubrication and/or misalignment can damage the bearings.

Common faults in induction motors may range from mechanical faults such as broken rotor bars, damaged motor bearings and air-gap eccentricities to electrical faults such as stator winding shorts and supply imbalance. Any combination of the above faults can cause failures of load critical machines, which can shut down an entire industrial process. Unplanned machine shut-downs cost time that could be avoided if an early warning system was available against impending faults. While preventive and periodic maintenance are techniques often employed in industry, unnecessary replacement of healthy motor parts is a major problem associated with them. Fault detection and diagnosis schemes are intended to provide advanced warnings of incipient faults, so that corrective action can be taken without detrimental interruption to

The journal model is *IEEE Transactions on Automatic Control*.

processes. Fault detection of electric motors, in particular, can lead to greater plant availability, extended plant life, higher quality products, smooth plant operations, and reduction in downtime [1].

B. Types of Induction Motor Faults

The main components of the induction machine that are susceptible to faults are the stator, the rotor, and the bearings. Faults in induction motors can be broadly classified into faults based on electrical condition (electrical faults) and faults based on the mechanical conditions (mechanical faults) of the motor. Electrical faults include excessive power supply imbalance, stator winding shorts, etc. Stator faults are usually interpreted as insulation related faults since one of the weakest component in any electric machine is the winding insulation. Mechanical faults include bearing defects, rotor faults, air-gap eccentricities, etc. Defective castings, poor joints, high temperatures, combination of various stresses and large centrifugal forces developed during transient motor operation, such as start-up, give rise to rotor bar faults. Fatigue failure is very common in rolling-element bearings even under normal operating conditions of balanced load and proper alignment. Improper lubrication and misalignment are other sources of bearing faults. An induction motor can also fail due to air-gap eccentricity. When the positioning of the stator or the rotor is incorrect or there are ovalities of the core, static air-gap eccentricity is caused. Dynamic air-gap eccentricity can be caused by bearing wear, bearing misalignment, bent rotor shaft, etc. Other types of mechanical faults that occur in induction motors are discussed in [2].

C. Literature Review

Numerous fault detection methods have been proposed for electric machines because of the potential savings offered by them. Fault detection in three-phase induction motors is generally performed by some combination of mechanical and electrical signal monitoring. Mechanical signal monitoring techniques have been in use for quite some time and are quite effective in assessing a machine's condition. However, mechanical sensors, such as accelerometers, are generally installed on only the most expensive and load-critical machines, if at all, where the cost of the continuous monitoring is justified. Moreover, condition monitoring techniques using mechanical signals are also limited in their ability to detect electrical faults, such as stator insulation failures. Electrical monitoring techniques have concentrated on the use of motor current negative sequence for detecting stator-winding failures, whereas spectral analysis of stator current has been employed for sensing rotor faults, such as broken rotor bars. Recently, electrical monitoring techniques using line currents, such as Motor Current Signature Analysis (MCSA), has become popular for motor fault detection [3]. For most purposes, current monitoring can be implemented inexpensively on most machines, by utilizing the current transformers (CTs) and potential transformers (PTs) already in place at the motor control centers or switch-gear. Use of the existing CTs and PTs which are standard installations in industries makes Electrical Signal Analysis (ESA) convenient for remote monitoring of large numbers of motors from a central location.

Venugopal [4] demonstrated the suitability of electrical monitoring techniques compared to mechanical techniques for effective detection of mechanical faults in induction motors. Venugopal compared vibration signatures and electric current signatures for detecting mechanical faults and concluded that in addition to mechanical

signatures, electrical signatures also provide a consistent indication of mechanical faults.

Payne et al. [5],[6] investigated the diagnosis of broken rotor bars by the use of vibration and phase current analysis. Emphasis was on demonstrating higher potential with the use of current spectra while experimental results proved encouraging for both current spectra-based and vibration spectra-based fault diagnosis. Schoen et al. [7] addressed the application of motor current spectral analysis for the detection of rolling element bearing damage in induction motors. Thomson et al. [8] were able to successfully demonstrate the identification of faults in the motor spectral components. An industrial case study was presented to show that the spectral components of the stator current associated with eccentricity were identifiable in the Fast Fourier Transform (FFT). These components were notably absent after the correction of the defect. Mechanical fault detection using MCSA has been demonstrated in [9],[10].

Electrical health assessment techniques are based primarily on the use of negative-sequence currents as indicators. Use of negative sequence currents to detect stator faults was first introduced by Williamson and Mirzoian [11], and the majority of the methods developed since then for detecting insulation faults are based on this technique. These methods are simple to implement but have a severe limitation in the sense that power supply imbalance and load variations will also produce effects that are similar to the appearance of negative sequence currents. Sottile and Kohler [12] modified the methods using negative sequence currents to compensate for the impact of unbalanced machine operation and have shown that use of negative sequence impedance is insensitive to voltage and current changes but are highly sensitive to stator defects. Kliman et al. [13] developed the injected negative sequence current that is not affected from an unbalanced supply voltage but is sensitive to load variations. Most of the proposed approaches for current-based motor condition monitoring ignore

the load effects or assume that the load is known and constant. Kim [14],[15] presents an alternative approach to MCSA by using the overall distortion of the stator current as an indicator for the presence of a fault. This approach has the advantage of being insensitive to uncertainties in the frequencies at which faults appear in the current spectrum. Benbouzid et al. [16] demonstrated the use of stator current processing for the detection and localization of faults in an induction motor.

D. Research Objectives and Proposed Approach

1. Objectives

The primary objective of the present research is to detect some of the most widely encountered mechanical and electrical faults in induction motors such as broken rotor faults, air-gap eccentricity, damaged bearings, mechanical imbalance and, stator winding shorts based only on electrical signatures. Another objective of this work is to be able to distinguish actual faults from false alarms by investigating the variability of the fault indicators at a certain “healthy” condition of the motor. As it is shown in this research, the scalability of the proposed approach enables application of the present fault detection scheme to induction motors of different ratings and manufacturers.

2. Proposed Approach

The fault features extracted from the electrical signals pertaining to a faulty motor are compared to the fault features of a healthy motor at various loading condition. If variations in these fault features between a healthy and a faulty motor are more than a threshold then a fault would be declared. A healthy data set for known loading level is obtained by recording all three phases of line voltages and currents which forms

the baseline for this comparison. A similar procedure is followed to obtain data sets for different faulty cases. Each staged faulty case is then considered individually with respect to the baseline healthy data.

Data sets obtained through the data acquisition medium is passed through a SIMULINK model to compute all of the fault indicators. To calculate the indicators, the pertained information is extracted from the spectrum of the current signal for healthy and faulty data sets. Fault indicators used in the present research includes a measure of the reciprocal of signal-to-noise ratio, the negative sequence, and the imbalance in three phases of motor current signals. After the computation of these indicators, the difference between the fault indicators for the faulty and healthy motors provides the information for the detection of faults. Statistical consistency is verified by repeating the processing for multiple sets of data. Variation in indicators for the healthy and faulty data sets is also calculated to make a distinction between actual faults and false alarms.

The above procedure to analyze the current spectra is repeated for motors of different ratings and manufacturers, to demonstrate the scalability of the comparison and the fault detection scheme. After the results from the electrical signatures are obtained, statistical analysis between healthy and faulty indicators is performed to validate the effectiveness of the approach.

E. Contributions of the Research

The following are the key contributions of this research towards fault detection of induction motors:

1. Investigation of the variability of fault features extracted for a particular motor condition, towards making distinctions between actual fault and false alarms.

2. Demonstration of the robustness of the developed fault detection approach to different loading conditions.
3. Demonstration of the adaptability of the developed fault detection approach to mechanical and electrical induction motor faults of different nature.
4. Demonstration of the scalability of the developed fault detection approach for induction motors of different ratings and manufacturers.

F. Organization of the Thesis

The rest of the thesis is organized as follows. In Chapter II an overview of the different fault detection methods is provided. This chapter also explains the various steps involved in the signal processing performed. This is done through descriptions of the various operating parameters and fault indicators. Chapter III presents the experimental set-ups for both small and large machines together with various experiments conducted. This chapter also presents the results for number of data sets with their mean indicator values and Fault Indicator Change (FIC) of faulty data as compared to healthy data. In Chapter IV the dependence of the indicator values and indicator change on loading condition is presented. Each fault is individually considered, and the corresponding results are graphically presented. Finally, in Chapter V a summary of this work is presented along with the conclusions drawn from the results.

CHAPTER II

PROPOSED FAULT DETECTION SCHEME

A. Fault Detection Methods

A fault detection method can be data-driven, knowledge-based or model-based. A data-driven fault detection scheme consists of 1) collecting data, 2) extracting relevant features from the data and evaluating these extracted features into a form of fault indicators, and 3) comparing these indicators to baseline observations formed from the normal condition system. Based on the results of this comparison, a fault can be declared. While knowledge-based methods involve developing relations between observed symptoms (effects) and unknown faults (causes) and thereby arriving at a logical conclusion to help diagnose faults, model-based methods use the system input and output data to estimate information about the system. A majority of the motor fault detection methods developed so far have been based on data-driven methods (also known as signal-based methods) when applied to statistically significant lengths of data sets. The focus of this research is on the application of advanced signal processing algorithms and development of current-based mechanical and electrical fault indicators for the detection of mechanical and electrical faults.

The indicators are calculated from the measured data, which in some way represent the state or behavior of the system. The idea is to compress or convert the large amount of on-line data collected from the system into a meaningful measures, and thereby assist the operators in determining the status of the system condition.

B. Signal Processing and Development of Fault Indicators

In the present research, there are two major signal processing procedures, the signal segmentation and the fault indicator generation process. The signal segmentation routine separates the quasi-stationary region of the signal from the non-stationary region and only the quasi-stationary signal is further processed to extract the fault features.

A FFT-based method is used in the fault indicator generation algorithm to obtain the fault indicators. The Fourier transform contains information on the frequencies of the signal at one time instant, and it does not account for variations over time. Thus, FFT is an effective method for the analysis of the signals if the frequency components do not vary over time significantly. Once the stationary regions are acquired, the FFT-based method can be used for the processing of the signals to compute the fault indicators. Reciprocal of signal-to-noise ratio of the current signal is developed to capture the fault signature of mechanical faults and negative-sequence component and degree of three phase imbalance of the current signal is developed to capture the fault signature of electrical faults. The procedures, for computing the fault indicators involves separation of the fundamental component from the remaining harmonic components. Once the signal segmentation is performed and quasi-stationary regions of the signal are obtained, the frequency component separation is achieved by FFT-based method.

This procedure is performed for healthy motor as well as for cases with specific staged faults in the motor. The indicators developed through the analysis of healthy motor condition and faulty motor condition forms the healthy baseline and fault indicators respectively. Figure 1 shows the various component involved in the signal processing approach. Each module is discussed in detail in the following subsections.

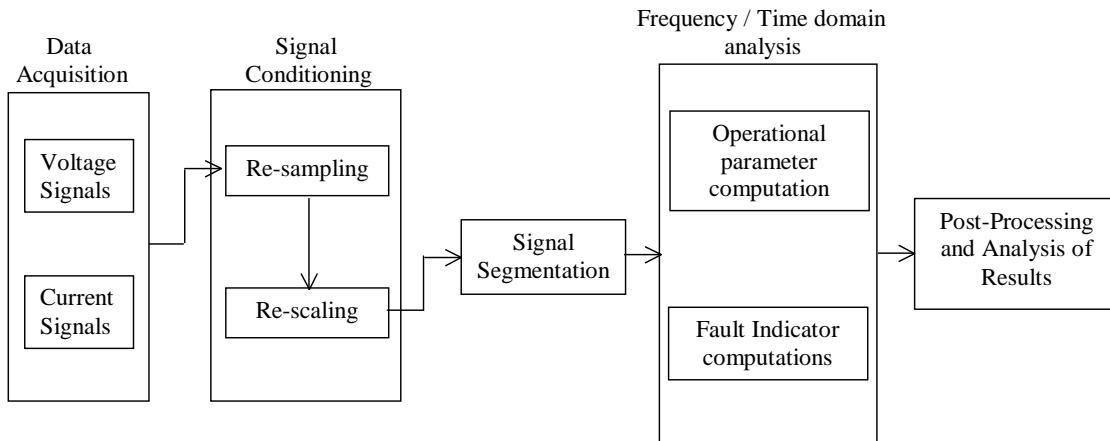


Fig. 1. Block diagram of signal processing approach.

1. Re-sampling and Scaling

Line voltages and phase currents are measured using CT's and PT's. These signals representing each of the three phases of currents and voltages are re-sampled. In small motor case, the data itself is acquired at a low sampling rate and hence does not need any re-sampling. Data sets obtained through the data acquisition system are joined together into arrays of data ready to be processed. Any biases that might have occurred during one or more of the experiments are taken care of by forcing a zero-mean to the signals.

2. Signal Segmentation

After re-sampling, the signal is passed through a signal segmentation algorithm and the output obtained is the quasi-stationary region of the signal. The signal segmentation into a piece-wise quasi-stationary signal is based on the fact that the magnitude of the fundamental component and the harmonic components of a signal should re-

main within certain limits over a period of time. Thus, in signal segmentation it is required to investigate the variations of the fundamental component as well as the harmonic components as a function of time. The magnitude variation of the frequency component is compared to a pre-selected threshold value. This threshold represents the allowed limit of magnitude variation for a signal to be considered quasi-stationary. All three measurements of the currents and voltages are tested for stationarity. The final decision for the stationarity of the signal is made only if all three current and voltage measurements are within the pre-specified threshold.

3. Operating Parameters

After signal segmentation, the quasi-stationary signal is passed through a fault indicator generation algorithm, which is written using SIMULINK, to obtain information about the actual condition of the machine. The following operating parameters are developed to identify the operating condition of the motor:

- moving window root mean square of all the three phases of voltages and currents
- three-phase voltage imbalance
- total harmonic distortion of the voltage signal
- reciprocal of signal-to-noise ratio of the voltage signal

Moving window root mean square algorithm: A moving window with no overlap is used to perform the root mean square algorithm, continuing through the length of the window. The window size is obtained through the product of sampling frequency and size of window in seconds.

The moving window root mean square value of a signal 'x(t)' over the time interval of $[t_1, t_N]$ is defined as follows

$$x_{RMS}(l) = \sqrt{\int_{t_1+lp}^{t_2+lp} x(t)^2 dt} \quad (2.1)$$

where $l = 0, 1, \dots, m$, $t_2 - t_1$ is the size of the moving window, with a moving window distance of p , and $m = (t_N - t_2)/p$.

Voltage imbalance: The degree of three-phase voltage imbalance is defined by

$$Imbalance_V(\%) = \frac{\max_X |V_X^{RMS} - V_{mean}^{RMS}|}{V_{mean}^{RMS}} \times 100, \quad (2.2)$$

where V_{mean}^{RMS} is the mean of three-phase voltages, and the subscript X stands for three-phase a, b, c. The major cause of imbalance at the point of utilization is that single-phase loads on a system are not uniformly applied to all three phases.

Total harmonic distortion: The Total Harmonic Distortion (THD) of a signal is defined as the ratio of sum of the powers of all integer harmonic frequencies above the fundamental frequency to the power of the fundamental frequency. The THD of the voltage signals is obtained by calculating Power Spectral Density (PSD) of the signal. The PSD of the three-phase voltage and current signal is calculated after windowing the signal with the Blackman window. The THD of the voltage signal is expressed as

$$THD_X = \frac{\sqrt{\sum_k F_{60k}^2}}{F_{60}} \quad (2.3)$$

where $k = 2, 3, \dots, 15$, F_{60} is power of fundamental frequency (60 Hz) of the voltage signal, F_{60k} is power of all integer harmonics above fundamental frequency, as k varies from 2 to 15, and subscript X stands for three-phase of voltage a, b, c.

Signal-to-noise ratio of voltage signal (SNR_V): The SNR_V value is the ratio of the peak power level (power of the fundamental frequency) to the remaining

noise power of a voltage signal. It is also defined as the ratio of the amplitude of the desired signal to the amplitude of noise signals at a given point in time. For calculating SNR_V , PSD of the voltage signal is used. In the present research, $1/SNR_V$ is taken as the operating parameter and it can be expressed as

$$1/SNR_V = \frac{\sum_n F_n^2}{F_{60}^2} \quad (2.4)$$

$$n = 1, \dots, N$$

$$n \neq 60k$$

where N is number of samples, $k = 1, \dots, 15$, F_{60} is power of fundamental frequency (60 Hz) of the voltage signal, F_n is power of all harmonics excluding power of all the integer harmonics, as k varies from 1 to 15. $1/SNR_V$ is calculated for each phases of voltage.

4. Development of Fault Indicators

Three fault indicators are developed in the present research depending on the operating condition of the motor. After passing the re-sampled current signals through the signal segmentation algorithm, the quasi-stationary signals are passed through fault indicator generation algorithm which generates five operating parameters and three fault indicators. Healthy baselines are obtained when processing current signals from the healthy motor data and an increase with respect to this baseline value of the fault indicators which are obtained from the analysis of faulty motor data indicate a fault in the motor.

Signal-to-noise ratio of current signal (SNR_I): The reciprocal of SNR_I is referred to as indicator-1 and is primarily used to detect mechanical faults in the motor. The PSD of the current signal is used to calculate SNR_I . The value of SNR_I is

calculated in the same way as described for voltage signals. The only difference in the computation is that while calculating for voltage, power of all the integer harmonics including fundamental frequency is subtracted from the power of the signal, whereas, in the case of current signal only the power of odd harmonics and fundamental is subtracted from the power of the signal. In this research, $1/SNR_I$ is taken as the one of the fault indicator and it can be expressed as

$$1/SNR_I = \frac{\sum_n F_n^2}{F_{60}^2} \quad (2.5)$$

$$n = 1, \dots, N$$

$$n \neq 60k$$

where N is number of samples, $k = 1, 3, 5, \dots, 15$, F_{60} is power of fundamental frequency (60 Hz) of the voltage signal, F_n is power of all harmonics excluding power of all the odd harmonics, as k varies from 1, 3, ..., 15. $1/SNR_I$ is calculated for each phases of current.

Current imbalance: The degree of three-phase current imbalance is referred to as indicator-2 and is developed to detect the electrical faults in motor. It is calculated the same way as voltage imbalance and is defined by

$$Imbalance_I(\%) = \frac{\max_X |I_X^{RMS} - I_{mean}^{RMS}|}{I_{mean}^{RMS}} \times 100, \quad (2.6)$$

where I_{mean}^{RMS} is the mean of three-phase currents, and the subscript X stands for three-phase a, b, c.

Negative-sequence component of the current signal: In this study, the negative-sequence component of the current signal is referred to as indicator-3 and is used as another fault indicator for detecting electrical faults. Separation of the signals into fundamental and harmonics is performed by an FFT because the underlying

signals are quasi-stationary. After the separation of the frequency components, the negative-sequence component of the current is obtained by the symmetrical component analysis of the fundamental of the three-phase current. When electrical fault occurs, the positive sequence currents do not change very much, but the negative-sequence current appear where there should be none because of the asymmetry in the current magnitudes. Thus the faults in the stator winding can be detected by monitoring the negative-sequence current. The symmetrical component of a three-phase current signal can be expressed as

$$\begin{bmatrix} I_0 \\ I_p \\ I_n \end{bmatrix} = \frac{1}{3} \begin{bmatrix} 1 & 1 & 1 \\ 1 & \alpha & \alpha^2 \\ 1 & \alpha^2 & \alpha \end{bmatrix} \begin{bmatrix} I_a \\ I_b \\ I_c \end{bmatrix}$$

where $\alpha = e^{j2\pi/3}$, I_0 , I_p and I_n are the zero-, positive-, and negative-sequence variables, I_a , I_b and I_c are the corresponding three-phase variables of the current signal. The negative sequence of the current can be obtained by symmetrical component theory as

$$\text{Negative sequence (neg_seq)} = \frac{1}{3}(I_{a,f} + \alpha^2 I_{b,f} + \alpha I_{c,f}) \quad (2.7)$$

where $\alpha = e^{j2\pi/3}$, $I_{a,f}$, $I_{b,f}$ and $I_{c,f}$ are the fundamental components of current signal.

C. Chapter Summary

In this chapter, the steps involved in the processing of the signals and the proposed algorithms for the fault detection system are explained. In the proposed scheme the signal segmentation technique is applied to get the quasi-stationary regions and the RMS-based and FFT-based methods are used for processing of the signals to compute the operating parameters and fault indicators.

CHAPTER III

EXPERIMENT DESCRIPTION AND EXPERIMENTAL RESULTS

A. Experimental Setup and Data Collection

1. Small Machine Set-up

Experiments for small machine are conducted on two motors: a) 3 - ϕ , 2 pole, 3 hp motor and b) 3 - ϕ , 4 pole, 1 hp motor. Both the 3 hp and 1 hp motor are manufactured by Marathon Incorporate and located at Networked Intelligent Machines Lab, 167 Wisenbaker Engineering Research Center, Texas A&M University. The motors are powered by means of an 3 - ϕ auto-transformer. The motor is connected to a gear box which is used to load the induction motor. Data are collected at steady state operation for various loading conditions. A 8-channel National Instruments data acquisition system containing anti-aliasing filter is used to collect and sample the data. Figure 2 shows the schematic diagram of the experimental setup used for small machine.

2. Large Machine Set-up

Experiments for large machine are conducted on 2 sets of motors. The first set consists of three motors: a) 3 - ϕ , 800 hp motor manufactured by Westinghouse Motor, b) 3 - ϕ , 6 pole, 500 hp motor manufactured by General Electric, c) 3 - ϕ , 8 pole, 800 hp motor manufactured by Allis Chalmers, and the second set consists of two motors: d) 3 - ϕ , 4 pole, 150 hp motor and e) 3 - ϕ , 6 pole, 700 hp motor. Data sets are collected at *Public Service Electric and Gas Motor Repair Facility, Sewaren, New Jersey*. The motors are connected to a dynamometer which is used to load the induction motor. Schematic diagrams of the experimental setup for the first set of

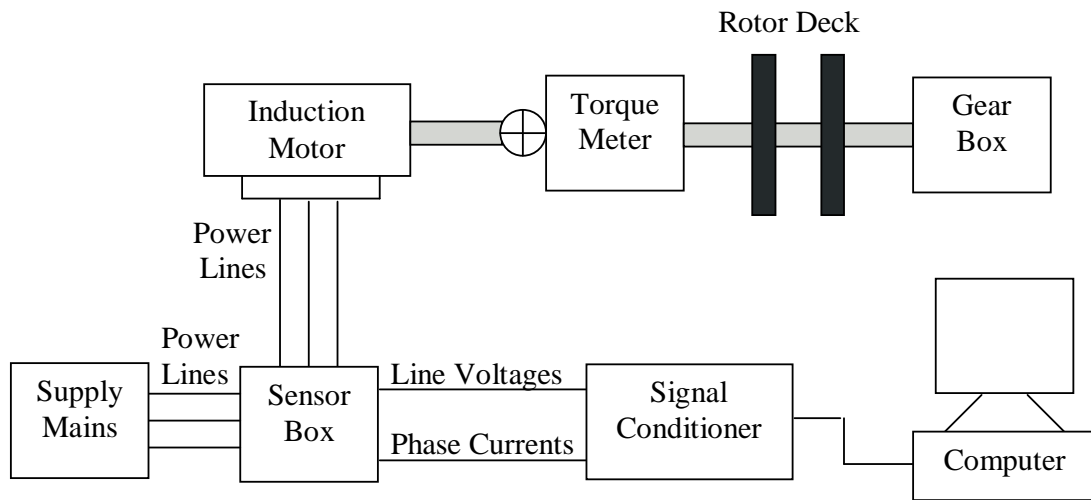


Fig. 2. Block diagram of the experimental set-up for small machines.

motors and the second set of motors are shown on Figure 3 and Figure 4 respectively. The experiments for first set of three motors were conducted in 1997 and a 13-channel *IOTech*TM data-acquisition system was used to record the data for three line voltages, the three phase currents, the speed and the six vibration signals at 40 kHz sampling frequency. The experiments for second set of two motors, 150 hp and 700 hp, were conducted in 2002 and NI DAQ was used to sample the three line voltages and three phase currents at 10 kHz sampling frequency.

B. Description of Experiments Conducted

1. Small Machines

Experiments are conducted on 3 hp and 1 hp motor for different cases of mechanical faults. The 3 hp motor is used to stage faults with different types of deteriorating

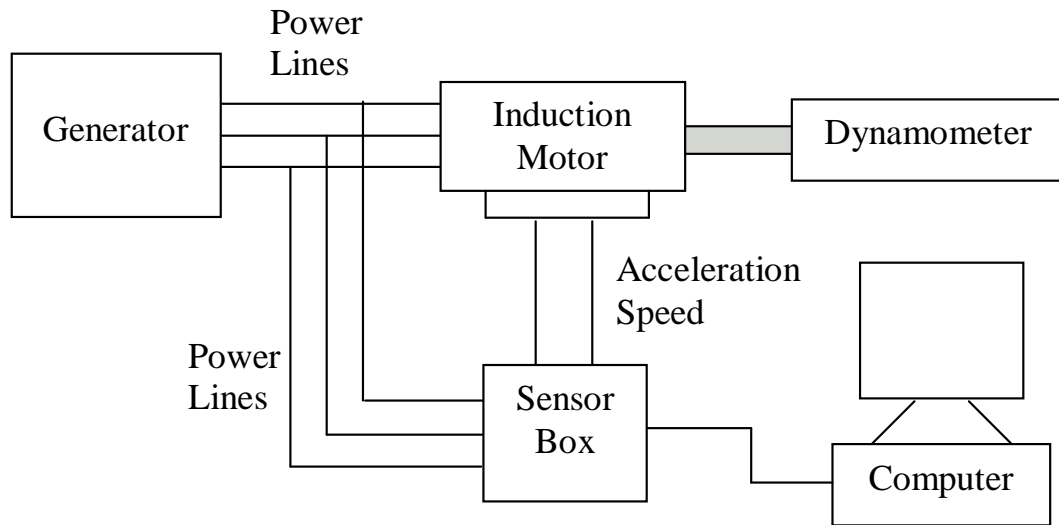


Fig. 3. Block diagram of the experimental set-up for first set of large machines.

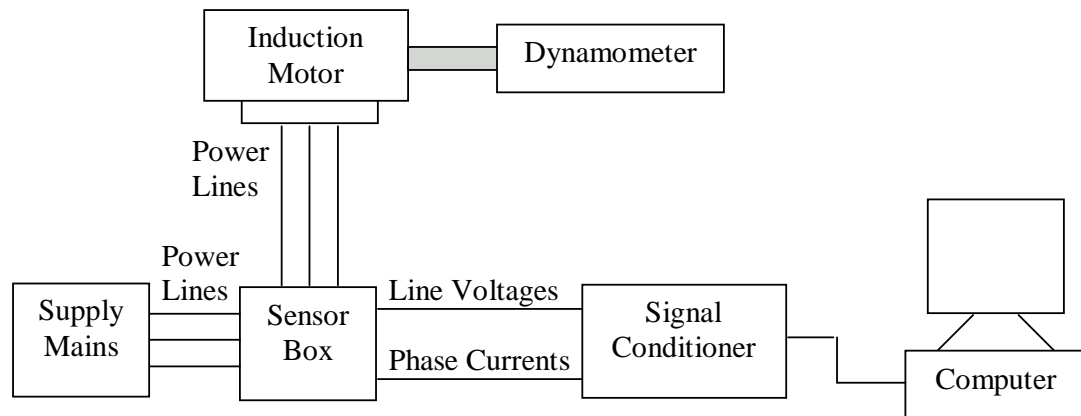


Fig. 4. Block diagram of the experimental set-up for second set of large machines.

bearing condition and 1 hp motor is configured for a load eccentricity fault. Table I shows the list of staged fault experiments with description of various cases of fault. While the healthy and faulty experiments of the 3 hp motor are carried out at no load and 25% load condition, the healthy and faulty experiments on the 1 hp motor are carried out at no load condition.

2. Large Machines

Experiments are conducted for different types of mechanical and electrical faults. Steady state data corresponding to 100%, 50% and 0% loading conditions are used for the different cases. For this research, data corresponding to mechanical faults namely broken rotor bars, air-gap eccentricity, mechanical imbalance and data corresponding to electrical faults namely stator imbalance, stator winding faults, ground wall insulation, and interlaminar insulation short, are used. As the data for the faults are from different motors, separate healthy baselines for the corresponding cases are considered for analysis. Table I and Table II show the list of staged mechanical and electrical fault experiments with description a of various cases of faults considered.

C. Detection of Mechanical Faults

For detecting the mechanical faults the reciprocal of signal-to-noise of the current signal ($1/\text{SNR}_I$) is primarily used as a fault indicator. The effectiveness of the developed indicator is examined by calculating the Fault Indicator-1 Change (FIC-1). Results obtained for different mechanical fault cases at different loading conditions are discussed in the following subsections.

Table I. List of staged mechanical fault experiments.

Fault	Fault-Case	Rating	Loading condition	Description of various cases
Fault I	Eccentric loading	1 hp ¹	0% load	Eccentric loading
Fault II	Bad Bearing	3 hp ¹	0% and 25% load	Single Bearing Fault: at fan end of the rotor Double Bearing Fault: at both end of the rotor
Fault III	Broken Rotor Bar - Case A	800 hp ²	0%, 50% and 100%	Half broken rotor bar One broken rotor bar Two broken rotor bar Four broken rotor bar
	Broken Rotor Bar - Case B	700 hp	50% and 100%	Grease on winding and two broken rotor bar
Fault IV	Air-gap Eccentricity - Case A	800 hp ²	0%, 50% and 100%	Case A1: Offset set to 25% Up Inboard Case A2: Offset set to 20% Down Outboard & 26% Right Inboard
	Air-gap Eccentricity - Case B	700 hp	50% and 100%	————
Fault V	Mechanical Imbalance	500 hp ³	0%, 50% and 100%	Rotor Imbalance

Note: Manufacturers; 1 - Marathon, 2 - Allis Chalmers, 3 - G.E.

Table II. List of staged electrical fault experiments.

Fault	Fault-Case	Rating	Loading condition	Description of various cases
Fault I	Stator Imbalance - Case A	150 hp	50% and 100%	Case A1: 0.012 Ω res. in series with phase A Case A2: 0.633 Ω res. in series with phase A
	Stator Imbalance - Case B	800 hp ⁴	0%, 50% and 100%	2.7 Ω resistor on A phase
Fault II	Stator Winding Shorts	500 hp	0%, 50% and 100%	Case 1: 2.7 Ω turn-turn res. 4.2 Amps C phase Case 2: 1.35 Ω turn-turn res. 8.3 Amps C phase
	Ground Wall Insulation	500 hp	0%, 50% and 100%	10 M Ω res. in C phase
Fault IV	Interlaminar Insulation Short	500 hp	0% and 100%	Damaged stator core, 3 groups near iron edge 1 group further inside

Note: Manufacturers; 4 - Westinghouse

1. Eccentric Loading

The healthy baseline data is obtained using the 1 hp motor operating under healthy conditions. Faulty cases are obtained by conducting experiments with eccentric loading on rotor. Number of different data sets of 30 seconds are processed with no loading condition. All the values of operating parameters and fault indicators for healthy condition and faulty condition are averaged over the respective number of data sets considered. Table III shows the magnitude of the operating parameters and the fault indicators for the healthy cases at 0% load condition. Table IV shows the same for the faulty cases with the corresponding values of FIC-1 at 0% load condition. The FIC-1 for eccentric loaded motor at 0% load is 126.73%.

2. Bad Bearings

The healthy baseline data is obtained using the 3 hp motor with healthy bearings at both ends. The measurements for the faulty bearings are collected with the installation of the bad bearings resulted from the defect of ball, inner and outer race. The 3 hp motor used in this work is originally designated to stage the rotor eccentricity experiments and it had an intrinsic 'looseness' of the rotor. The said condition has affected healthy and faulty cases alike.

a. Single Deteriorating Bearing

On the 3 hp motor, for the single deteriorating bearing cases, bearings are replaced at one end of the rotor (fan end) while maintaining the bearing at the other end (shaft end) healthy. Table V and Table VI show the magnitude of the operating parameters and the fault indicators for the healthy cases at 0% and 25% load condition. Table VII and Table VIII show the same for the faulty cases with the corresponding values

Table III. Fault I: 1 hp motor at 0% load (healthy).

Operational Parameter						Fault Indicator		
D.S.No.	RMS_V (p.u.)	RMS_I (p.u.)	Imb_V (%)	THD_V ($\times 10^{-2}$)	$(\frac{1}{SNR})_V$ ($\times 10^{-5}$)	Ind-1 ($\times 10^{-3}$)	Ind-2 (%)	Ind-3
1	1.00	0.23	0.43	1.90	4.78	1.36	0.91	9.39
2	0.99	0.23	0.42	1.92	1.02	1.31	0.83	8.66
3	0.99	0.23	0.43	1.90	3.20	1.34	0.85	8.68
4	0.99	0.23	0.43	1.92	1.63	1.32	0.84	8.45
5	0.99	0.23	0.43	1.92	1.96	1.32	0.87	9.15
6	0.99	0.23	0.42	1.52	30.55	1.80	0.88	8.29
7	0.99	0.23	0.40	1.69	19.69	1.61	0.94	8.47
8	0.99	0.23	0.40	1.68	19.41	1.62	1.14	11.02
9	0.99	0.23	0.41	1.92	1.72	1.33	1.10	10.90
10	0.99	0.23	0.40	1.89	4.57	1.37	1.12	11.43
Mean	1.00	0.23	0.42	1.83	8.86	1.44	0.95	9.45

Note: D.S.No. is Data Set Number

Table IV. Fault I: 1 hp motor at 0% load (eccentric loading).

Operational Parameter						Fault Indicator		
D.S.No.	RMS_V (p.u.)	RMS_I (p.u.)	Imb_V (%)	THD_V ($\times 10^{-2}$)	$(\frac{1}{SNR})_V$ ($\times 10^{-5}$)	Ind-1 ($\times 10^{-3}$)	Ind-2 (%)	Ind-3
1	1.00	0.23	0.42	1.13	59.50	2.30	1.09	10.73
2	1.00	0.23	0.41	0.84	89.60	2.68	1.13	10.69
3	1.00	0.23	0.41	0.57	138.58	3.25	1.12	10.08
4	1.00	0.23	0.40	0.52	147.97	3.35	1.18	10.11
5	1.00	0.23	0.40	1.02	67.69	2.39	1.17	10.48
6	1.00	0.23	0.41	0.91	83.59	2.59	1.07	9.55
7	1.00	0.23	0.41	0.30	245.63	4.37	1.00	8.01
8	1.00	0.23	0.41	0.36	198.45	3.87	1.13	9.79
9	1.00	0.23	0.41	0.28	250.08	4.40	1.16	10.24
10	1.00	0.23	0.41	0.40	180.30	3.68	1.18	10.33
11	1.00	0.23	0.40	0.58	125.27	3.08	1.17	10.62
Mean	1.00	0.23	0.41	0.63	144.24	3.27	1.13	10.06
FIC(%)						126.73	18.20	6.45

Note: D.S.No. is Data Set Number

of FIC-1 at 0% and 25% load condition. While the FIC-1 for single bearing fault at 0% load is 16.97%, the FIC-1 at 25% load is 2.79%.

Table V. Fault II: 3 hp motor at 0% load (healthy).

Operational Parameter						Fault Indicator		
D.S.No.	RMS_V (p.u.)	RMS_I (p.u.)	Imb_V (%)	THD_V ($\times 10^{-2}$)	$(\frac{1}{SNR})_V$ ($\times 10^{-5}$)	Ind-1 ($\times 10^{-3}$)	Ind-2 (%)	Ind-3
1	1.01	0.31	0.44	0.87	23.83	1.37	1.20	11.77
2	1.00	0.31	0.43	1.32	13.13	1.16	1.15	12.72
3	1.00	0.31	0.43	1.20	6.12	1.02	1.14	12.13
4	1.00	0.31	0.43	1.20	10.42	1.09	1.08	12.11
5	1.01	0.31	0.43	0.59	18.81	1.23	1.09	11.55
6	1.01	0.31	0.44	0.23	15.78	1.19	0.87	7.68
7	1.01	0.31	0.43	0.26	2.04	0.94	1.14	11.00
8	1.01	0.31	0.43	0.52	16.66	1.20	1.15	11.93
9	1.01	0.31	0.42	0.71	6.42	1.02	1.26	13.53
10	1.01	0.31	0.42	0.89	4.97	0.99	1.25	13.44
11	1.01	0.31	0.42	1.42	32.58	1.49	1.21	13.32
12	1.01	0.31	0.43	1.44	11.43	1.11	1.15	12.90
Mean	1.01	0.31	0.43	0.89	13.52	1.15	1.14	12.01

Note: D.S.No. is Data Set Number

b. Double Deteriorating Bearing

For the double deteriorating bearing cases, the single faulty bearing is maintained at the fan end, the other end is introduced with a faulty bearing. Table IX and Table

Table VI. Fault II: 3 hp motor at 25% load (healthy).

Operational Parameter						Fault Indicator		
D.S.No.	RMS_V (p.u.)	RMS_I (p.u.)	Imb_V (%)	THD_V ($\times 10^{-2}$)	$(\frac{1}{SNR})_V$ ($\times 10^{-5}$)	Ind-1 ($\times 10^{-3}$)	Ind-2 (%)	Ind-3
1	1.00	0.46	0.47	2.09	2.42	0.71	1.96	37.69
2	1.00	0.46	0.47	2.09	5.13	0.79	1.92	36.38
3	1.00	0.45	0.47	1.93	16.29	1.29	1.94	35.90
4	1.00	0.45	0.47	2.12	2.35	0.69	1.90	36.07
5	1.00	0.45	0.48	2.14	0.99	0.64	1.91	36.96
6	1.00	0.45	0.47	1.98	12.05	1.08	1.90	34.55
7	1.00	0.45	0.47	1.85	18.96	1.45	1.48	25.48
8	1.00	0.44	0.48	1.77	25.81	1.76	1.85	33.33
9	1.00	0.44	0.47	2.12	1.47	0.67	1.73	31.80
10	1.00	0.44	0.47	2.12	2.02	0.69	1.64	29.39
11	1.00	0.44	0.48	2.10	3.17	0.73	1.68	30.52
Mean	1.00	0.45	0.47	2.03	8.24	0.96	1.81	33.46

Note: D.S.No. is Data Set Number

Table VII. Fault II: 3 hp motor at 0% load (single bearing fault).

Operational Parameter						Fault Indicator		
D.S.No.	RMS_V	RMS_I	Imb_V	THD_V	$(\frac{1}{SNR})_V$	Ind-1	Ind-2	Ind-3
	(p.u.)	(p.u.)	(%)	($\times 10^{-2}$)	($\times 10^{-5}$)	($\times 10^{-3}$)	(%)	
1	1.00	0.31	0.31	2.17	0.99	0.89	5.59	84.16
2	1.00	0.31	0.30	1.79	25.72	1.29	5.40	77.95
3	1.00	0.31	0.30	2.09	6.89	0.98	5.64	83.19
4	1.00	0.31	0.30	2.13	5.07	0.95	5.62	83.74
5	1.00	0.31	0.32	2.16	2.03	0.89	5.69	85.75
6	1.00	0.31	0.30	1.85	22.3	1.23	5.82	84.72
7	1.00	0.31	0.29	1.71	30.75	1.37	5.80	82.22
8	1.00	0.31	0.32	2.15	2.78	0.91	5.63	84.20
9	1.00	0.31	0.27	1.89	20.5	1.21	5.53	79.87
10	1.00	0.31	0.32	0.69	104.83	2.49	5.62	75.09
11	1.00	0.31	0.33	0.64	111.71	2.59	5.60	74.89
Mean	1.00	0.31	0.31	1.75	30.32	1.35	5.63	81.43
FIC(%)						16.97	393.13	578.27

Note: D.S.No. is Data Set Number

Table VIII. Fault II: 3 hp motor at 25% load (single bearing fault).

Operational Parameter						Fault Indicator		
D.S.No.	RMS_V	RMS_I	Imb_V	THD_V	$(\frac{1}{SNR})_V$	Ind-1	Ind-2	Ind-3
	(p.u.)	(p.u.)	(%)	($\times 10^{-2}$)	($\times 10^{-5}$)	($\times 10^{-3}$)	(%)	
1	0.99	0.46	0.31	2.12	1.17	0.68	5.09	113.12
2	0.99	0.46	0.30	2.08	4.81	0.75	5.03	109.32
3	0.99	0.45	0.30	1.96	13.27	1.09	4.85	102.36
4	0.99	0.45	0.30	2.03	9.39	0.95	5.21	110.21
5	1.00	0.45	0.41	1.89	143.78	2.81	5.36	107.32
6	0.99	0.44	0.30	2.09	4.44	0.78	5.21	108.40
7	0.99	0.44	0.29	2.14	1.29	0.66	5.35	112.26
8	0.99	0.43	0.30	2.13	2.05	0.69	5.30	108.80
9	0.99	0.43	0.30	2.12	2.96	0.72	5.39	110.49
10	0.99	0.43	0.33	2.12	2.06	0.68	5.57	112.02
Mean	0.99	0.45	0.31	2.07	18.52	0.98	5.24	109.43
FIC(%)						2.79	189.34	227.04

Note: D.S.No. is Data Set Number

X show the magnitude of the operating parameters and the fault indicators for the double deteriorating bearing cases with the corresponding values of FIC-1 at 0% and 25% load condition. The FIC-1 for double bearing fault at 0% load is 140.56% and 25% is 76.22%.

Table IX. Fault II: 3 hp motor at 0% load (double bearing fault).

Operational Parameter						Fault Indicator		
D.S.No.	RMS_V (p.u.)	RMS_I (p.u.)	Imb_V (%)	THD_V ($\times 10^{-2}$)	$(\frac{1}{SNR})_V$ ($\times 10^{-5}$)	Ind-1 ($\times 10^{-3}$)	Ind-2 (%)	Ind-3
1	1.00	0.31	0.41	2.04	101.15	3.06	3.52	51.08
2	1.00	0.31	0.41	2.20	56.06	2.27	3.45	50.41
3	1.00	0.31	0.41	2.32	64.63	2.42	3.53	53.00
4	1.00	0.31	0.42	2.24	63.95	2.41	3.58	52.91
5	1.00	0.31	0.41	2.12	138.39	3.46	3.52	51.02
6	1.00	0.31	0.40	2.15	160.52	3.72	3.51	51.07
7	1.00	0.31	0.44	2.29	118.02	3.25	3.36	49.94
8	1.00	0.31	0.42	2.30	90.81	2.86	3.50	52.80
9	1.00	0.31	0.41	1.89	48.96	2.09	3.48	49.28
10	1.00	0.31	0.42	2.22	50.34	2.11	3.36	47.56
Mean	1.00	0.31	0.41	2.18	89.28	2.77	3.48	50.91
FIC(%)						140.56	204.85	324.00

Note: D.S.No. is Data Set Number

Table X. Fault II: 3 hp motor at 25% load (double bearing fault).

Operational Parameter						Fault Indicator		
D.S.No.	RMS_V (p.u.)	RMS_I (p.u.)	Imb_V (%)	THD_V ($\times 10^{-2}$)	$(\frac{1}{SNR})_V$ ($\times 10^{-5}$)	Ind-1 ($\times 10^{-3}$)	Ind-2 (%)	Ind-3
1	1.00	0.48	0.44	2.14	16.33	1.28	2.64	50.36
2	1.00	0.47	0.44	1.94	28.13	1.81	2.30	42.62
3	1.00	0.47	0.44	2.18	14.41	1.17	2.71	52.36
4	1.00	0.46	0.44	1.55	54.43	2.78	2.56	45.30
5	1.00	0.46	0.43	1.57	55.47	2.75	2.64	46.73
6	1.00	0.46	0.44	1.64	46.91	2.49	2.64	47.12
7	1.00	0.46	0.44	2.22	9.25	0.96	2.66	49.78
8	1.00	0.46	0.44	2.00	23.16	1.55	2.33	42.53
9	1.00	0.45	0.44	2.10	17.65	1.30	2.75	49.21
10	1.00	0.45	0.44	2.02	22.84	1.50	2.78	50.39
11	1.00	0.45	0.45	2.24	8.28	0.94	2.61	47.83
Mean	1.00	0.46	0.44	1.96	26.99	1.68	2.60	47.66
FIC(%)						76.22	43.71	42.42

Note: D.S.No. is Data Set Number

3. Broken Rotor Bars - Case A

On the 800 hp, Allis Chalmers motor, the healthy baseline data is obtained using a motor operating under healthy conditions. Faulty cases are obtained by conducting experiments with half broken rotor bar, one broken rotor bar, two broken rotor bars and four broken rotor bars for different load levels. For the present research, only steady state data obtained at 0%, 50% and 100% loading levels are used.

a. Half Broken Rotor Bar

Table XI, Table XII and Table XIII show the magnitude of the operating parameters and the fault indicators for the healthy cases at 0%, 50% and 100% load condition. Table XIV, Table XV and Table XVI show the same for the faulty cases with the corresponding values of FIC-1 at 0%, 50% and 100% load condition. The FIC-1 for half broken rotor bar fault at 0% load is 51.17%, at 50% load is 86.5% and at 100% load is 5.49%. At 50% loading the increase in the fault indicator is larger as compared to the corresponding increase at 0% loading.

b. One Broken Rotor Bar

Table XVII, Table XVIII and Table XIX show the the magnitude of the operating parameters and the fault indicators for the faulty cases with the corresponding values of FIC-1 at 0%, 50% and 100% load condition. The FIC-1 for one broken rotor bar fault at 0% load is 44.13%, at 50% load is 51.05% and at 100% load is 17.99%. At 100% loading, we can observe that the FIC-1 is higher that the half broken rotor bar.

Table XI. Fault III: 800 hp motor at 0% load (healthy).

Operational Parameter						Fault Indicator		
D.S.No.	RMS_V (p.u.)	RMS_I (p.u.)	Imb_V (%)	THD_V ($\times 10^{-2}$)	$(\frac{1}{SNR})_V$ ($\times 10^{-5}$)	Ind-1 ($\times 10^{-3}$)	Ind-2 (%)	Ind-3
1	1.01	0.33	1.32	1.60	11.80	0.26	2.19	32.84
2	1.01	0.33	1.32	1.60	17.07	0.31	2.19	32.95
3	1.01	0.33	1.31	1.60	12.92	0.27	2.19	32.86
4	1.01	0.33	1.31	1.59	13.96	0.29	2.19	32.99
5	1.01	0.33	1.26	1.62	13.22	0.26	2.20	33.46
6	1.01	0.33	1.15	1.60	14.71	0.32	2.17	32.84
7	1.01	0.33	1.15	1.60	15.30	0.33	2.17	32.82
Mean	1.01	0.33	1.26	1.60	14.14	0.29	2.19	32.97

Note: D.S.No. is Data Set Number

Table XII. Fault III: 800 hp motor at 50% load (healthy).

Operational Parameter						Fault Indicator		
D.S.No.	RMS_V (p.u.)	RMS_I (p.u.)	Imb_V (%)	THD_V ($\times 10^{-2}$)	$(\frac{1}{SNR})_V$ ($\times 10^{-5}$)	Ind-1 ($\times 10^{-3}$)	Ind-2 (%)	Ind-3
1	1.01	0.54	1.23	1.18	16.56	0.19	1.56	40.16
2	1.01	0.62	1.23	1.06	21.31	0.23	1.48	41.79
3	1.01	0.61	1.22	1.06	23.11	0.25	1.49	41.37
4	1.01	0.61	1.22	1.06	22.03	0.24	1.49	41.31
5	1.01	0.61	1.22	1.07	26.36	0.28	1.49	41.35
6	1.01	0.61	1.21	1.06	24.02	0.26	1.49	41.30
7	1.01	0.64	1.11	1.04	18.44	0.21	1.46	35.22
8	1.01	0.63	1.11	1.06	21.87	0.25	1.47	28.87
Mean	1.01	0.61	1.19	1.07	21.71	0.24	1.49	38.92

Note: D.S.No. is Data Set Number

Table XIII. Fault III: 800 hp motor at 100% load (healthy).

Operational Parameter						Fault Indicator		
D.S.No.	RMS_V (p.u.)	RMS_I (p.u.)	Imb_V (%)	THD_V ($\times 10^{-2}$)	$(\frac{1}{SNR})_V$ ($\times 10^{-5}$)	Ind-1 ($\times 10^{-3}$)	Ind-2 (%)	Ind-3
1	1.00	0.91	1.17	0.97	49.25	0.53	1.20	95.80
2	1.00	0.93	1.16	0.99	38.57	0.42	1.18	56.78
3	1.00	0.96	1.16	0.99	39.63	0.40	1.15	55.35
4	1.00	0.99	1.14	1.00	39.00	0.41	1.14	67.02
5	1.00	0.99	1.13	1.01	55.82	0.58	1.14	39.68
6	1.00	1.01	1.11	1.01	51.68	0.53	1.13	37.46
7	1.00	1.01	1.11	1.03	52.64	0.54	1.13	58.43
Mean	1.00	0.97	1.14	0.99	46.65	0.49	1.15	58.65

Note: D.S.No. is Data Set Number

Table XIV. Fault III: 800 hp motor at 0% load (half broken rotor bar).

Operational Parameter						Fault Indicator		
D.S.No.	RMS_V (p.u.)	RMS_I (p.u.)	Imb_V (%)	THD_V ($\times 10^{-2}$)	$(\frac{1}{SNR})_V$ ($\times 10^{-5}$)	Ind-1 ($\times 10^{-3}$)	Ind-2 (%)	Ind-3
1	1.01	0.33	1.30	1.55	26.54	0.50	2.13	32.38
2	1.01	0.33	1.30	1.55	25.43	0.50	2.13	32.15
3	1.01	0.33	1.30	1.57	14.33	0.35	2.13	32.17
4	1.01	0.33	1.29	1.58	13.38	0.31	2.13	32.35
5	1.01	0.33	1.29	1.56	22.14	0.44	2.13	32.19
6	1.01	0.33	1.25	1.53	27.48	0.54	2.13	33.38
Mean	1.01	0.33	1.29	1.56	21.55	0.44	2.13	32.44
FIC(%)						51.17	-2.51	-1.61

Note: D.S.No. is Data Set Number

Table XV. Fault III: 800 hp motor at 50% load (half broken rotor bar).

Operational Parameter						Fault Indicator		
D.S.No.	RMS_V (p.u.)	RMS_I (p.u.)	Imb_V (%)	THD_V ($\times 10^{-2}$)	$(\frac{1}{SNR})_V$ ($\times 10^{-5}$)	Ind-1 ($\times 10^{-3}$)	Ind-2 (%)	Ind-3
1	1.01	0.63	1.21	0.98	57.87	0.57	1.60	37.27
2	1.01	0.63	1.21	0.99	50.99	0.54	1.60	42.61
3	1.01	0.63	1.21	1.02	30.50	0.33	1.60	49.02
4	1.01	0.63	1.21	0.99	29.44	0.33	1.60	47.58
5	1.01	0.61	1.09	1.02	28.39	0.33	1.63	35.23
6	1.01	0.62	1.10	0.99	43.88	0.46	1.62	41.47
7	1.01	0.62	1.10	1.01	51.40	0.56	1.62	62.08
Mean	1.01	0.62	1.16	1.00	41.78	0.45	1.61	45.04
FIC(%)						86.50	8.06	15.72

Note: D.S.No. is Data Set Number

Table XVI. Fault III: 800 hp motor at 100% load (half broken rotor bar).

Operational Parameter						Fault Indicator		
D.S.No.	RMS_V (p.u.)	RMS_I (p.u.)	Imb_V (%)	THD_V ($\times 10^{-2}$)	$(\frac{1}{SNR})_V$ ($\times 10^{-5}$)	Ind-1 ($\times 10^{-3}$)	Ind-2 (%)	Ind-3
1	1.00	0.99	1.15	0.96	46.10	0.45	1.27	83.16
2	1.00	0.98	1.15	0.95	60.61	0.61	1.28	57.48
3	1.00	0.99	1.14	0.99	45.24	0.48	1.28	51.65
Mean	1.00	0.99	1.15	0.97	50.65	0.51	1.28	64.10
FIC(%)						5.49	11.08	9.29

Note: D.S.No. is Data Set Number

Table XVII. Fault III: 800 hp motor at 0% load (one broken rotor bar).

Operational Parameter						Fault Indicator		
D.S.No.	RMS_V (p.u.)	RMS_I (p.u.)	Imb_V (%)	THD_V ($\times 10^{-2}$)	$(\frac{1}{SNR})_V$ ($\times 10^{-5}$)	Ind-1 ($\times 10^{-3}$)	Ind-2 (%)	Ind-3
1	1.01	0.33	1.19	1.55	19.60	0.45	2.12	32.08
2	1.01	0.33	1.19	1.57	22.07	0.44	2.12	32.10
3	1.01	0.33	1.18	1.59	17.83	0.37	2.12	32.39
Mean	1.01	0.33	1.18	1.57	19.83	0.42	2.12	32.19
FIC(%)						44.13	-3.00	-2.36

Note: D.S.No. is Data Set Number

Table XVIII. Fault III: 800 hp motor at 50% load (one broken rotor bar).

Operational Parameter						Fault Indicator		
D.S.No.	RMS_V (p.u.)	RMS_I (p.u.)	Imb_V (%)	THD_V ($\times 10^{-2}$)	$(\frac{1}{SNR})_V$ ($\times 10^{-5}$)	Ind-1 ($\times 10^{-3}$)	Ind-2 (%)	Ind-3
1	1.01	0.63	1.14	1.02	30.16	0.32	1.63	43.46
2	1.01	0.63	1.14	0.99	38.84	0.41	1.63	43.47
3	1.01	0.63	1.14	1.02	31.80	0.38	1.63	43.58
4	1.01	0.62	1.06	1.03	36.87	0.45	1.63	59.58
5	1.01	0.61	1.05	1.06	29.68	0.36	1.64	57.56
6	1.01	0.61	1.06	1.07	19.71	0.25	1.66	46.71
Mean	1.01	0.62	1.10	1.03	31.18	0.36	1.64	49.06
FIC(%)						51.05	9.79	26.05

Note: D.S.No. is Data Set Number

Table XIX. Fault III: 800 hp motor at 100% load (one broken rotor bar).

Operational Parameter						Fault Indicator		
D.S.No.	RMS_V (p.u.)	RMS_I (p.u.)	Imb_V (%)	THD_V ($\times 10^{-2}$)	$(\frac{1}{SNR})_V$ ($\times 10^{-5}$)	Ind-1 ($\times 10^{-3}$)	Ind-2 (%)	Ind-3
1	1.00	1.00	1.10	1.01	53.65	0.58	1.29	68.33
2	1.00	0.99	1.09	0.99	52.71	0.54	1.30	99.25
3	1.00	0.98	1.08	1.01	35.85	0.40	1.31	78.30
4	1.00	0.98	1.08	0.98	67.16	0.73	1.31	80.66
5	1.00	0.98	1.07	0.98	56.26	0.59	1.30	74.43
6	1.00	0.98	1.07	0.97	55.81	0.60	1.31	36.60
Mean	1.00	0.99	1.08	0.99	53.57	0.57	1.30	72.93
FIC(%)						17.99	13.25	24.35

Note: D.S.No. is Data Set Number

c. Two Broken Rotor Bars

Table XX, Table XXI and Table XXII show the the magnitude of the operating parameters and the fault indicators for the faulty cases with the corresponding values of FIC-1 at 0%, 50% and 100% load condition. The FIC-1 for two broken rotor bar fault at 0% load is 9.6%, at 50% load is 66.62% and at 100% load is 22.44%. At 50% and 100% loading, we can observe that the FIC-1 is higher than the one broken rotor bar case, as it is more severe fault than the previous fault. The FIC-1 is much larger when the motor is operating at 50% as compared to 0% loading conditions.

Table XX. Fault III: 800 hp motor at 0% load (two broken rotor bars).

Operational Parameter						Fault Indicator		
D.S.No.	RMS_V (p.u.)	RMS_I (p.u.)	Imb_V (%)	THD_V ($\times 10^{-2}$)	$(\frac{1}{SNR})_V$ ($\times 10^{-5}$)	Ind-1 ($\times 10^{-3}$)	Ind-2 (%)	Ind-3
1	1.01	0.33	1.15	1.60	13.44	0.31	2.11	31.83
2	1.01	0.33	1.15	1.60	13.96	0.32	2.11	31.86
3	1.01	0.33	1.15	1.60	12.59	0.30	2.11	31.96
4	1.01	0.33	1.15	1.60	11.07	0.30	2.12	31.96
5	1.01	0.33	1.15	1.59	17.68	0.37	2.12	31.99
Mean	1.01	0.33	1.15	1.60	13.75	0.32	2.11	31.92
FIC(%)						9.60	-3.35	-3.18

Note: D.S.No. is Data Set Number

Table XXI. Fault III: 800 hp motor at 50% load (two broken rotor bars).

Operational Parameter						Fault Indicator		
D.S.No.	RMS_V (p.u.)	RMS_I (p.u.)	Imb_V (%)	THD_V ($\times 10^{-2}$)	$(\frac{1}{SNR})_V$ ($\times 10^{-5}$)	Ind-1 ($\times 10^{-3}$)	Ind-2 (%)	Ind-3
1	1.01	0.64	1.10	1.01	29.33	0.36	1.56	42.70
2	1.01	0.62	1.04	1.05	23.27	0.31	1.58	50.49
3	1.01	0.61	1.04	1.03	41.19	0.51	1.58	41.74
4	1.01	0.61	1.03	1.06	35.40	0.42	1.59	20.81
Mean	1.01	0.62	1.05	1.04	32.30	0.40	1.58	38.93
FIC(%)						66.62	5.77	0.03

Note: D.S.No. is Data Set Number

Table XXII. Fault III: 800 hp motor at 100% load (two broken rotor bars).

Operational Parameter						Fault Indicator		
D.S.No.	RMS_V (p.u.)	RMS_I (p.u.)	Imb_V (%)	THD_V ($\times 10^{-2}$)	$(\frac{1}{SNR})_V$ ($\times 10^{-5}$)	Ind-1 ($\times 10^{-3}$)	Ind-2 (%)	Ind-3
1	1.00	0.99	1.05	1.00	63.61	0.71	1.24	79.99
2	1.00	1.00	1.05	1.01	43.33	0.51	1.24	62.28
3	1.00	1.00	1.05	0.99	57.12	0.64	1.24	42.73
4	1.00	0.99	1.04	1.02	45.92	0.53	1.25	50.56
Mean	1.00	1.00	1.05	1.01	52.49	0.60	1.24	58.89
FIC(%)						22.44	8.07	0.41

Note: D.S.No. is Data Set Number

d. Four Broken Rotor Bars

Table XXIII, Table XXIV and Table XXV show the the magnitude of the operating parameters and the fault indicators for the faulty cases with the corresponding values of FIC-1 at 0%, 50% and 100% load condition. The FIC-1 for four broken rotor bar fault at 0% load is 61.53%, at 50% load is 243.4% and at 100% load is 156.67%. The four broken bar case show the maximum increase in the indicator magnitude as compared to the other cases. Figure 5 shows the broken rotor bar test at 100% of rated load steady state. The top of figure show the raw current signal of healthy and faulty(4 cut rotor bars) case and the bottom shows the motor current spectra with healthy and 4 broken rotor bars. In case of 4 broken rotor bars, the sideband around the power line frequency is clearly apparent.

Table XXIII. Fault III: 800 hp motor at 0% load (four broken rotor bars).

Operational Parameter						Fault Indicator		
D.S.No.	RMS_V (p.u.)	RMS_I (p.u.)	Imb_V (%)	THD_V ($\times 10^{-2}$)	$(\frac{1}{SNR})_V$ ($\times 10^{-5}$)	Ind-1 ($\times 10^{-3}$)	Ind-2 (%)	Ind-3
1	1.01	0.33	1.14	1.58	21.30	0.50	2.04	30.39
2	1.01	0.33	1.14	1.58	21.31	0.49	2.05	30.65
3	1.01	0.33	1.14	1.59	15.98	0.42	2.06	30.89
Mean	1.01	0.33	1.14	1.582	19.53	0.47	2.05	30.64
FIC(%)						61.53	-6.26	-7.04

Note: D.S.No. is Data Set Number

In abstract, for all of the above cases, it is observed that FIC-1 is higher at 50% as compared to FIC-1 at 100%, which is counter intuitive. This is because of the

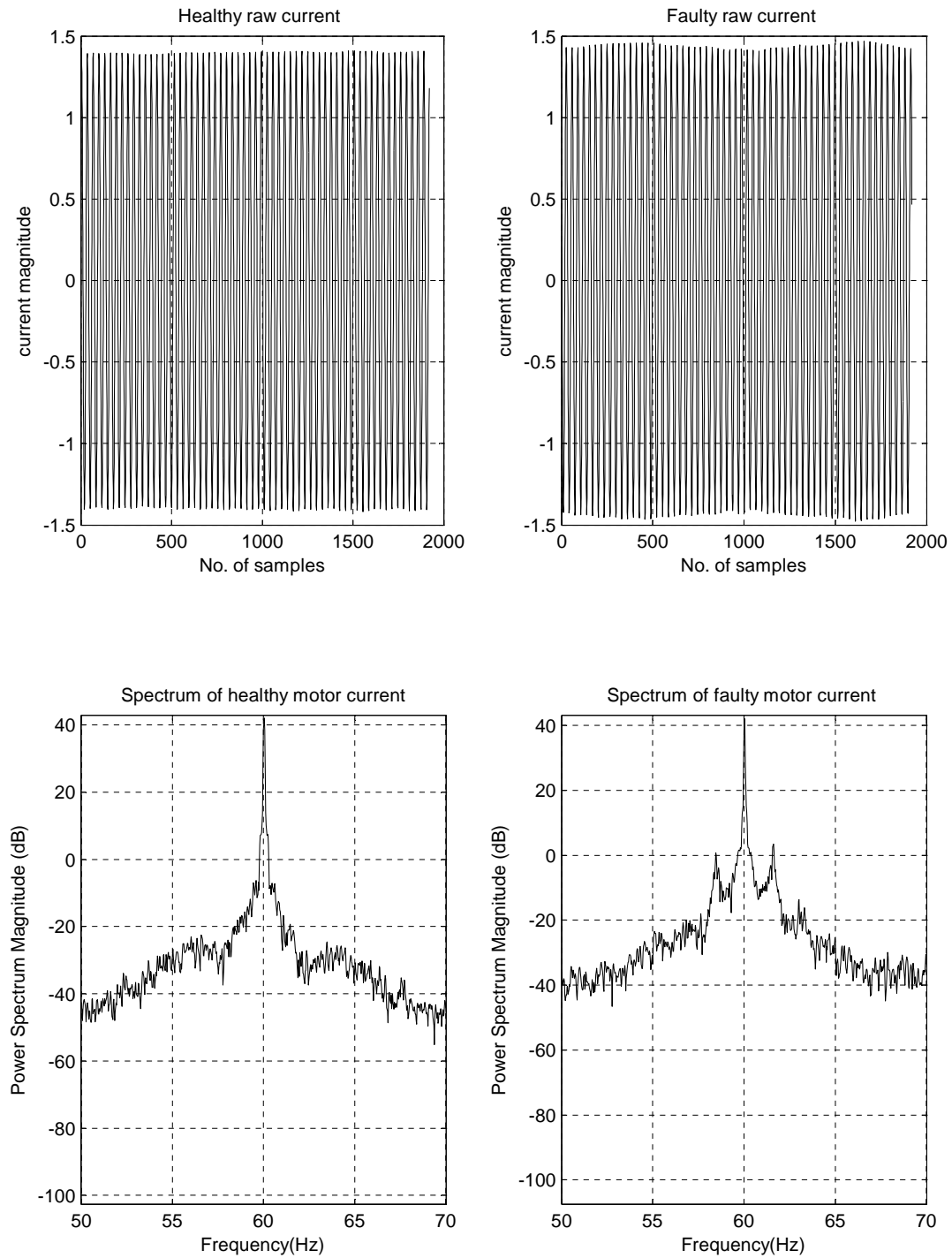


Fig. 5. Four rotor broken bar test for 800 hp motor; raw motor current (top), motor current spectra (bottom).

Table XXIV. Fault III: 800 hp motor at 50% load (four broken rotor bars).

Operational Parameter						Fault Indicator		
D.S.No.	RMS_V (p.u.)	RMS_I (p.u.)	Imb_V (%)	THD_V ($\times 10^{-2}$)	$(\frac{1}{SNR})_V$ ($\times 10^{-5}$)	Ind-1 ($\times 10^{-3}$)	Ind-2 (%)	Ind-3
1	1.01	0.64	1.03	1.07	29.65	0.82	1.56	28.70
2	1.01	0.63	1.04	1.08	47.93	0.85	1.57	39.49
3	1.01	0.62	1.04	1.08	36.02	0.94	1.58	20.62
4	1.01	0.62	1.04	1.08	35.98	0.68	1.57	15.59
Mean	1.01	0.63	1.04	1.08	37.40	0.82	1.57	26.10
FIC(%)						243.40	5.31	-32.94

Note: D.S.No. is Data Set Number

discrepancy in the raw data at 100% load. We observe that at fully loaded conditions the increase in the fault indicator magnitude from healthy to faulty ranges from 6% for the half broken rotor bar to about 160% for the four broken rotor bars.

4. Broken Rotor Bars - Case B

On the 700 hp motor, the healthy baseline data is obtained using a motor operating under healthy conditions. Table XXVI and Table XXVII show the magnitude of the operating parameters and the fault indicators for the healthy cases at 50% and 100% load condition. Faulty cases are obtained by conducting experiments with grease on winding and two rotor bars cut side by side for different load levels. In this case, steady state data obtained at 50% and 100% loading levels are used. Table XXVIII and Table XXIX show the the magnitude of the operating parameters and the fault indicators for the faulty cases with the corresponding values of FIC-1 at 50% and

Table XXV. Fault III: 800 hp motor at 100% load (four broken rotor bars).

Operational Parameter						Fault Indicator		
D.S.No.	RMS_V	RMS_I	Imb_V	THD_V	$(\frac{1}{SNR})_V$	Ind-1	Ind-2	Ind-3
	(p.u.)	(p.u.)	(%)	($\times 10^{-2}$)	($\times 10^{-5}$)	($\times 10^{-3}$)	(%)	
1	1.00	1.01	1.06	1.04	75.84	1.35	1.26	46.00
2	1.00	1.00	1.06	1.09	42.14	1.07	1.25	35.32
3	1.00	1.01	1.05	1.06	63.00	1.18	1.26	112.60
4	1.00	1.01	1.05	1.06	68.43	1.30	1.25	94.70
5	1.00	1.01	1.04	1.04	74.24	1.33	1.26	66.13
Mean	1.00	1.01	1.05	1.06	64.73	1.25	1.26	70.95
FIC(%)						156.67	9.16	20.98

Note: D.S.No. is Data Set Number

100% load condition. The FIC-1 for two broken rotor bar fault at 50% load is 3.33% and at 100% load is 8.13%.

Table XXVI. Fault III: 700 hp motor at 50% load (healthy).

Operational Parameter						Fault Indicator		
D.S.No.	RMS_V (p.u.)	RMS_I (p.u.)	Imb_V (%)	THD_V ($\times 10^{-2}$)	$(\frac{1}{SNR})_V$ ($\times 10^{-5}$)	Ind-1 ($\times 10^{-3}$)	Ind-2 (%)	Ind-3
1	1.03	0.61	0.19	1.19	9.95	2.52	1.16	123.93
2	1.03	0.61	0.13	1.56	10.12	2.58	1.46	231.05
Mean	1.03	0.61	0.16	1.38	10.03	2.55	1.31	177.49

Note: D.S.No. is Data Set Number

5. Air-Gap Eccentricity - Case A

Air-gap eccentricity - Case A tests are performed considering two different cases on 800 hp, Allis Chalmers motor. The first case is a condition of moving the rotating center 25% upward at the inboard end, and the other case is a condition of moving the rotating center 20% downward at the outboard end and 26% right at the inboard end.

a. Air-gap Eccentricity - Case A1

The data from experiments conducted with this setting, is compared to data from healthy operating condition of the same motor. In this case steady state data only at 50% and 100% loading condition is available. Table XXX and Table XXXI show the the magnitude of the operating parameters and the fault indicators for the present case with the corresponding values of FIC-1 at 50% and 100% load condition. At

Table XXVII. Fault III: 700 hp motor at 100% load (healthy).

Operational Parameter						Fault Indicator		
D.S.No.	RMS_V (p.u.)	RMS_I (p.u.)	Imb_V (%)	THD_V ($\times 10^{-2}$)	$(\frac{1}{SNR})_V$ ($\times 10^{-5}$)	Ind-1 ($\times 10^{-3}$)	Ind-2 (%)	Ind-3
1	0.99	1.01	0.22	1.18	10.98	0.95	0.61	145.82
2	1.00	1.00	0.22	1.28	9.01	0.98	0.66	217.91
3	0.99	1.01	0.22	1.16	7.12	0.94	0.62	255.05
4	1.01	0.99	0.22	1.72	9.22	0.96	0.68	265.73
Mean	1.00	1.00	0.22	1.34	9.08	0.95	0.65	221.13

Note: D.S.No. is Data Set Number

100% loading conditions, the FIC-1 is non-indicative of the fault being present in the system. The FIC-1 at 50% loading is 29.12% which is higher as compared to those obtained at 100% loading. As in this type of fault the rotor is present at an offset from the rotating center, it produces imbalance in the current signal which can be seen in the FIC for negative-sequence. This type of fault can be said as a electro-mechanical fault.

b. Air-gap Eccentricity - Case A2

Table XXXII, Table XXXIII and Table XXXIV show the the magnitude of the operating parameters and the fault indicators for the faulty cases with the corresponding values of FIC-1 at 0%, 50% and 100% load condition. The FIC-1 for the present case at 0% load is 258.56%, at 50% load is 89.22% and at 100% load is 37.55%. We can observe that the FIC-1 for the present case is higher than the previous case, as it is more severe fault than the previous fault. It is also observe that at high levels of

Table XXVIII. Fault III: 700 hp motor at 50% load (grease on winding and two broken rotor bars).

Operational Parameter						Fault Indicator		
D.S.No.	RMS_V	RMS_I	Imb_V	THD_V	$(\frac{1}{SNR})_V$	Ind-1	Ind-2	Ind-3
	(p.u.)	(p.u.)	(%)	($\times 10^{-2}$)	($\times 10^{-5}$)	($\times 10^{-3}$)	(%)	
1	1.03	0.61	0.06	2.07	12.98	2.79	1.71	170.20
2	1.02	0.60	0.07	1.67	9.02	2.65	1.68	204.43
3	1.02	0.60	0.07	1.65	5.80	2.57	1.64	309.46
4	1.02	0.60	0.07	1.58	6.02	2.60	1.63	360.44
5	1.02	0.60	0.07	1.68	5.70	2.59	1.62	420.66
6	1.02	0.60	0.07	1.63	6.51	2.62	1.57	398.12
Mean	1.02	0.60	0.07	1.71	7.67	2.64	1.64	310.55
FIC(%)						3.33	25.28	74.97

Note: D.S.No. is Data Set Number

Table XXIX. Fault III: 700 hp motor at 100% load (grease on winding and two broken rotor bars).

Operational Parameter						Fault Indicator		
D.S.No.	RMS_V	RMS_I	Imb_V	THD_V	$(\frac{1}{SNR})_V$	Ind-1	Ind-2	Ind-3
	(p.u.)	(p.u.)	(%)	($\times 10^{-2}$)	($\times 10^{-5}$)	($\times 10^{-3}$)	(%)	
1	1.00	1.01	0.21	1.38	6.29	0.99	0.69	468.82
2	1.00	0.99	0.22	1.31	8.52	1.01	0.71	612.85
3	1.00	0.97	0.21	1.31	7.23	1.03	0.73	120.04
4	1.00	0.96	0.21	1.31	9.00	1.09	0.78	99.62
5	1.00	0.96	0.21	1.47	7.75	1.06	0.78	129.90
6	1.01	0.98	0.20	1.59	8.86	1.01	0.77	202.05
7	1.00	0.97	0.20	1.31	7.34	1.10	0.75	104.30
8	1.00	1.00	0.20	1.31	6.70	0.99	0.78	183.73
9	1.00	0.99	0.22	1.30	9.47	1.01	0.73	310.06
Mean	1.00	0.98	0.21	1.37	7.91	1.03	0.75	247.93
FIC(%)						8.13	15.57	12.12

Note: D.S.No. is Data Set Number

Table XXX. Fault IV: 800 hp motor at 50% load (air-gap eccentricity - case A1).

Operational Parameter						Fault Indicator		
D.S.No.	RMS _V	RMS _I	Imb _V	THD _V	$(\frac{1}{SNR})_V$	Ind-1	Ind-2	Ind-3
	(p.u.)	(p.u.)	(%)	($\times 10^{-2}$)	($\times 10^{-5}$)	($\times 10^{-3}$)	(%)	
1	1.01	0.59	1.20	1.62	12.15	0.28	24.56	361.12
2	1.01	0.59	1.20	1.61	17.63	0.35	24.56	360.20
3	1.01	0.59	1.20	1.61	12.66	0.29	24.56	361.87
4	1.01	0.59	1.20	1.60	17.76	0.37	24.56	360.13
5	1.01	0.59	1.20	1.61	12.16	0.30	24.56	359.63
6	1.01	0.56	1.14	1.05	25.06	0.29	23.64	316.28
7	1.01	0.56	1.14	1.06	26.40	0.29	23.65	316.59
Mean	1.01	0.58	1.18	1.45E-02	17.69	0.31	24.30	347.97
FIC(%)						29.21	1529.50	794.06

Note: D.S.No. is Data Set Number

Table XXXI. Fault IV: 800 hp motor at 100% load (air-gap eccentricity - case A1).

Operational Parameter						Fault Indicator		
D.S.No.	RMS_V	RMS_I	Imb_V	THD_V	$(\frac{1}{SNR})_V$	Ind-1	Ind-2	Ind-3
	(p.u.)	(p.u.)	(%)	($\times 10^{-2}$)	($\times 10^{-5}$)	($\times 10^{-3}$)	(%)	
1	1.00	0.85	1.11	1.02	27.75	0.32	23.24	488.90
2	1.00	0.88	1.10	1.04	33.01	0.36	23.20	478.92
3	1.00	0.89	1.10	1.02	43.805	0.45	23.20	475.00
4	1.00	0.89	1.09	1.03	52.33	0.54	23.20	515.00
5	1.00	0.89	1.09	1.03	44.38	0.44	23.20	453.28
6	1.00	0.89	1.09	1.02	36.12	0.38	23.20	469.80
7	1.00	0.88	1.09	1.02	48.39	0.49	23.21	464.42
Mean	1.00	0.88	1.10	1.02	40.83	0.43	23.21	477.90
FIC(%)						-12.36	1915.60	714.90

Note: D.S.No. is Data Set Number

loading, the fault signatures are weak. However, at lower levels of loading, we can see a significant increase in the fault indicator. Figure 6 show the air-gap eccentricity test at 100% of rated load steady state. The top of figure shows the raw current signal of healthy and faulty(air-gap eccentricity) case and the bottom shows the motor current spectra with healthy and eccentric air-gap. The distinction of the air-gap eccentricity spectrum from the motor current spectrum is very difficult, so by simply observing the motor current spectrum, the detectability of the air-gap eccentricity faults is very unlikely.

Table XXXII. Fault IV: 800 hp motor at 0% load (air-gap eccentricity - case A2).

Operational Parameter						Fault Indicator		
D.S.No.	RMS_V (p.u.)	RMS_I (p.u.)	Imb_V (%)	THD_V ($\times 10^{-2}$)	$(\frac{1}{SNR})_V$ ($\times 10^{-5}$)	Ind-1 ($\times 10^{-3}$)	Ind-2 (%)	Ind-3
1	1.01	0.06	1.18	1.60	16.94	1.00	24.89	36.28
2	1.01	0.06	1.18	1.60	29.28	1.13	24.90	36.00
3	1.01	0.06	1.18	1.60	15.16	0.99	24.89	36.20
Mean	1.01	0.06	1.18	1.60	20.46	1.04	24.89	36.16
FIC(%)						258.56	1038.70	9.69

Note: D.S.No. is Data Set Number

6. Air-Gap Eccentricity - Case B

Air-gap eccentricity - Case B test is performed on 700 hp motor. The data from experiments conducted is compared to data from healthy operating condition of the same motor. Table XXXV and Table XXXVI show the magnitude of the operating parameters and the fault indicators for the faulty cases with the corresponding values

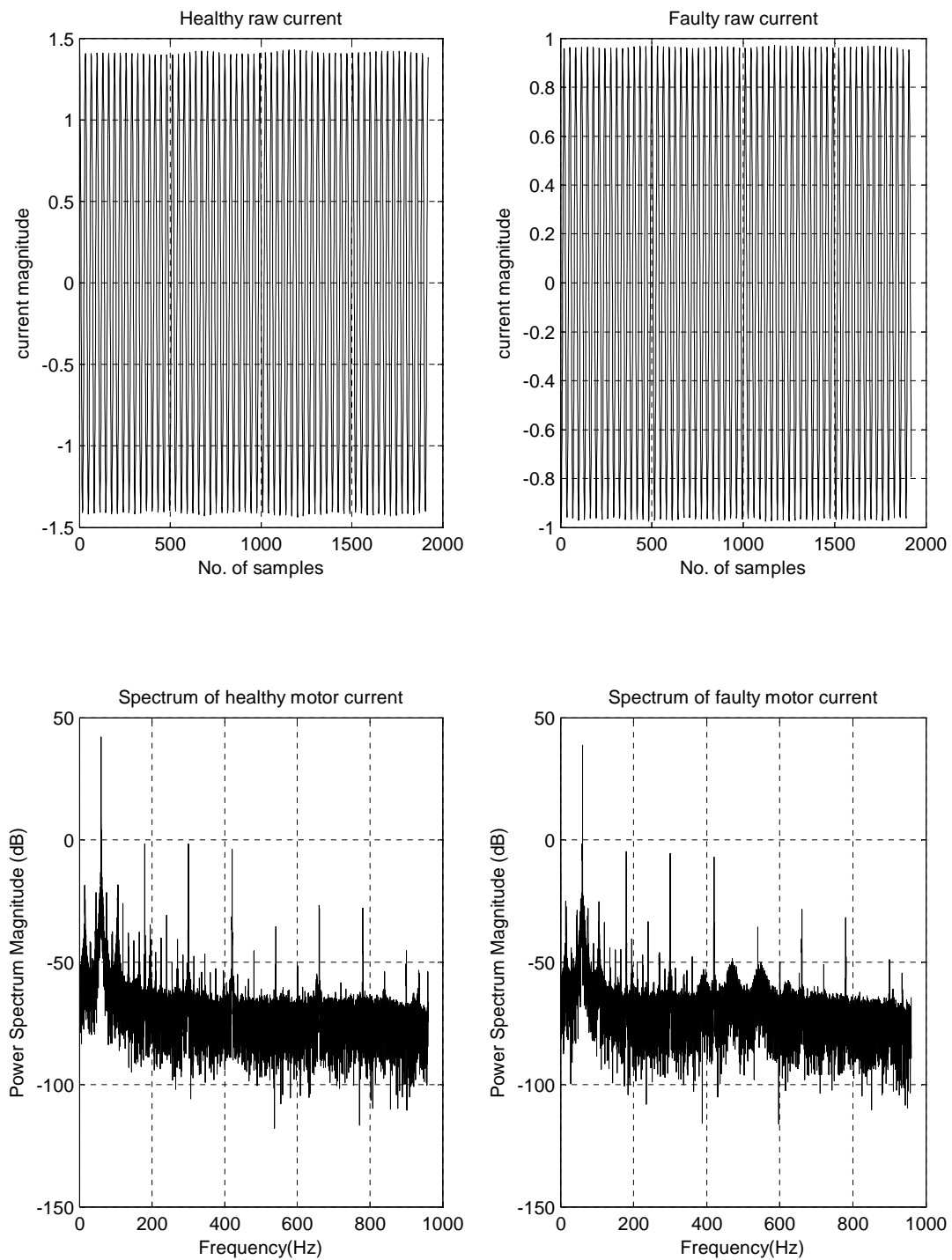


Fig. 6. Air-gap eccentricity test for 800 hp motor; raw motor current (top), motor current spectra (bottom).

Table XXXIII. Fault IV: 800 hp motor at 50% load (air-gap eccentricity - case A2).

Operational Parameter						Fault Indicator		
D.S.No.	RMS _V	RMS _I	Imb _V	THD _V	$(\frac{1}{SNR})_V$	Ind-1	Ind-2	Ind-3
	(p.u.)	(p.u.)	(%)	($\times 10^{-2}$)	($\times 10^{-5}$)	($\times 10^{-3}$)	(%)	
1	1.01	0.47	1.16	1.20	43.40	0.48	23.86	271.99
2	1.01	0.57	1.15	1.04	45.17	0.46	23.58	319.78
3	1.01	0.56	1.08	1.06	40.32	0.43	23.60	320.08
Mean	1.01	0.53	1.13	1.10	42.96	0.45	23.68	303.95
FIC(%)						89.22	1488.00	680.95

Note: D.S.No. is Data Set Number

Table XXXIV. Fault IV: 800 hp motor at 100% load (air-gap eccentricity - case A2).

Operational Parameter						Fault Indicator		
D.S.No.	RMS _V	RMS _I	Imb _V	THD _V	$(\frac{1}{SNR})_V$	Ind-1	Ind-2	Ind-3
	(p.u.)	(p.u.)	(%)	($\times 10^{-2}$)	($\times 10^{-5}$)	($\times 10^{-3}$)	(%)	
1	1.00	0.88	1.11	1.03	50.97	0.54	23.15	451.66
2	1.00	0.88	1.10	1.01	68.93	0.70	23.15	440.67
3	1.00	0.88	1.10	1.02	75.71	0.76	23.16	478.82
Mean	1.00	0.88	1.10	1.02	65.20	0.67	23.15	457.05
FIC(%)						37.55	1910.70	679.34

Note: D.S.No. is Data Set Number

of FIC-1 at 50% and 100% load condition. The FIC-1 for air-gap eccentricity - Case B fault at 50% load is 17.3% and at 100% load is 11.09%.

Table XXXV. Fault IV: 700 hp motor at 50% load (air-gap eccentricity - case B).

Operational Parameter						Fault Indicator		
D.S.No.	RMS_V (p.u.)	RMS_I (p.u.)	Imb_V (%)	THD_V ($\times 10^{-2}$)	$(\frac{1}{SNR})_V$ ($\times 10^{-2}$)	Ind-1 ($\times 10^{-3}$)	Ind-2 (%)	Ind-3
1	0.02	0.58	0.21	3.53	1.59	2.93	1.82	65.36
2	0.02	0.58	0.27	2.95	1.60	2.89	1.70	236.43
3	0.02	0.58	0.28	2.85	1.62	2.96	1.67	362.98
4	0.02	0.58	0.23	3.41	1.59	2.96	1.77	151.69
5	0.02	0.58	0.25	2.78	1.63	3.08	1.73	241.24
6	0.02	0.57	0.27	2.58	1.62	3.13	1.67	84.58
Mean	0.02	0.58	0.25	3.02	1.612	2.99	1.73	190.38
FIC(%)						17.30	31.71	7.26

Note: D.S.No. is Data Set Number

7. Mechanical Imbalance

A 500 hp, General Electric motor is used to conduct experiments for this fault. The healthy baseline is obtained from healthy condition of motor and is compared with a mechanically unbalanced condition of the motor (unbalanced rotor).

Table XXXVII, Table XXXVIII and Table XXXIX show the magnitude of the operating parameters and the fault indicators for the healthy cases at 0%, 50% and 100% load condition. Table XL, Table XLI and Table XLII show the same for the faulty cases with the corresponding values of FIC-1 at 0%, 50% and 100% load con-

Table XXXVI. Fault IV: 700 hp motor at 100% load (air-gap eccentricity - case B).

Operational Parameter						Fault Indicator		
D.S.No.	RMS_V (p.u.)	RMS_I (p.u.)	Imb_V (%)	THD_V ($\times 10^{-2}$)	$(\frac{1}{SNR})_V$ ($\times 10^{-2}$)	Ind-1 ($\times 10^{-3}$)	Ind-2 (%)	Ind-3
1	0.02	0.97	0.36	2.30	1.63	1.11	1.60	153.00
2	0.02	0.97	0.42	2.06	1.65	1.06	1.14	339.76
3	0.02	0.98	0.51	1.76	1.64	1.00	0.84	460.74
Mean	0.02	0.97	0.43	2.04	1.64	1.06	1.19	317.83
FIC(%)						11.09	84.51	43.73

Note: D.S.No. is Data Set Number

dition. At 0% loading conditions, indicator is non indicative of the fault present. At 50% and 100% loading condition, it is observed that the increase in the value of fault indicator as compared to healthy baseline is 13.04% and 41.17% respectively. At 100% loading, the fault signatures are more indicative of the fault present in the system.

D. Detection of Electrical Faults

For detecting the electrical faults the degree of three-phase current imbalance and the negative-sequence component of the current signal are primarily used as a fault indicator to indicate electrical fault in the motor. The effectiveness of the indicator-2 and indicator-3 developed are examined by calculating the Fault Indicator-2 Change, (FIC-2) for current imbalance and Fault Indicator-3 Change (FIC-3) for negative sequence.

Table XXXVII. Fault V: 500 hp motor at 0% load (healthy).

Operational Parameter						Fault Indicator		
D.S.No.	RMS_V (p.u.)	RMS_I (p.u.)	Imb_V (%)	THD_V ($\times 10^{-2}$)	$(\frac{1}{SNR})_V$ ($\times 10^{-5}$)	Ind-1 ($\times 10^{-3}$)	Ind-2 (%)	Ind-3
1	1.01	0.24	1.54	1.38	30.71	1.25	3.96	42.43
2	1.01	0.24	1.54	1.37	49.91	1.45	3.97	42.93
3	1.01	0.24	1.53	1.36	41.34	1.45	3.95	42.64
4	1.01	0.24	1.53	1.39	30.65	1.19	3.96	42.58
5	1.01	0.24	1.53	1.37	34.25	1.31	3.97	42.36
Mean	1.01	0.24	1.53	1.37	37.37	1.33	3.96	42.59

Note: D.S.No. is Data Set Number

Table XXXVIII. Fault V: 500 hp motor at 50% load (healthy).

Operational Parameter						Fault Indicator		
D.S.No.	RMS_V (p.u.)	RMS_I (p.u.)	Imb_V (%)	THD_V ($\times 10^{-2}$)	$(\frac{1}{SNR})_V$ ($\times 10^{-5}$)	Ind-1 ($\times 10^{-3}$)	Ind-2 (%)	Ind-3
1	1.00	0.60	1.46	0.99	30.33	0.41	1.93	52.72
2	1.00	0.61	1.46	0.99	30.83	0.41	1.92	52.62
3	1.00	0.61	1.42	0.99	30.57	0.43	1.93	52.82
4	1.00	0.61	1.42	0.97	36.16	0.46	1.93	52.96
5	1.00	0.61	1.42	0.99	38.43	0.50	1.92	53.79
Mean	1.00	0.61	1.43	0.99	33.26	0.44	1.92	52.98

Note: D.S.No. is Data Set Number

Table XXXIX. Fault V: 500 hp motor at 100% load (healthy).

Operational Parameter						Fault Indicator		
D.S.No.	RMS _V (p.u.)	RMS _I (p.u.)	Imb _V (%)	THD _V ($\times 10^{-2}$)	$(\frac{1}{SNR})_V$ ($\times 10^{-5}$)	Ind-1 ($\times 10^{-3}$)	Ind-2 (%)	Ind-3
1	1.00	1.04	1.40	0.79	59.85	0.61	1.35	62.16
2	1.00	0.99	1.40	0.75	90.91	0.93	1.39	60.17
3	1.00	1.00	1.40	0.79	78.72	0.83	1.37	61.39
4	1.00	1.00	1.40	0.79	42.06	0.44	1.38	61.10
Mean	1.00	1.01	1.40	0.78	67.88	0.70	1.37	61.21

Note: D.S.No. is Data Set Number

Table XL. Fault V: 500 hp motor at 0% load (mechanical imbalance).

Operational Parameter						Fault Indicator		
D.S.No.	RMS _V (p.u.)	RMS _I (p.u.)	Imb _V (%)	THD _V ($\times 10^{-2}$)	$(\frac{1}{SNR})_V$ ($\times 10^{-5}$)	Ind-1 ($\times 10^{-3}$)	Ind-2 (%)	Ind-3
1	1.00	0.24	1.50	1.38	38.68	1.30	4.04	42.56
2	1.00	0.24	1.50	1.37	28.28	1.25	4.04	42.32
3	1.00	0.24	1.50	1.42	32.27	1.07	4.04	42.49
4	1.00	0.24	1.50	1.40	24.75	1.11	4.03	42.46
5	1.00	0.24	1.50	1.38	39.46	1.33	4.03	42.19
Mean	1.00	0.24	1.50	1.39	32.69	1.21	4.04	42.40
FIC(%)						-8.81	1.86	-0.43

Note: D.S.No. is Data Set Number

Table XLI. Fault V: 500 hp motor at 50% load (mechanical imbalance).

Operational Parameter						Fault Indicator		
D.S.No.	RMS_V (p.u.)	RMS_I (p.u.)	Imb_V (%)	THD_V ($\times 10^{-2}$)	$(\frac{1}{SNR})_V$ ($\times 10^{-5}$)	Ind-1 ($\times 10^{-3}$)	Ind-2 (%)	Ind-3
1	1.00	0.62	1.45	0.98	38.49	0.49	1.91	53.11
2	1.00	0.56	1.46	1.05	28.86	0.42	2.02	52.14
3	1.00	0.52	1.46	1.08	38.89	0.59	2.13	51.22
Mean	1.00	0.57	1.46	1.04	35.42	0.50	2.02	52.16
FIC(%)						13.04	4.92	-1.56

Note: D.S.No. is Data Set Number

Table XLII. Fault V: 500 hp motor at 100% load (mechanical imbalance).

Operational Parameter						Fault Indicator		
D.S.No.	RMS_V (p.u.)	RMS_I (p.u.)	Imb_V (%)	THD_V ($\times 10^{-2}$)	$(\frac{1}{SNR})_V$ ($\times 10^{-5}$)	Ind-1 ($\times 10^{-3}$)	Ind-2 (%)	Ind-3
1	1.00	0.98	1.40	0.80	106.67	1.04	1.39	60.96
2	1.00	0.94	1.40	0.79	92.25	0.95	1.43	60.18
Mean	1.00	0.96	1.40	0.80	99.46	0.99	1.41	60.57
FIC(%)						41.17	2.65	-1.03

Note: D.S.No. is Data Set Number

1. Stator Imbalance - Case A

Experiments are performed bridging the stator winding with resistors to implement stator imbalance. On the 150 hp motor, two different tests are conducted. The first case is resistance of 0.012 ohms in series with phase A, and second case is resistance of 0.633 ohms in series with phase A.

a. Stator Imbalance - Case A1

The healthy baseline is obtained from healthy condition of 150 hp motor and is compared with a stator imbalanced condition of the motor. Table XLIII and Table XLIV show the magnitude of the operating parameters and the fault indicators for the healthy cases at 50% and 100% load condition. Table XLV and Table XLVI show the same for the faulty cases with the corresponding values of FIC-2 and FIC-3 at 50% and 100% load condition. For the present case, the FIC-2 at 50% load is 64.81% and at 100% load is 25.65% and the FIC-3 at 50% load is 29.79% and at 100% load is 31.83%.

Table XLIII. Fault I: 150 hp motor at 50% load (healthy).

Operational Parameter						Fault Indicator		
D.S.No.	RMS_V (p.u.)	RMS_I (p.u.)	Imb_V (%)	THD_V ($\times 10^{-2}$)	$(\frac{1}{SNR})_V$ ($\times 10^{-1}$)	Ind-1 ($\times 10^{-1}$)	Ind-2 (%)	Ind-3
1	0.96	0.51	2.97	7.81	1.65	1.69	1.78	37.29
2	0.97	0.51	2.91	7.27	2.77	2.78	1.68	37.39
3	0.96	0.51	2.67	6.40	1.69	1.70	1.29	16.33
Mean	0.96	0.51	2.85	7.16	2.03	2.06	1.58	30.34

Note: D.S.No. is Data Set Number

Table XLIV. Fault I: 150 hp motor at 100% load (healthy).

Operational Parameter						Fault Indicator		
D.S.No.	RMS_V (p.u.)	RMS_I (p.u.)	Imb_V (%)	THD_V ($\times 10^{-2}$)	$(\frac{1}{SNR})_V$ ($\times 10^{-1}$)	Ind-1 ($\times 10^{-1}$)	Ind-2 (%)	Ind-3
1	1.00	1.07	2.81	7.44	2.10	2.04	1.52	30.13
2	1.00	1.06	2.88	8.38	2.67	2.62	1.73	37.26
3	1.00	1.02	2.88	7.91	3.43	3.43	1.62	21.78
4	1.00	1.03	2.82	7.48	2.19	2.16	1.53	25.16
5	1.00	1.02	2.81	7.94	3.97	3.89	1.45	22.22
6	1.00	1.00	2.82	7.80	1.62	1.59	1.47	25.68
Mean	1.00	1.03	2.84	7.82	2.66	2.62	1.55	27.04

Note: D.S.No. is Data Set Number

b. Stator Imbalance - Case A2

Table XLVII and Table XLVIII show the magnitude of the operating parameters and the fault indicators for the faulty cases with the corresponding values of FIC-2 and FIC-3 at 50% and 100% load condition. In this case, the FIC-2 at 50% load is 2172.7% and at 100% load is 1971.1% and the FIC-3 at 50% load is 1108.4% and at 100% load is 1899.9%. The increase in the value of fault indicators as compared to healthy baseline in this case is much higher than the case A1, as it is more severe fault than the previous fault.

Table XLV. Fault I: 150 hp motor at 50% load (stator imbalance - case A1).

Operational Parameter						Fault Indicator		
D.S.No.	RMS_V (p.u.)	RMS_I (p.u.)	Imb_V (%)	THD_V ($\times 10^{-2}$)	$(\frac{1}{SNR})_V$ ($\times 10^{-1}$)	Ind-1 ($\times 10^{-1}$)	Ind-2 (%)	Ind-3
1	1.02	0.54	3.12	5.87	3.58	3.60	2.61	34.99
2	1.02	0.54	3.11	5.14	2.68	2.73	2.51	32.61
3	1.02	0.54	3.12	4.79	2.96	2.97	2.63	42.32
4	1.02	0.54	3.12	4.84	1.56	1.58	2.60	40.85
5	1.02	0.53	3.16	6.02	3.24	3.25	2.84	48.13
6	1.02	0.51	3.12	4.81	2.15	2.19	2.46	37.35
Mean	1.02	0.53	3.13	5.25	2.70	2.72	2.61	39.37
FIC(%)						32.31	64.81	29.79

Note: D.S.No. is Data Set Number

Table XLVI. Fault I: 150 hp motor at 100% load (stator imbalance - case A1).

Operational Parameter						Fault Indicator		
D.S.No.	RMS_V (p.u.)	RMS_I (p.u.)	Imb_V (%)	THD_V ($\times 10^{-2}$)	$(\frac{1}{SNR})_V$ ($\times 10^{-1}$)	Ind-1 ($\times 10^{-1}$)	Ind-2 (%)	Ind-3
1	1.01	1.05	3.11	7.04	3.44	3.43	1.93	36.55
2	1.01	1.05	3.11	7.86	5.01	4.94	2.01	40.50
3	1.01	1.04	3.09	7.34	5.13	5.08	1.93	33.97
4	1.01	1.02	3.09	7.55	4.25	4.26	1.94	31.55
Mean	1.01	1.04	3.10	7.45	4.46	4.43	1.95	35.64
FIC(%)						68.86	25.65	31.83

Note: D.S.No. is Data Set Number

2. Stator Imbalance - Case B

Experiments for stator imbalance - Case B are performed on 800 hp Westinghouse motor. The healthy baseline data is obtained using the 800 hp motor operating under healthy conditions. Faulty cases are obtained by conducting experiments with 2.7Ω resistor on A phase. Table XLIX, Table L and Table LI show the magnitude of the operating parameters and the fault indicators for the healthy cases at 0%, 50% and 100% load condition. Table LII, Table LIII and Table LIV show the same for the faulty cases with the corresponding values of FIC-2 and FIC-3 at 0%, 50% and 100% load condition. In this case, the FIC-2 at 0% load is 148.41%, at 50% load is 342.45% and at 100% load is 574.65% and the FIC-3 at 0% load is 468.11%, at 50% load is 652.48% and at 100% load is 816.29%. As there is imbalance in the power supply, a huge increase in the value of the fault indicator as compared to the healthy baseline

Table XLVII. Fault I: 150 hp motor at 50% load (stator imbalance - case A2).

Operational Parameter						Fault Indicator		
D.S.No.	RMS _V	RMS _I	Imb _V	THD _V	$(\frac{1}{SNR})_V$	Ind-1	Ind-2	Ind-3
	(p.u.)	(p.u.)	(%)	($\times 10^{-2}$)	($\times 10^{-1}$)	($\times 10^{-1}$)	(%)	
1	0.97	0.37	9.74	4.37	2.63	2.83	30.87	401.27
2	0.97	0.36	9.60	4.96	2.51	2.68	30.82	321.44
3	0.97	0.36	9.54	6.09	4.84	5.02	30.74	369.41
4	0.97	0.36	9.55	5.75	5.85	6.08	30.77	198.32
5	0.97	0.36	9.59	5.38	4.78	4.99	30.66	195.05
6	0.97	0.36	9.67	5.88	4.14	4.33	30.78	253.30
Mean	0.97	0.36	9.61	5.40	4.12	4.32	30.77	289.80
FIC(%)						111.52	2172.70	1108.40

Note: D.S.No. is Data Set Number

Table XLVIII. Fault I: 150 hp motor at 100% load (stator imbalance - case A2).

Operational Parameter						Fault Indicator		
D.S.No.	RMS_V (p.u.)	RMS_I (p.u.)	Imb_V (%)	THD_V ($\times 10^{-2}$)	$(\frac{1}{SNR})_V$ ($\times 10^{-1}$)	Ind-1 ($\times 10^{-1}$)	Ind-2 (%)	Ind-3
1	0.94	0.66	15.50	7.71	6.92	6.90	32.17	646.16
2	0.95	0.63	14.96	8.58	8.56	8.64	32.16	435.28
3	0.95	0.62	14.89	7.44	7.52	7.63	32.26	493.65
Mean	0.94	0.64	15.23	8.14	7.74	7.77	32.17	540.72
FIC(%)						196.51	1971.10	1899.90

Note: D.S.No. is Data Set Number

is seen.

3. Stator Winding Shorts

Stator winding shorts tests are performed considering two different cases on 500 hp, General Electric motor. Case 1 represents the turn-to-turn short bridged with 2.7Ω , resulting in the shorted current of 4.2 A flowing on phase C winding. Case 2 represents the turn-to-turn short bridged with 1.35Ω , resulting in the shorted current of 8.3 A flowing on phase C winding.

a. Stator Winding Shorts - Case 1

The data from experiments conducted with this setting, is compared to data from healthy operating condition of the same motor. Table LV, Table LVI and Table LVII show the the magnitude of the operating parameters and the fault indicators for the

Table XLIX. Fault I: 800 hp motor at 0% load (healthy).

Operational Parameter						Fault Indicator		
D.S.No.	RMS_V (p.u.)	RMS_I (p.u.)	Imb_V (%)	THD_V ($\times 10^{-2}$)	$(\frac{1}{SNR})_V$ ($\times 10^{-5}$)	Ind-1 ($\times 10^{-3}$)	Ind-2 (%)	Ind-3
1	1.01	0.20	9.16	1.65	34.49	3.70	4.91	41.71
2	1.01	0.20	9.15	1.66	41.03	3.70	4.92	41.93
3	1.01	0.20	9.16	1.65	40.23	3.75	4.93	42.09
4	1.01	0.20	9.14	1.67	48.72	3.75	4.93	42.13
5	1.01	0.20	9.15	1.67	36.84	3.61	4.93	42.20
6	1.01	0.20	9.14	1.69	31.16	3.41	4.92	42.02
7	1.01	0.20	8.55	1.71	52.85	3.29	4.89	42.41
8	1.01	0.20	8.58	1.69	36.41	3.27	4.89	42.28
9	1.01	0.20	8.61	1.68	48.34	3.48	4.88	42.29
Mean	1.01	0.20	8.96	1.67	41.12	3.55	4.91	42.12

Note: D.S.No. is Data Set Number

Table L. Fault I: 800 hp motor at 50% load (healthy).

Operational Parameter						Fault Indicator		
D.S.No.	RMS_V (p.u.)	RMS_I (p.u.)	Imb_V (%)	THD_V ($\times 10^{-2}$)	$(\frac{1}{SNR})_V$ ($\times 10^{-5}$)	Ind-1 ($\times 10^{-3}$)	Ind-2 (%)	Ind-3
1	1.00	0.49	9.03	1.49	200.56	2.25	2.04	45.33
2	1.00	0.55	9.01	1.45	146.44	1.69	1.85	44.25
3	1.00	0.51	9.00	1.53	150.73	1.84	1.97	46.05
4	1.00	0.46	8.99	1.54	69.79	1.10	2.13	44.75
5	1.00	0.46	8.99	1.51	62.06	1.17	2.14	44.89
Mean	1.00	0.49	9.01	1.50	125.9	1.61	2.03	45.05

Note: D.S.No. is Data Set Number

present case with the corresponding values of FIC-2 and FIC-3 at 0%, 50% and 100% load condition. The FIC-2 at 0% load is 0.44%, at 50% load is 15.29% and at 100% load is 14.09% and the FIC-3 at 0% load is 3.5%, at 50% load is 8.92% and at 100% load is 15.65%. At 0% load both the FIC are non indicative of the fault present in the system. It is observe that, the FIC increases with the increase in loading condition.

b. Stator Winding Shorts - Case 2

Table LVIII, Table LIX and Table LX show the magnitude of the operating parameters and the fault indicators for the case 2 with the corresponding values of FIC-2 and FIC-3 at 0%, 50% and 100% load condition. The FIC-2 at 0% load is 1.4%, at 50% load is 15.21% and at 100% load is 14% and the FIC-3 at 0% load is 4.23%, at 50% load is 13% and at 100% load is 21%. In this case, the same trend of increase in the FIC is observed with increase in the loading condition. In case 2, the increase in the

Table LI. Fault I: 800 hp motor at 100% load (healthy).

Operational Parameter						Fault Indicator		
D.S.No.	RMS_V (p.u.)	RMS_I (p.u.)	Imb_V (%)	THD_V ($\times 10^{-2}$)	$(\frac{1}{SNR})_V$ ($\times 10^{-5}$)	Ind-1 ($\times 10^{-3}$)	Ind-2 (%)	Ind-3
1	1.00	0.86	8.88	1.35	81.91	0.99	1.27	46.85
2	1.00	0.84	8.87	1.33	159.43	1.78	1.30	45.74
3	1.00	0.81	8.86	1.40	117.29	1.29	1.34	46.16
4	1.00	0.82	8.86	1.35	96.14	1.07	1.33	46.53
5	1.00	0.80	8.85	1.40	78.89	0.93	1.36	46.63
6	1.00	0.82	8.84	1.35	95.16	1.05	1.32	46.64
7	1.00	1.01	8.69	1.38	116.14	1.20	1.11	47.04
8	1.00	1.02	8.67	1.37	174.13	1.88	1.10	47.93
9	1.00	1.01	8.66	1.39	94.66	1.03	1.10	48.42
Mean	1.00	0.89	8.80	1.37	112.6	1.25	1.25	46.88

Note: D.S.No. is Data Set Number

Table LII. Fault I: 800 hp motor at 0% load (stator imbalance - case B).

Operational Parameter						Fault Indicator		
D.S.No.	RMS_V	RMS_I	Imb_V	THD_V	$(\frac{1}{SNR})_V$	Ind-1	Ind-2	Ind-3
	(p.u.)	(p.u.)	(%)	($\times 10^{-2}$)	($\times 10^{-5}$)	($\times 10^{-3}$)	(%)	
1	1.00	0.40	2.50	1.36	13.09	1.13	12.14	239.73
2	1.00	0.40	2.49	1.35	25.52	1.35	12.17	239.02
3	1.00	0.40	2.49	1.37	10.21	1.09	12.19	239.54
4	1.00	0.40	2.49	1.36	15.41	1.17	12.20	239.72
5	1.00	0.40	2.48	1.36	11.23	1.16	12.22	238.80
6	1.00	0.40	2.49	1.36	15.12	1.22	12.22	238.94
7	1.00	0.40	2.48	1.34	19.15	1.36	12.22	238.30
8	1.00	0.40	2.48	1.34	26.64	1.44	12.23	239.88
9	1.00	0.40	2.48	1.36	21.60	1.25	12.23	239.52
Mean	1.00	0.40	2.49	1.36	17.55	1.24	12.20	239.27
FIC(%)						-65.04	148.41	468.11

Note: D.S.No. is Data Set Number

Table LIII. Fault I: 800 hp motor at 50% load (stator imbalance - case B).

Operational Parameter						Fault Indicator		
D.S.No.	RMS _V	RMS _I	Imb _V	THD _V	$(\frac{1}{SNR})_V$	Ind-1	Ind-2	Ind-3
	(p.u.)	(p.u.)	(%)	($\times 10^{-2}$)	($\times 10^{-5}$)	($\times 10^{-3}$)	(%)	
1	0.99	0.74	3.17	1.15	54.72	1.13	9.07	328.97
2	0.99	0.79	3.26	1.12	87.76	1.34	8.88	344.02
3	0.99	0.79	3.25	1.11	64.93	1.31	8.96	344.04
Mean	0.99	0.77	3.23	1.13	69.14	1.26	8.97	339.01
FIC(%)						-21.70	342.45	652.48

Note: D.S.No. is Data Set Number

Table LIV. Fault I: 800 hp motor at 100% load (stator imbalance - case B).

Operational Parameter						Fault Indicator		
D.S.No.	RMS _V	RMS _I	Imb _V	THD _V	$(\frac{1}{SNR})_V$	Ind-1	Ind-2	Ind-3
	(p.u.)	(p.u.)	(%)	($\times 10^{-2}$)	($\times 10^{-5}$)	($\times 10^{-3}$)	(%)	
1	0.99	1.02	3.60	1.03	66.18	0.91	8.45	429.60
2	0.99	1.05	3.64	0.99	30.47	0.55	8.44	428.28
3	0.97	0.98	5.03	0.92	92.31	1.06	8.35	399.27
4	0.97	1.00	5.08	0.91	93.29	0.98	8.39	467.36
5	0.97	1.01	5.11	0.95	70.65	0.79	8.43	423.37
Mean	0.98	1.01	4.49	0.96	70.58	0.86	8.41	429.58
FIC(%)						-31.24	574.65	816.29

Note: D.S.No. is Data Set Number

Table LV. Fault II: 500 hp motor at 0% load (stator winding shorts - case 1).

Operational Parameter						Fault Indicator		
D.S.No.	RMS_V (p.u.)	RMS_I (p.u.)	Imb_V (%)	THD_V ($\times 10^{-2}$)	$(\frac{1}{SNR})_V$ ($\times 10^{-5}$)	Ind-1 ($\times 10^{-3}$)	Ind-2 (%)	Ind-3
1	1.01	0.24	2.10	1.37	22.87	1.19	4.00	44.04
2	1.01	0.24	2.10	1.37	34.39	1.53	4.01	43.97
3	1.01	0.24	2.10	1.36	34.17	1.37	4.00	44.00
4	1.01	0.24	2.10	1.37	28.70	1.23	4.00	44.52
5	1.00	0.25	2.09	1.37	30.74	1.27	3.95	43.96
6	1.00	0.25	2.09	1.38	19.55	1.11	3.95	43.89
7	1.00	0.25	2.09	1.36	34.25	1.33	3.95	44.16
Mean	1.01	0.24	2.09	1.37	29.24	1.29	3.98	44.08
FIC(%)						-3.12	0.44	3.50

Note: D.S.No. is Data Set Number

Table LVI. Fault II: 500 hp motor at 50% load (stator winding shorts - case 1).

Operational Parameter						Fault Indicator		
D.S.No.	RMS_V (p.u.)	RMS_I (p.u.)	Imb_V (%)	THD_V ($\times 10^{-2}$)	$(\frac{1}{SNR})_V$ ($\times 10^{-5}$)	Ind-1 ($\times 10^{-3}$)	Ind-2 (%)	Ind-3
1	1.00	0.56	2.05	0.99	51.99	0.51	2.21	57.85
2	1.00	0.57	2.05	1.01	35.52	0.51	2.20	57.53
3	1.00	0.56	2.05	0.99	125.92	0.58	2.21	58.05
4	1.00	0.57	2.04	1.02	54.93	0.67	2.20	58.14
5	0.99	0.56	2.19	1.03	136.22	1.22	2.22	57.99
6	1.00	0.55	2.04	1.00	65.22	0.85	2.24	56.99
7	1.00	0.54	2.04	1.05	85.28	1.07	2.26	57.40
Mean	1.00	0.56	2.06	1.01	79.30	0.77	2.22	57.71
FIC(%)						75.90	15.29	8.92

Note: D.S.No. is Data Set Number

Table LVII. Fault II: 500 hp motor at 100% load (stator winding shorts - case 1).

Operational Parameter						Fault Indicator		
D.S.No.	RMS_V (p.u.)	RMS_I (p.u.)	Imb_V (%)	THD_V ($\times 10^{-2}$)	$(\frac{1}{SNR})_V$ ($\times 10^{-5}$)	Ind-1 ($\times 10^{-3}$)	Ind-2 (%)	Ind-3
1	1.00	0.97	2.01	0.79	33.12	0.35	1.61	69.62
2	1.00	1.08	2.00	0.78	31.84	0.37	1.51	72.78
3	1.00	0.96	2.00	0.76	52.89	0.55	1.61	69.26
4	1.00	1.04	2.00	0.75	79.90	0.85	1.54	71.47
Mean	1.00	1.01	2.00	0.77	49.44	0.53	1.57	70.78
FIC(%)						-24.62	14.09	15.64

Note: D.S.No. is Data Set Number

value of fault indicators as compared to healthy baseline is higher than that of the previous case 1.

4. Ground Wall Insulation

Experiments for ground wall insulation fault is performed on 500 hp, G.E. motor by bridging C phase with 10 megohm resistor. Data from these experiments is compared to the healthy baseline of the same motor. Table LXI, Table LXII and Table LXIII show the the magnitude of the operating parameters and the fault indicators for the faulty cases with the corresponding values of FIC-2 and FIC-3 at 0%, 50% and 100% load condition. In this case, the FIC-2 at 0% load is 4.28%, at 50% load is 17.59% and at 100% load is 18.41% and the FIC-3 at 0% load is 5.75%, at 50% load is 12.91% and at 100% load is 18.47%.

Table LVIII. Fault II: 500 hp motor at 0% load (stator winding shorts - case 2).

Operational Parameter						Fault Indicator		
D.S.No.	RMS _V (p.u.)	RMS _I (p.u.)	Imb _V (%)	THD _V ($\times 10^{-2}$)	$(\frac{1}{SNR})_V$ ($\times 10^{-5}$)	Ind-1 ($\times 10^{-3}$)	Ind-2 (%)	Ind-3
1	1.00	0.24	2.09	1.38	18.39	1.10	4.01	44.26
2	1.00	0.24	2.09	1.36	26.85	1.25	4.02	44.18
3	1.00	0.24	2.09	1.39	17.48	1.06	4.01	44.41
4	1.00	0.25	2.09	1.37	28.43	1.28	4.03	44.71
Mean	1.00	0.24	2.09	1.38	22.79	1.17	4.02	44.39
FIC(%)						-11.77	1.40	4.24

Note: D.S.No. is Data Set Number

5. Interlaminar Insulation Short

Interlaminar insulation short is also performed on 500 hp, G.E. motor by damaging stator core. FIC is obtained by comparing the data from the experiment to the healthy baseline of 500 hp, G.E. motor. Table LXIV and Table LXV show the magnitude of the operating parameters and the fault indicators for the interlaminar insulation short fault cases with the corresponding values of FIC-2 and FIC-3 at 50% and 100% load condition. At 0% loading condition, fault indicators are non indicative of the present fault. At 100% load, the FIC-2 is 17.76% and FIC-3 is 17.63%.

E. Chapter Summary

In this chapter, the experimental set-ups and specifications for the data acquisition for the small as well as large machines are described. The experiments conducted for

Table LIX. Fault II: 500 hp motor at 50% load (stator winding shorts - case 2).

Operational Parameter						Fault Indicator		
D.S.No.	RMS_V (p.u.)	RMS_I (p.u.)	Imb_V (%)	THD_V ($\times 10^{-2}$)	$(\frac{1}{SNR})_V$ ($\times 10^{-5}$)	Ind-1 ($\times 10^{-3}$)	Ind-2 (%)	Ind-3
1	1.00	0.59	2.04	1.00	40.26	0.52	2.20	60.55
2	1.00	0.60	2.04	0.94	74.57	0.88	2.18	60.65
3	1.00	0.61	2.04	0.95	65.29	0.76	2.17	60.83
4	1.00	0.59	2.02	0.97	64.22	0.70	2.21	59.64
5	1.00	0.56	2.02	1.00	54.23	0.62	2.26	58.37
6	1.00	0.55	2.03	1.01	71.94	0.92	2.27	59.18
Mean	1.00	0.59	2.03	0.98	61.75	0.73	2.22	59.87
FIC(%)						66.14	15.21	13.00

Note: D.S.No. is Data Set Number

Table LX. Fault II: 500 hp motor at 100% load (stator winding shorts - case 2).

Operational Parameter						Fault Indicator		
D.S.No.	RMS_V (p.u.)	RMS_I (p.u.)	Imb_V (%)	THD_V ($\times 10^{-2}$)	$(\frac{1}{SNR})_V$ ($\times 10^{-5}$)	Ind-1 ($\times 10^{-3}$)	Ind-2 (%)	Ind-3
1	1.00	1.04	1.99	.77	55.66	0.58	1.59	73.34
2	1.00	1.08	1.99	.77	97.42	0.99	1.55	74.39
3	1.00	1.08	1.99	.73	101.9	1.04	1.55	74.45
Mean	1.00	1.07	1.99	0.76	84.99	0.87	1.56	74.06
FIC(%)						23.82	13.99	21.00

Note: D.S.No. is Data Set Number

Table LXI. Fault III: 500 hp motor at 0% load (ground wall insulation).

Operational Parameter						Fault Indicator		
D.S.No.	RMS_V (p.u.)	RMS_I (p.u.)	Imb_V (%)	THD_V ($\times 10^{-2}$)	$(\frac{1}{SNR})_V$ ($\times 10^{-5}$)	Ind-1 ($\times 10^{-3}$)	Ind-2 (%)	Ind-3
1	1.00	0.24	2.18	1.43	24.15	0.98	4.14	45.10
2	1.00	0.24	2.19	1.39	153.33	2.44	4.13	44.80
3	1.00	0.24	2.18	1.42	26.96	0.99	4.13	45.22
Mean	1.00	0.24	2.18	1.41	68.15	1.47	4.13	45.04
FIC(%)						10.52	4.28	5.75

Note: D.S.No. is Data Set Number

Table LXII. Fault III: 500 hp motor at 50% load (ground wall insulation).

Operational Parameter						Fault Indicator		
D.S.No.	RMS_V (p.u.)	RMS_I (p.u.)	Imb_V (%)	THD_V ($\times 10^{-2}$)	$(\frac{1}{SNR})_V$ ($\times 10^{-5}$)	Ind-1 ($\times 10^{-3}$)	Ind-2 (%)	Ind-3
1	1.00	0.62	2.13	0.94	59.60	0.74	2.20	59.86
2	1.00	0.58	2.13	1.03	47.23	0.61	2.28	60.20
3	1.00	0.58	2.13	1.03	49.01	0.57	2.29	59.50
4	1.00	0.58	2.13	1.05	51.83	0.62	2.29	59.73
Mean	1.00	0.59	2.13	1.01	51.92	0.63	2.26	59.82
FIC(%)						44.05	17.59	12.91

Note: D.S.No. is Data Set Number

Table LXIII. Fault III: 500 hp motor at 100% load (ground wall insulation).

Operational Parameter						Fault Indicator		
D.S.No.	RMS_V (p.u.)	RMS_I (p.u.)	Imb_V (%)	THD_V ($\times 10^{-2}$)	$(\frac{1}{SNR})_V$ ($\times 10^{-5}$)	Ind-1 ($\times 10^{-3}$)	Ind-2 (%)	Ind-3
1	1.00	0.99	2.09	0.84	75.55	0.77	1.66	71.86
2	1.00	1.04	2.09	0.80	104.4	1.05	1.63	73.41
3	1.00	1.07	2.09	0.81	81.20	0.86	1.60	72.65
4	1.00	1.06	2.09	0.77	63.90	0.67	1.61	72.13
Mean	1.00	1.04	2.09	0.81	81.26	0.84	1.62	72.51
FIC(%)						19.29	18.41	18.47

Note: D.S.No. is Data Set Number

Table LXIV. Fault IV: 500 hp motor at 0% load (interlaminar insulation short).

Operational Parameter						Fault Indicator		
D.S.No.	RMS_V (p.u.)	RMS_I (p.u.)	Imb_V (%)	THD_V ($\times 10^{-2}$)	$(\frac{1}{SNR})_V$ ($\times 10^{-5}$)	Ind-1 ($\times 10^{-3}$)	Ind-2 (%)	Ind-3
1	1.01	0.24	1.90	1.32	20.99	1.38	3.88	42.31
2	1.01	0.24	1.90	1.35	19.60	1.24	3.88	42.48
3	1.01	0.24	1.90	1.33	22.52	1.36	3.87	42.38
4	1.01	0.24	1.90	1.29	33.65	1.59	3.87	42.24
5	1.01	0.24	1.90	1.33	21.21	1.37	3.87	42.34
6	1.01	0.24	1.90	1.34	21.39	1.31	3.87	42.50
7	1.01	0.24	1.90	1.33	22.26	1.37	3.87	42.27
8	1.01	0.24	1.90	1.31	24.70	1.46	3.86	42.24
9	1.01	0.24	1.90	1.30	29.06	1.54	3.86	42.30
10	1.01	0.24	1.90	1.32	28.09	1.47	3.86	42.39
11	1.01	0.24	1.90	1.34	28.84	1.39	3.86	42.24
12	1.00	0.24	1.90	1.33	22.10	1.36	3.85	42.33
Mean	1.01	0.24	1.90	1.33	24.53	1.40	3.87	42.34
FIC(%)						5.35	-2.42	-0.59

Note: D.S.No. is Data Set Number

Table LXV. Fault IV: 500 hp motor at 100% load (interlaminar insulation short).

Operational Parameter						Fault Indicator		
D.S.No.	RMS_V (p.u.)	RMS_I (p.u.)	Imb_V (%)	THD_V ($\times 10^{-2}$)	$(\frac{1}{SNR})_V$ ($\times 10^{-5}$)	Ind-1 ($\times 10^{-3}$)	Ind-2 (%)	Ind-3
1	1.00	1.00	1.80	0.77	48.39	0.51	1.63	70.83
2	1.00	1.06	1.80	0.73	45.55	0.46	1.57	72.28
3	1.00	0.99	1.80	0.78	77.23	0.78	1.65	72.34
4	1.00	1.00	1.80	0.74	42.40	0.45	1.63	71.29
5	1.00	0.99	1.80	0.75	65.55	0.67	1.64	70.59
6	1.00	1.03	1.80	0.74	139.85	1.4	1.61	72.01
7	1.00	1.03	1.80	0.77	56.31	0.59	1.62	72.45
8	1.00	1.04	1.80	0.78	69.75	0.73	1.60	73.05
9	1.00	1.06	1.80	0.76	75.51	0.78	1.59	73.11
Mean	1.00	1.02	1.80	0.76	68.95	0.71	1.62	71.99
FIC(%)						0.50	17.76	17.63

Note: D.S.No. is Data Set Number

different type of staged mechanical and electrical faults in the small machines and large machines are also described. The developed fault detection system is tested with a total 19 cases of induction motor faults including different conditions of bad bearings, broken rotor bars, air-gap eccentricity, unbalanced stator, and stator turn-to-turn winding short at different loading conditions. The results for the various experiments are discussed. The operating parameters and fault indicators are computed and presented along with FIC for all fault indicators. The results show the effectiveness of the proposed fault indicators for both mechanical and electrical faults. A significant number of tests are performed and the results show satisfactory detection effectiveness for the developed fault detection system.

CHAPTER IV

COMPARISON OF FAULT SIGNATURES

A. Comparison of Mechanical Fault Based on Load Levels

The experiments for the bad bearing, broken rotor bars, air-gap eccentricity cases and mechanical imbalance are performed at different loading levels with motors of different rating. The maximum, minimum and average value of the fault indicator-1 for the number of data sets used for a particular condition is calculated and the variability of the fault Indicator-1 at a certain “healthy” condition of the motor is investigated by using error bar plots of the indicator values for healthy and faulty condition of motor. The Fault Indicator-1 Change(%) is presented in the form of bar plots.

The bearing fault experiments, conducted on 3 hp motor at 0% and 25% loading conditions, comprise of experiments with single faulty bearing in the rotor and both the rotor bearings faulty. When we look at the Figure 7 and Figure 8, we can clearly see the expected pattern according the severity of the fault. We can observe that in both the cases the FIC-1 is more at 0% load as compared to 25% loading condition. For single bearing fault, at 25% load, it is very difficult to detect the fault as the FIC-1 is very less. It can be also observed that the FIC-1 is much higher for the double faulty cases as compared to the single faulty cases.

Broken rotor bar experiments are done on a 800 hp and 700 hp motor. Experiments on the 800 hp motor comprise of half, one, two and, four broken rotor bars. Figure 9, Figure 10, Figure 11 and Figure 12 show the load dependence of Indicator-1 and FIC-1 for 800 hp motor with half, one, two, and four broken rotor bar respectively. For half broken rotor bar, at 100% loading, the FIC-1 do not clearly indicate

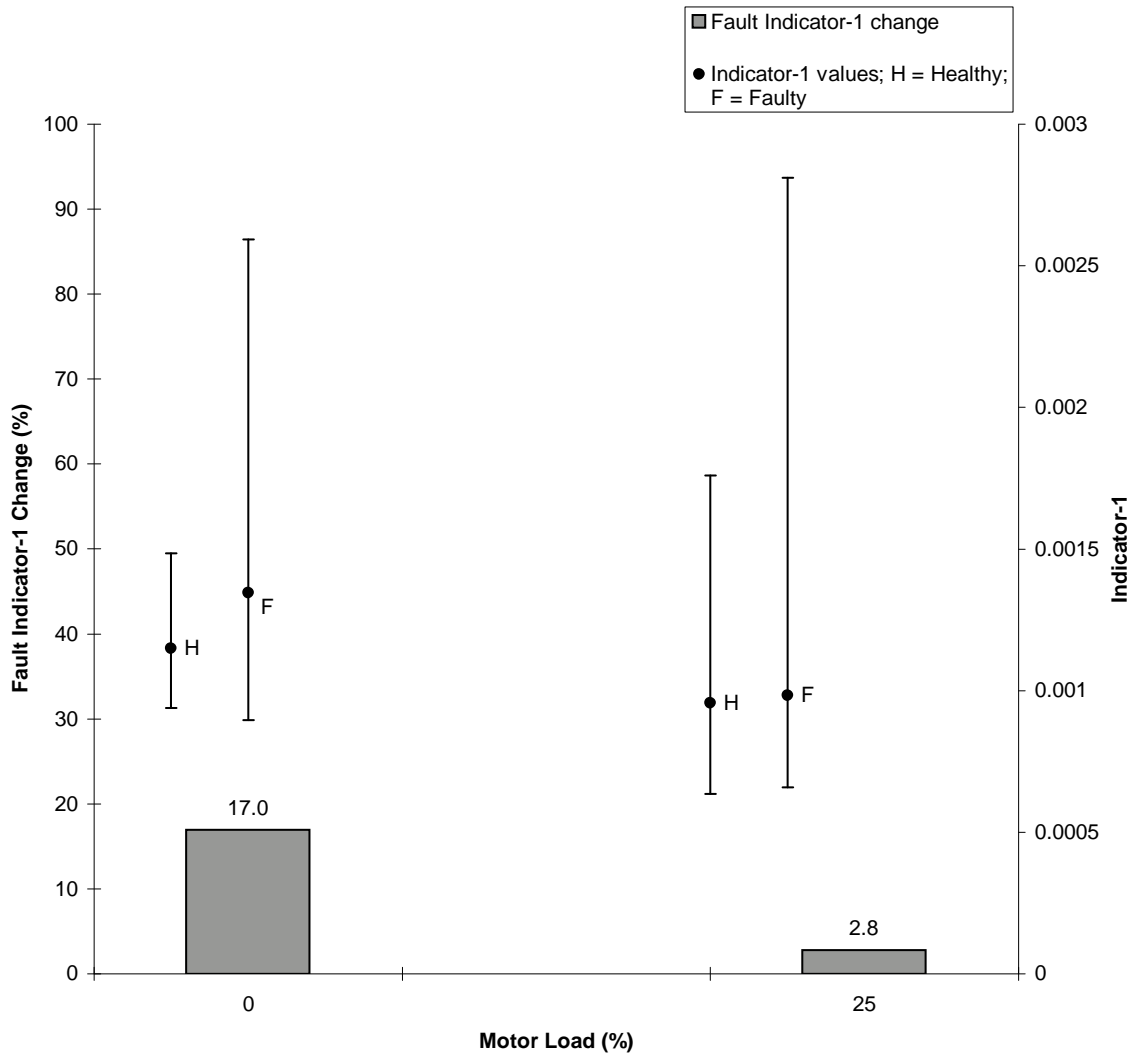


Fig. 7. Load dependence of Indicator-1 and Fault Indicator-1 Change for 3 hp motor; single bad bearing.

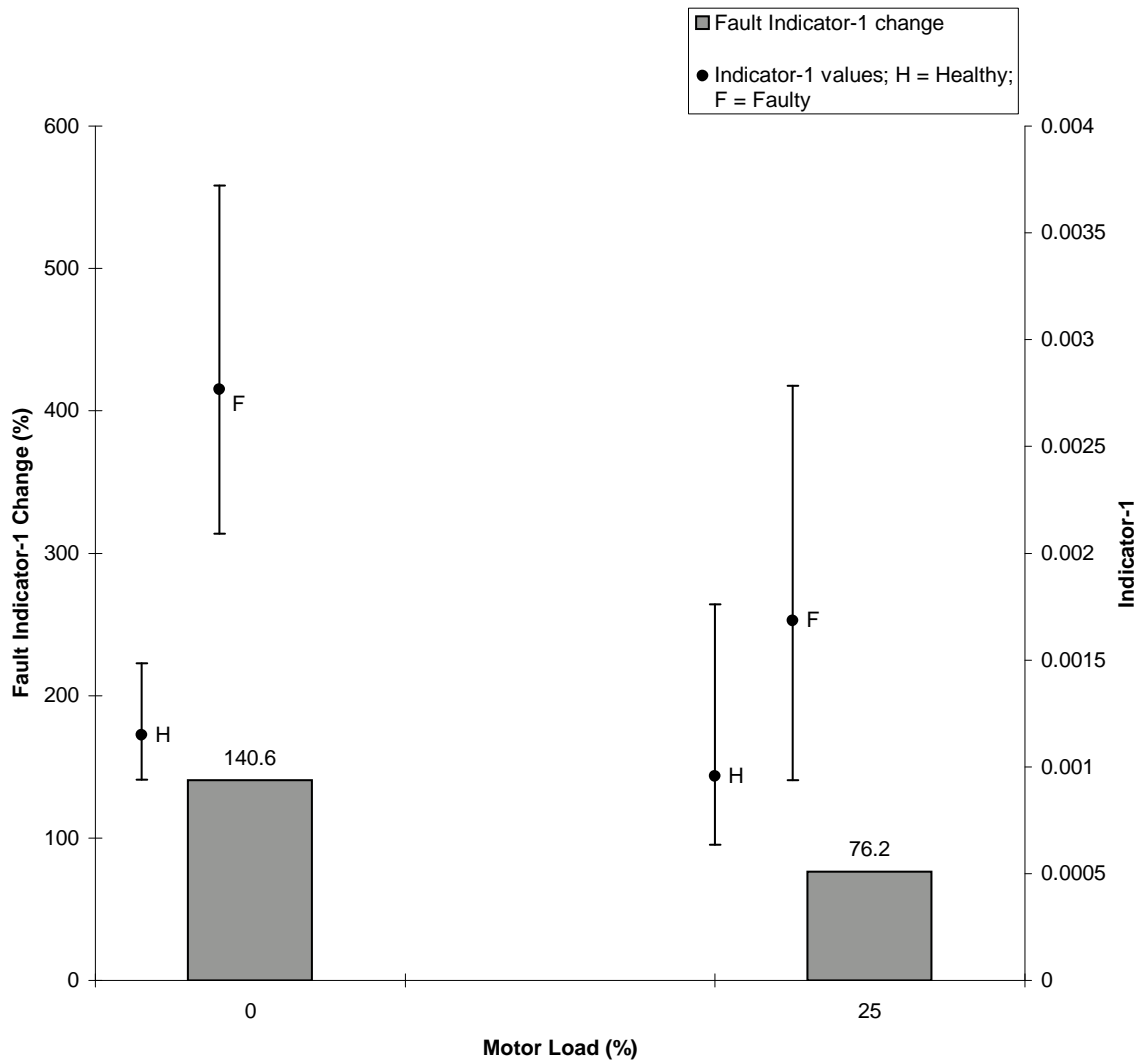


Fig. 8. Load dependence of Indicator-1 and Fault Indicator-1 Change for 3 hp motor; double bad bearing.

a significant increase from healthy to faulty condition, and is hence little indicative of the fault condition. At 50% loading the FIC-1 is much larger as compared to corresponding FIC-1 at 100% loading. For one broken rotor bar, at 100% loading, the FIC-1 is higher than the half broken rotor bar. The same pattern of load dependency can be observed for the case of two broken rotor bars. The four broken rotor bar case shows the maximum FIC-1 as compared to the other cases at all loading conditions. In all of the above cases, it is observed that FIC-1 is higher at 50% as compared to FIC-1 at 100%, which is counter intuitive. This is because of the discrepancy in the raw data at 100% load.

On the 700 hp motor, faulty cases are obtained by conducting experiments with grease on winding and two rotor bars cut side by side for different load levels. Figure 13 shows the load dependence of Indicator-1 and FIC-1 for 700 hp motor with two broken rotor bar. Both at 50% and 100% loading conditions, the FIC-1 is less indicative of the fault condition.

Experiments for air-gap eccentricity are done on 800 hp and 700 hp motor. On 800 hp motor, there is an offset set to 20% down at outboard end and 26% right at inboard end. The data from experiments conducted with this setting, is compared to data from healthy operating conditions of same motor. Figure 14 shows the load dependence of Indicator-1 and FIC-1 for 800 hp motor with air-gap eccentricity. At 0% loading, the FIC-1 is much larger as compared to corresponding FIC-1 at 50% and 100% loading. At 0% and 50% loading, from the error bar plot, the faulty indicator-1 values can be easily distinguished from the healthy indicator-1 values. For this fault type, we could see that at high levels of loading, the FIC-1 is more indicative of the fault as compared to lower levels of loading.

Figure 15 shows the load dependence of Indicator-1 and FIC-1 for 700 hp motor with air-gap eccentricity. On 700 hp motor, both at 50% and 100% loading conditions,

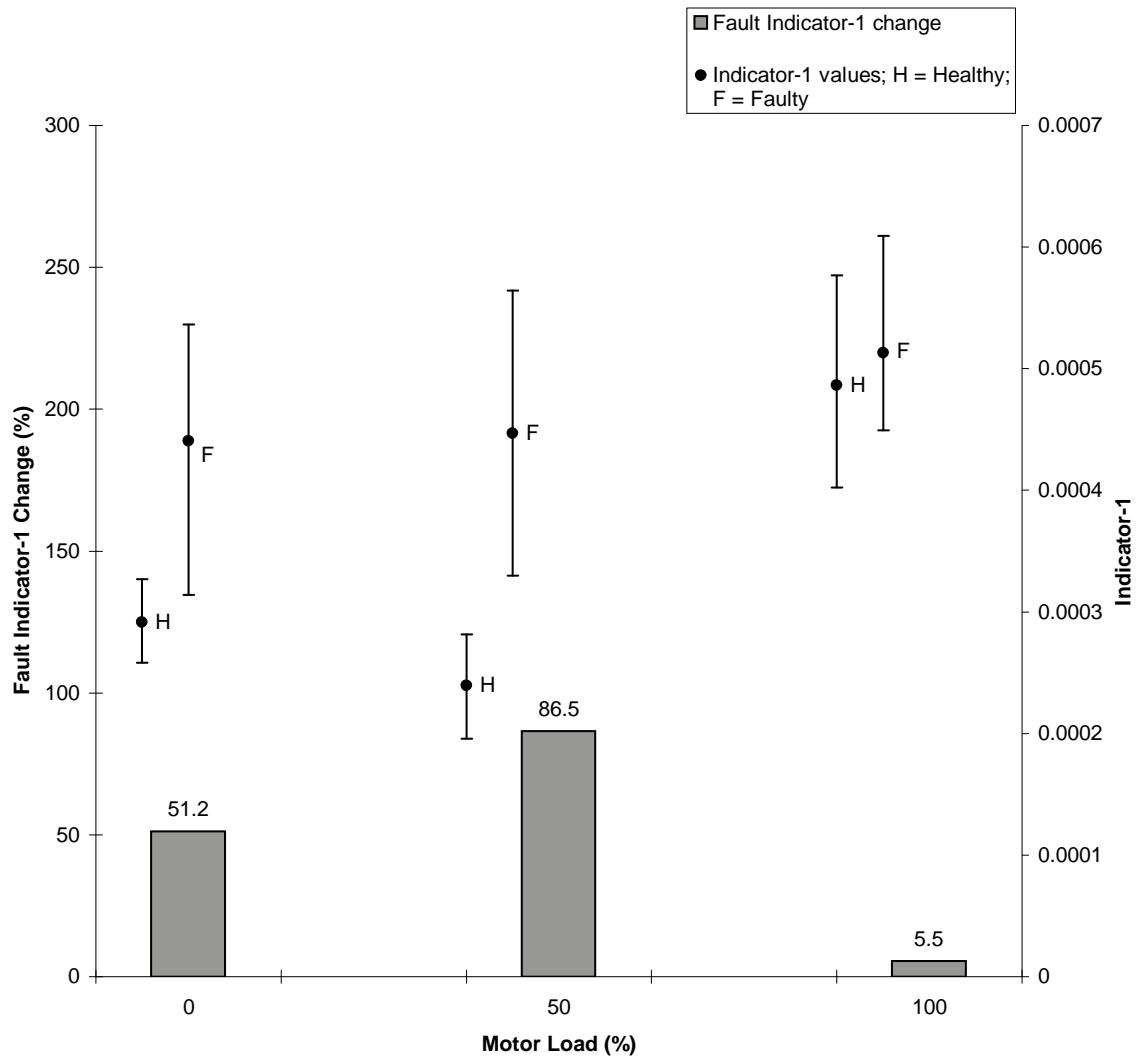


Fig. 9. Load dependence of Indicator-1 and Fault Indicator-1 Change for 800 hp motor; half broken rotor bar.

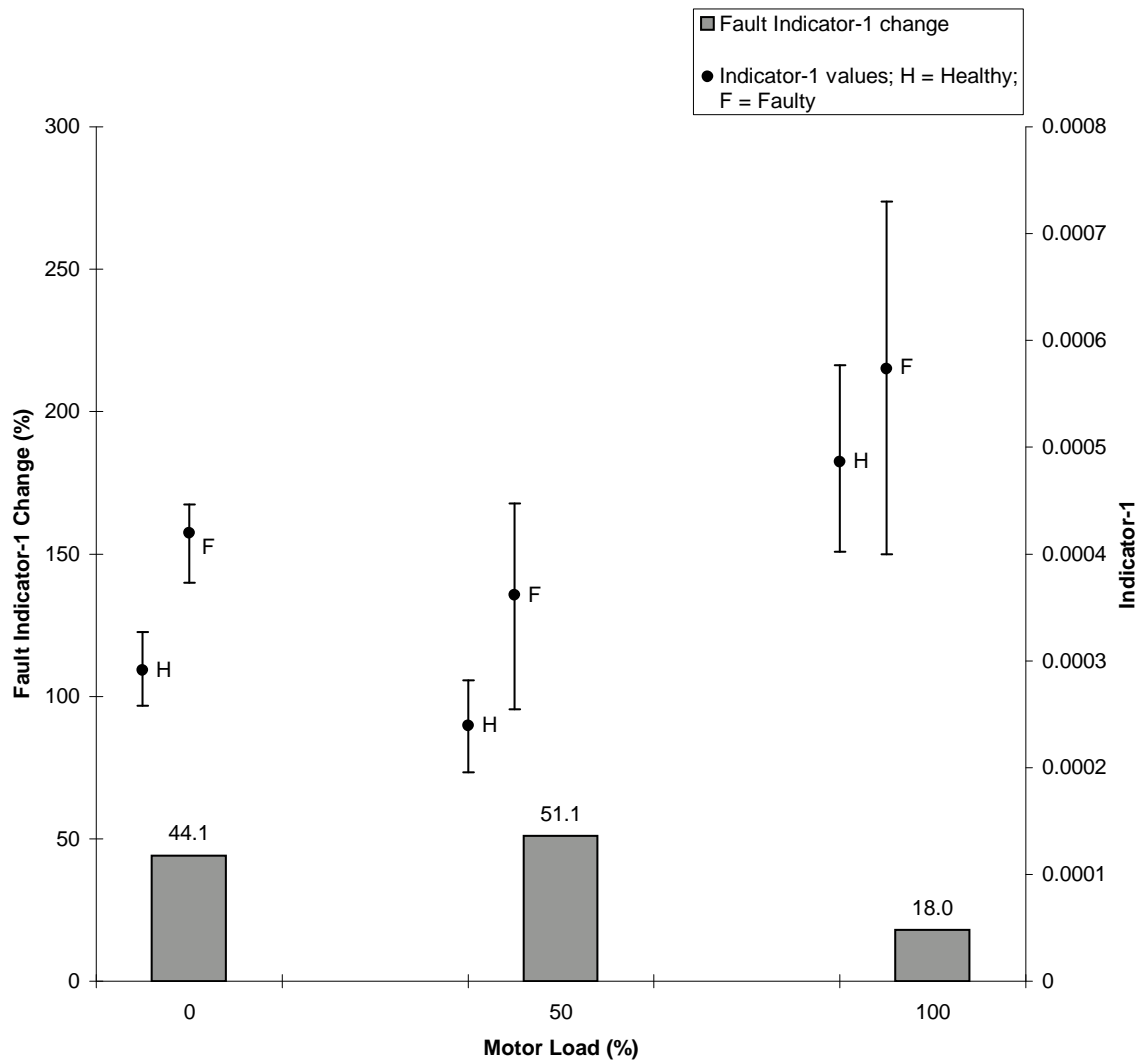


Fig. 10. Load dependence of Indicator-1 and Fault Indicator-1 Change for 800 hp motor; one broken rotor bar.

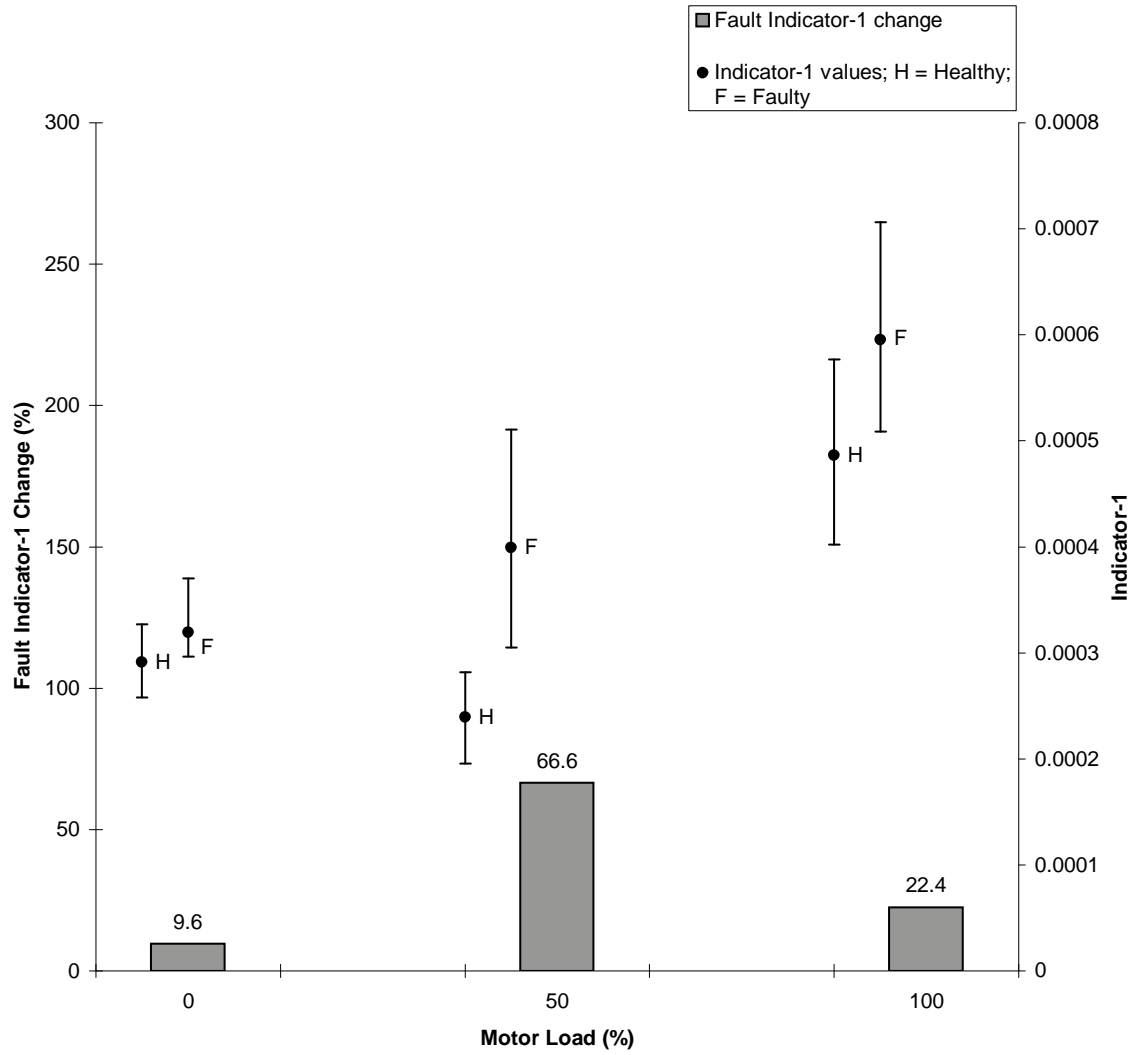


Fig. 11. Load dependence of Indicator-1 and Fault Indicator-1 Change for 800 hp motor; two broken rotor bars.

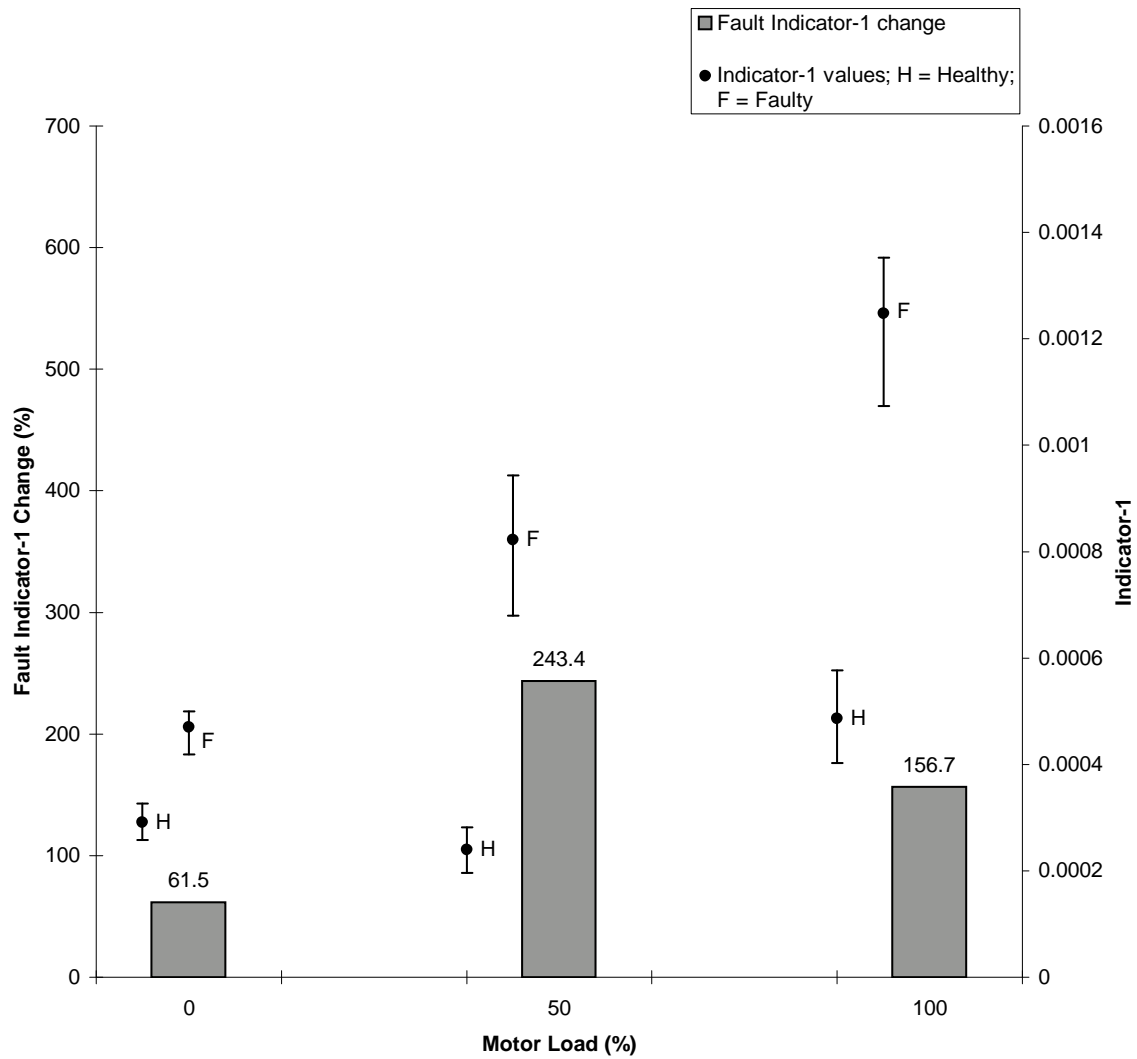


Fig. 12. Load dependence of Indicator-1 and Fault Indicator-1 Change for 800 hp motor; four broken rotor bars.

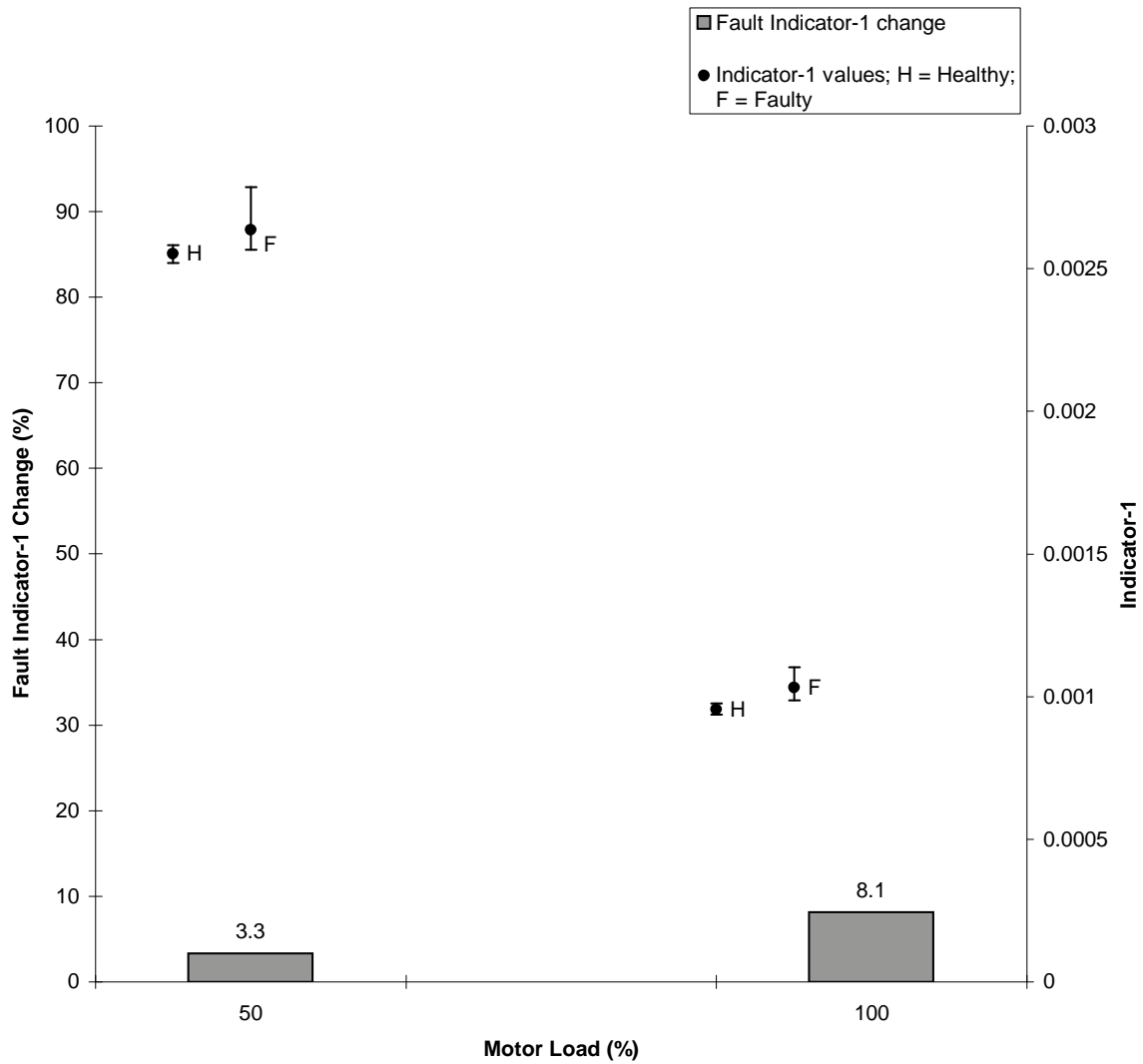


Fig. 13. Load dependence of Indicator-1 and Fault Indicator-1 Change for 700 hp motor; grease on winding and two broken rotor bars - case B.

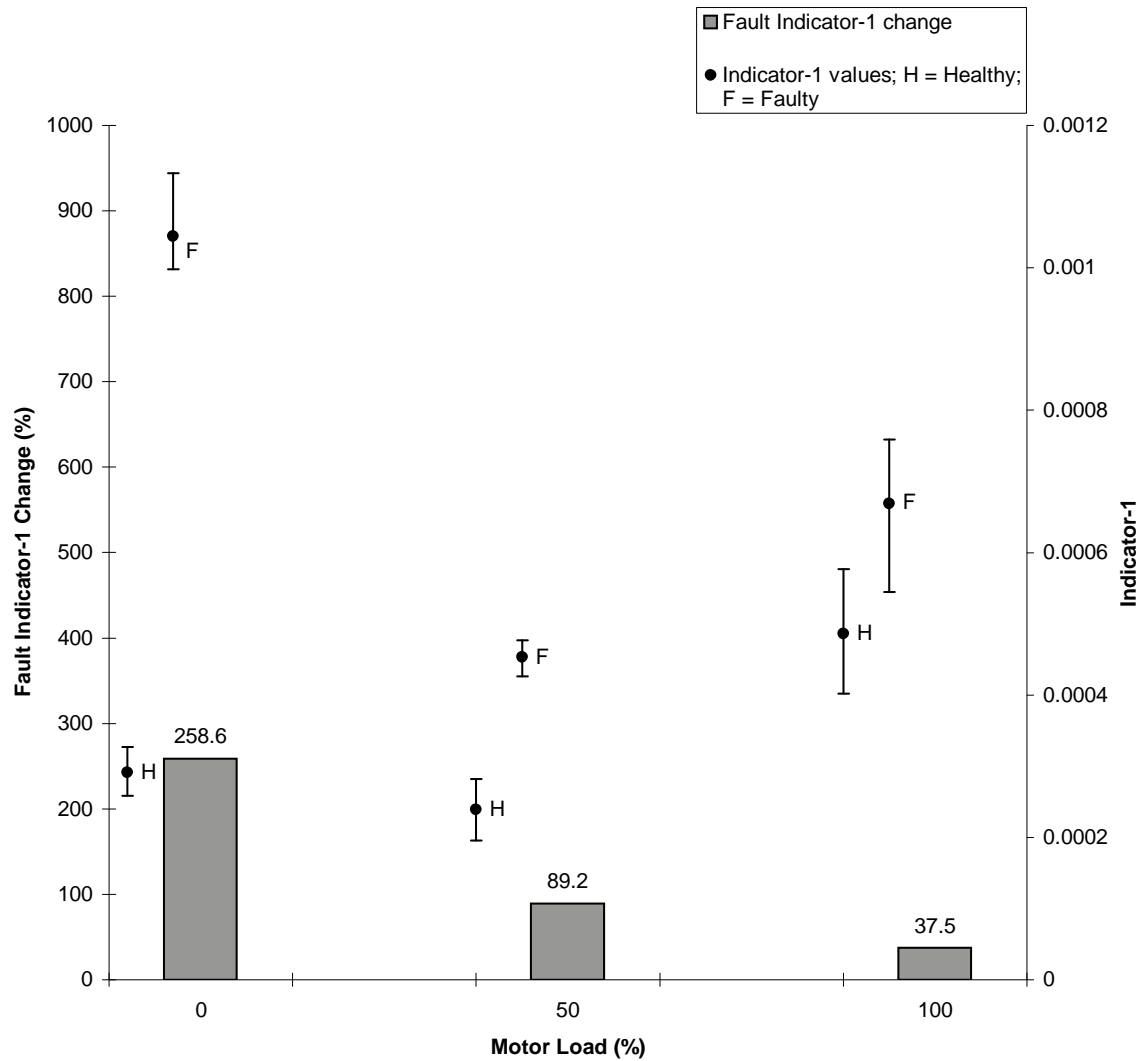


Fig. 14. Load dependence of Indicator-1 and Fault Indicator-1 Change for 800 hp motor; air-gap eccentricity - case A2.

the FIC-1 is less indicative of the fault condition as compared to FIC-1 for 800 hp motor. At 50% loading, the FIC-1 is larger as compared to corresponding FIC-1 at 100% loading.

Mechanical imbalance experiments are done on a 500 hp motor. Figure 16 shows the load dependence of Indicator-1 and FIC-1 for 500 hp motor with mechanical imbalance. At 100% loading, the fault signatures are more indicative of the fault present in the system. While the FIC-1 at 100% loading is 41.2%, it is 13% at 50% loading.

B. Comparison of Electrical Fault Based on Load Levels

The experiments for the different cases of stator imbalance, stator winding shorts, ground wall insulation, and interlaminar insulation short are performed at different loading levels with motors of different rating. The maximum, minimum and average value of the fault indicators for the number of data sets used for a particular condition is calculated and the variability of the fault Indicator-2 and Indicator-3 at a certain “healthy” condition of the motor is investigated by using error bar plots of the indicator values for healthy and faulty condition of motor. The Fault Indicator-2 Change(%) and Fault Indicator-3 Change(%) is presented in the form of bar plots.

Different cases of stator imbalance are performed on 150 hp and 800 hp motor. On 150 hp motor, for stator imbalance case A1, there is an resistance of 0.012 Ω in series with phase A. Figure 17 and Figure 18 show the load dependence of Indicator-2 and FIC-2 and Indicator-3 and FIC-3 for 150 hp motor with stator imbalance - case A1. At 50% and 100% loading, indicator-2 is more indicative of the fault being present as compared to indicator-3. At 100% loading, indicator-2 is less indicative of the fault as compared to the corresponding indicator at 50% loading. Figure 19 and

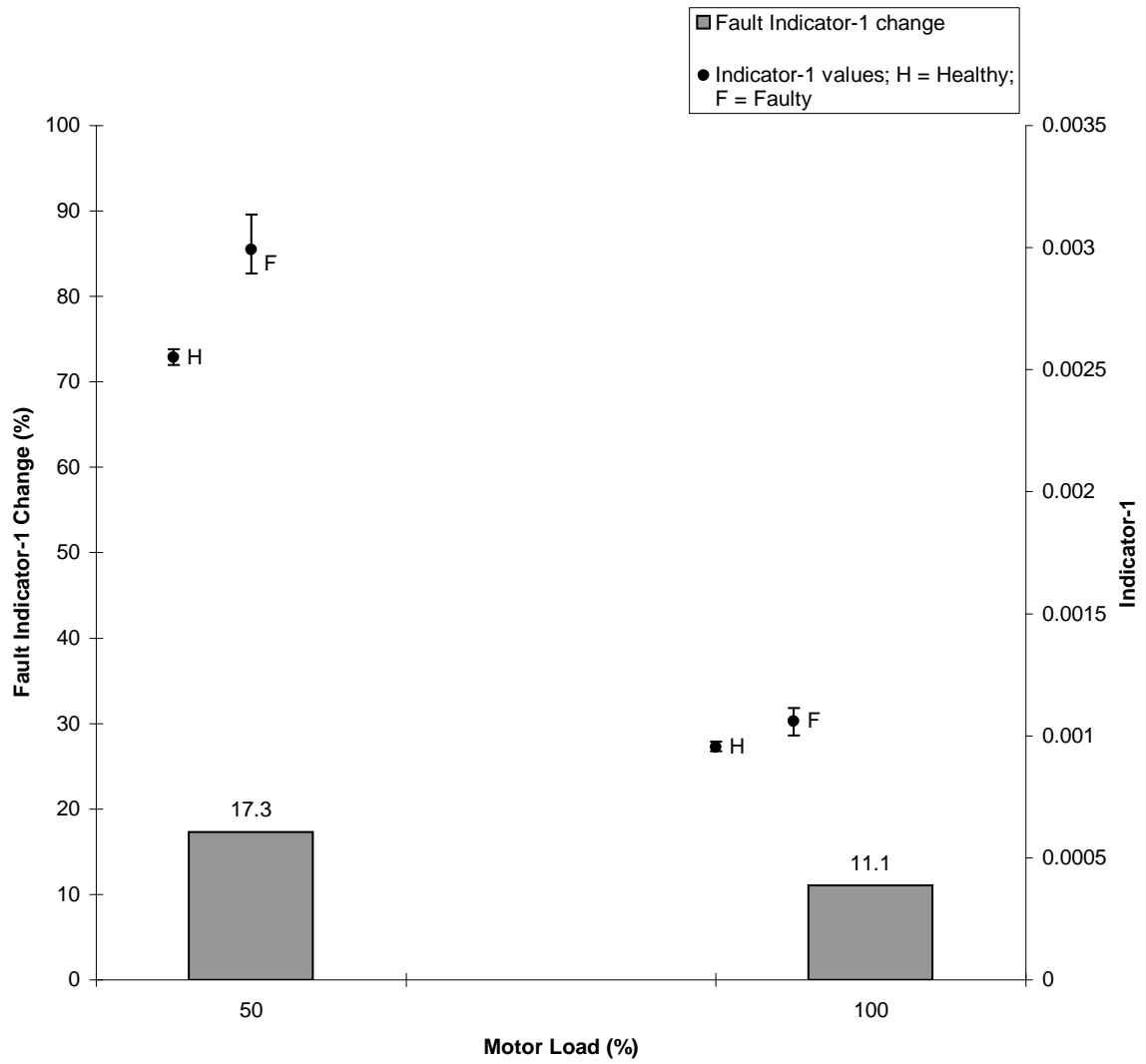


Fig. 15. Load dependence of Indicator-1 and Fault Indicator-1 Change for 700 hp motor; air-gap eccentricity - case B.

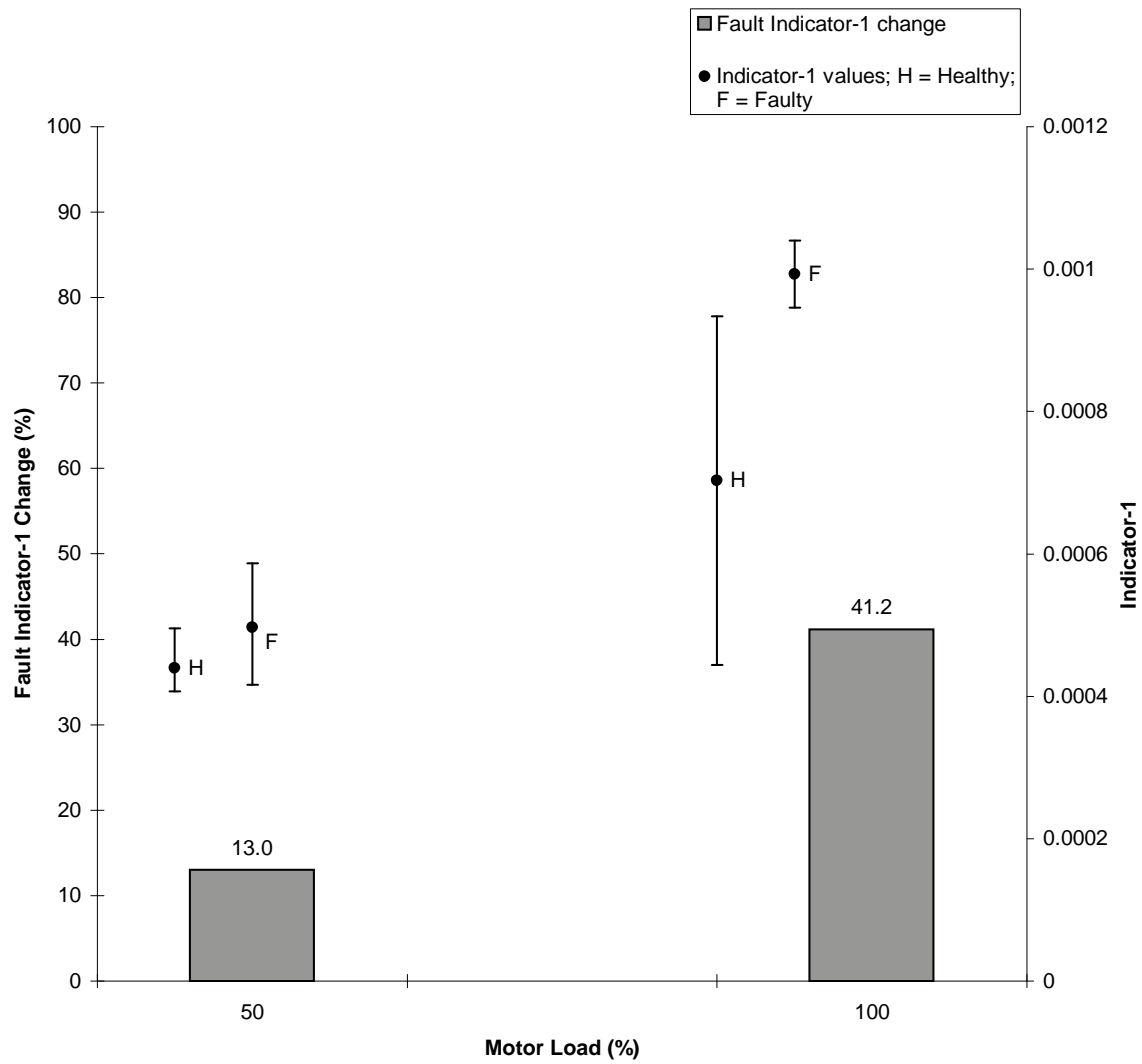


Fig. 16. Load dependence of Indicator-1 and Fault Indicator-1 Change for 500 hp motor; mechanical imbalance.

Figure 20 show the load dependence of Indicator-2 and FIC-2 and Indicator-3 and FIC-3 for 150 hp motor with stator imbalance - case A2. For stator short case A2, there is an resistance of 0.633Ω in series with phase A. At both loading conditions, the FIC-2 and FIC-3 are huge as compared to FIC-2 and FIC-3 for stator short case A1 because of the severity of the fault. At 50% and 100% loading condition, the variability of indicator-2 values is much less than the variability of indicator-3 values.

Experiments for stator imbalance - Case B are performed on 800 hp motor. Figure 21 and Figure 22 show the load dependence of Indicator-2 and FIC-2 and Indicator-3 and FIC-3 for 800 hp motor with stator imbalance - case B. At all loading conditions, both the indicators are good indicative of the fault present. As there is imbalance in the stator, a huge increase in the value of the fault indicator as compared to the healthy baseline is seen. As the load increases, the FIC- and FIC-3 also increases. From the Figure 22 we can observe that indicator-3 values for healthy condition of motor does not change with load.

On the 500 hp motor, for stator short case 1, there is an turn to turn short with an resistance of 2.7Ω in series with phase C. Figure 23 and Figure 24 show the load dependence of Indicator-2 and FIC-2 and Indicator-3 and FIC-3 for 500 hp motor with stator short - case 1. At 0% loading, both the indicators are non-indicative of the fault being present. At 50% loading, FIC-2 is more than as compared to FIC-3. For fault indicator-3, FIC-3 increases with the increase in the motor load. For stator short case 2, there is an turn to turn short with an resistance of 1.35Ω in series with phase C. Figure 25 and Figure 26 show the load dependence of Indicator-2 and FIC-2 and Indicator-3 and FIC-3 for 500 hp motor with stator short - case 2. For all loading conditions, the FIC-3 is more than the FIC-3 for the previous case 1. The FIC-3 follows the same trend of increasing with increase in the motor load.

Experiments for ground wall insulation are done on 500 hp motor. On the 500

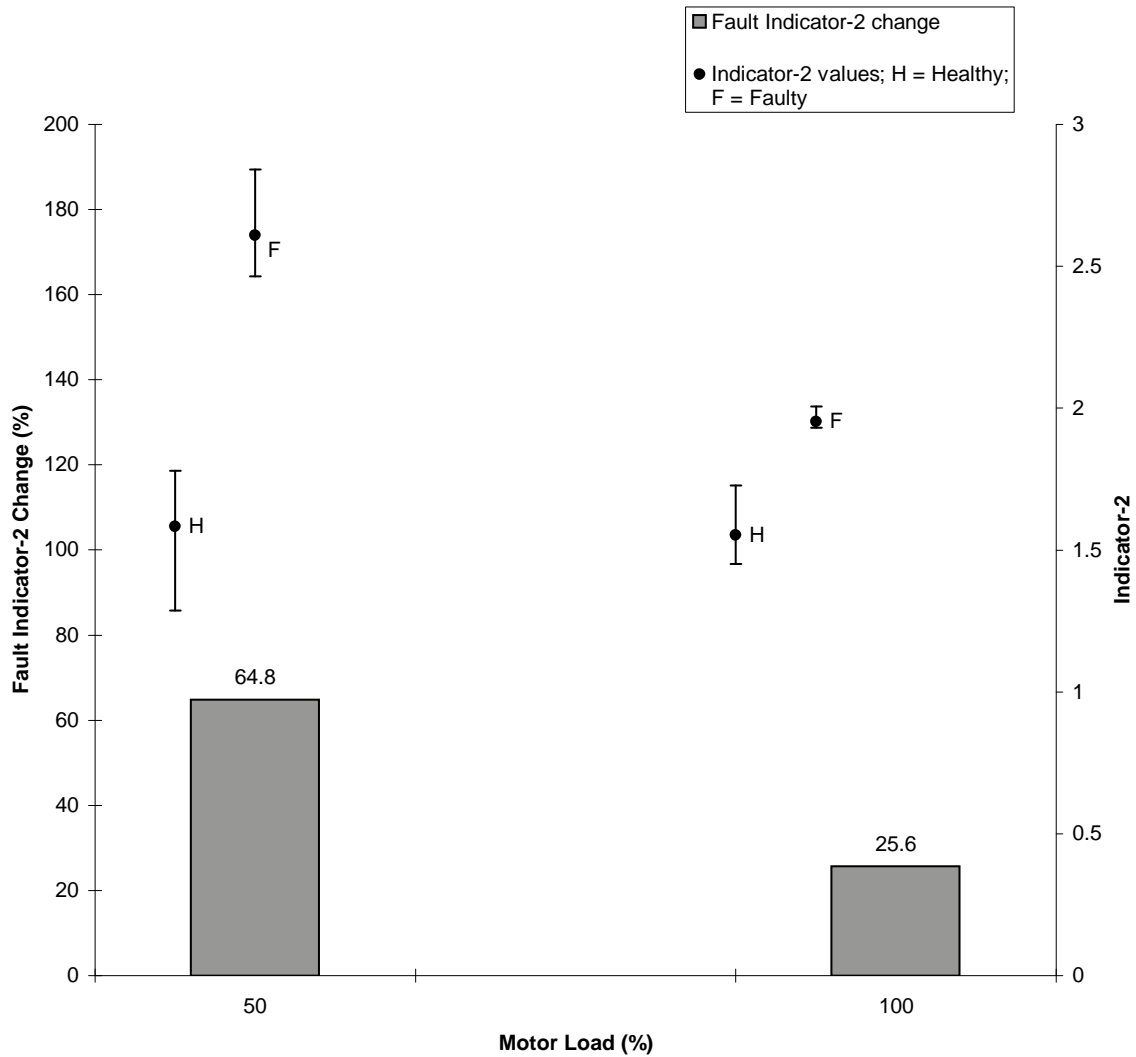


Fig. 17. Load dependence of Indicator-2 and Fault Indicator-2 Change for 150 hp motor; stator imbalance - case A1 (resistance of 0.012Ω in series with phase A).

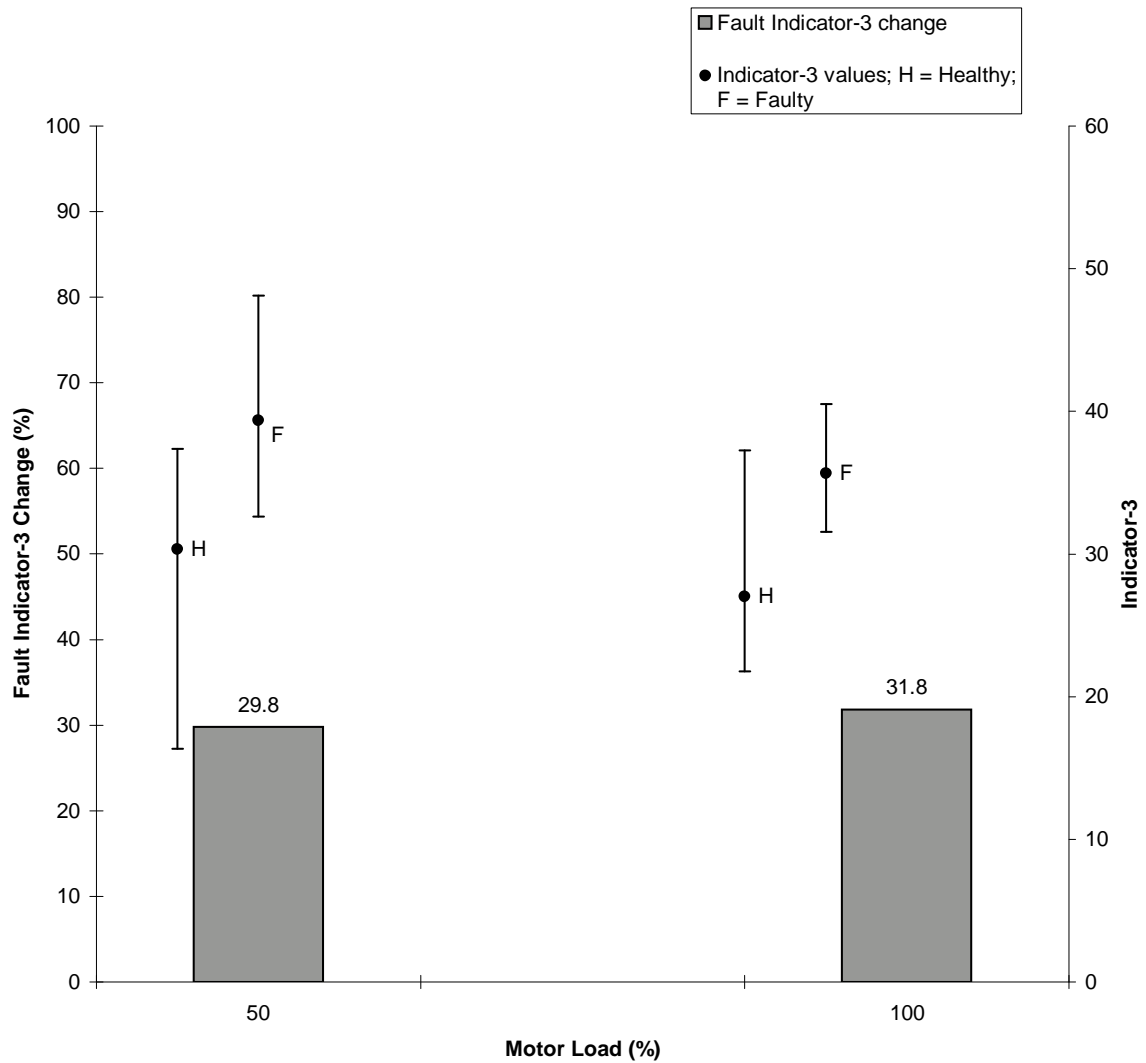


Fig. 18. Load dependence of Indicator-3 and Fault Indicator-3 Change for 150 hp motor; stator imbalance - case A1 (resistance of 0.012Ω in series with phase A).

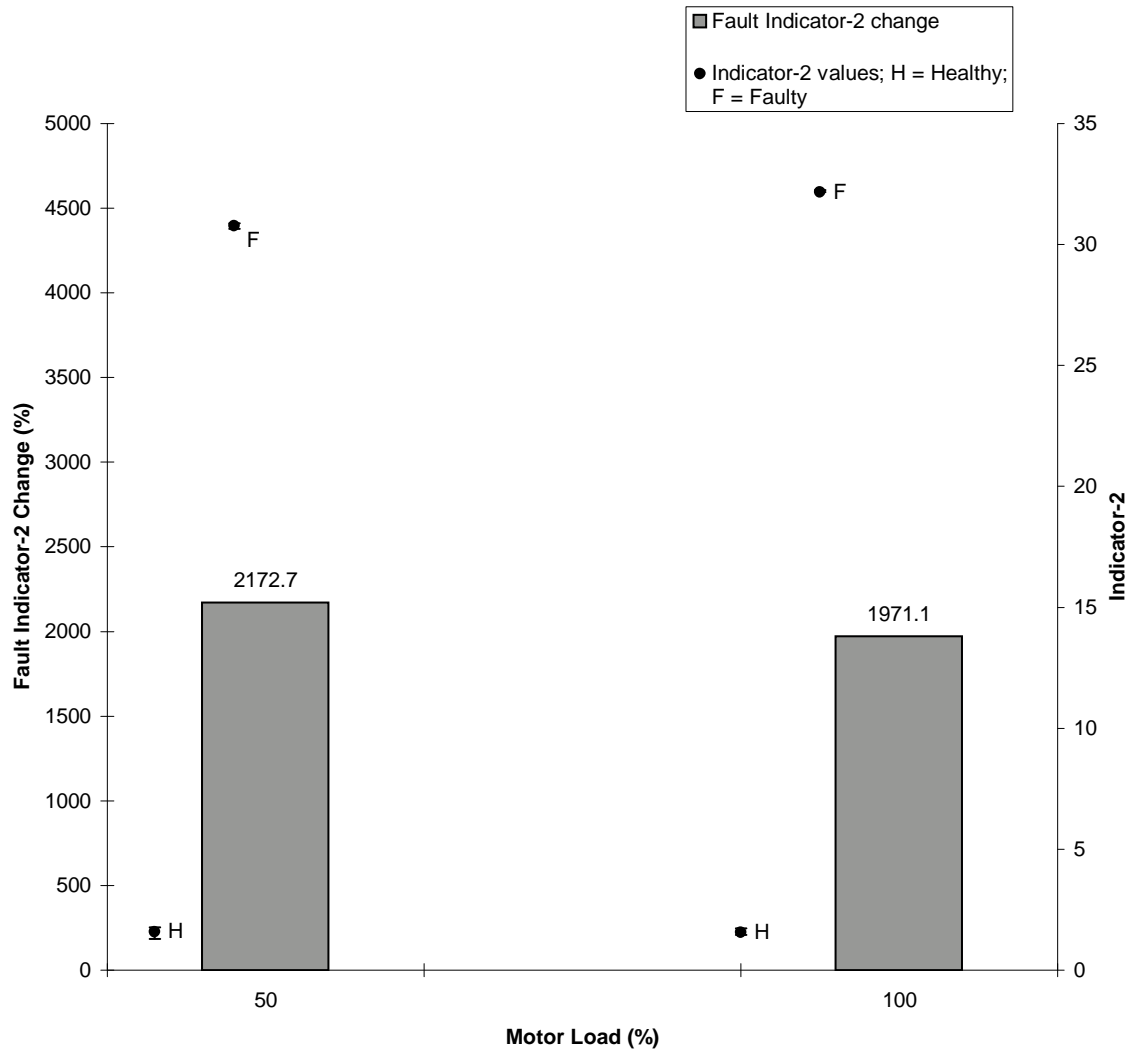


Fig. 19. Load dependence of Indicator-2 and Fault Indicator-2 Change for 150 hp motor; stator imbalance - case A2 (resistance of 0.633Ω in series with phase A).

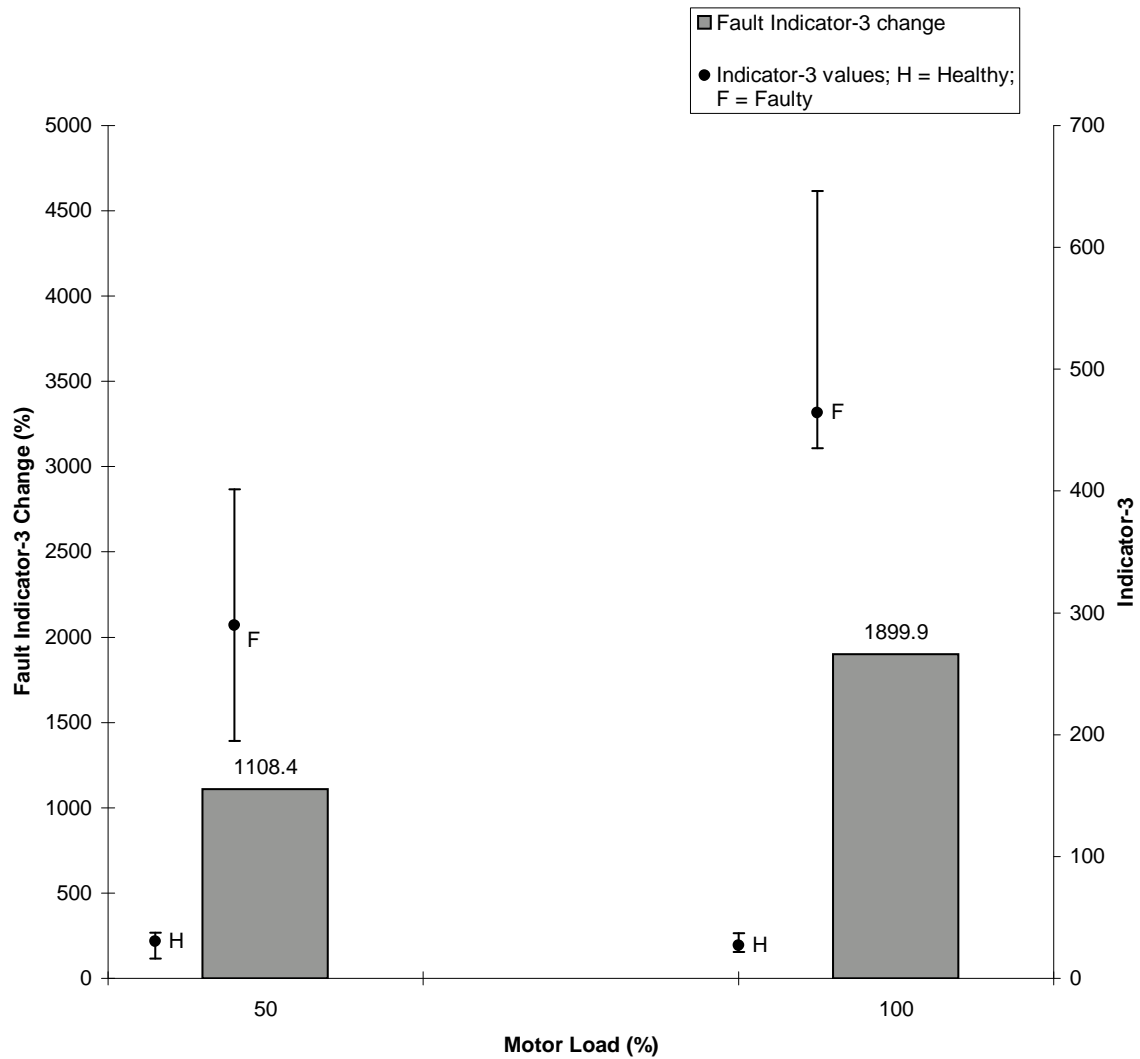


Fig. 20. Load dependence of Indicator-3 and Fault Indicator-3 Change for 150 hp motor; stator imbalance - case A2 (resistance of 0.633Ω in series with phase A).

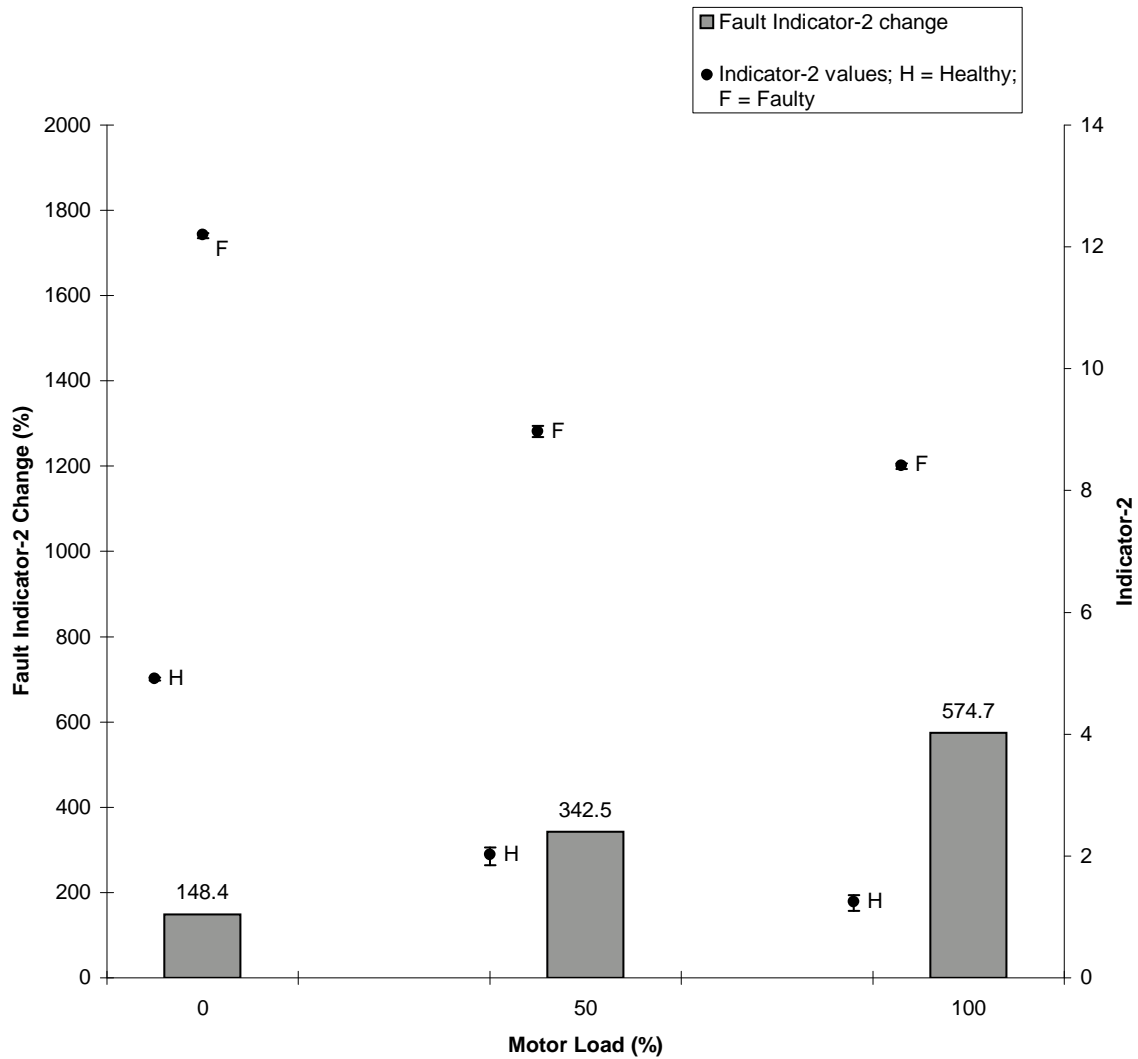


Fig. 21. Load dependence of Indicator-2 and Fault Indicator-2 Change for 800 hp motor; stator imbalance - case B (2.7Ω resistor in phase A).

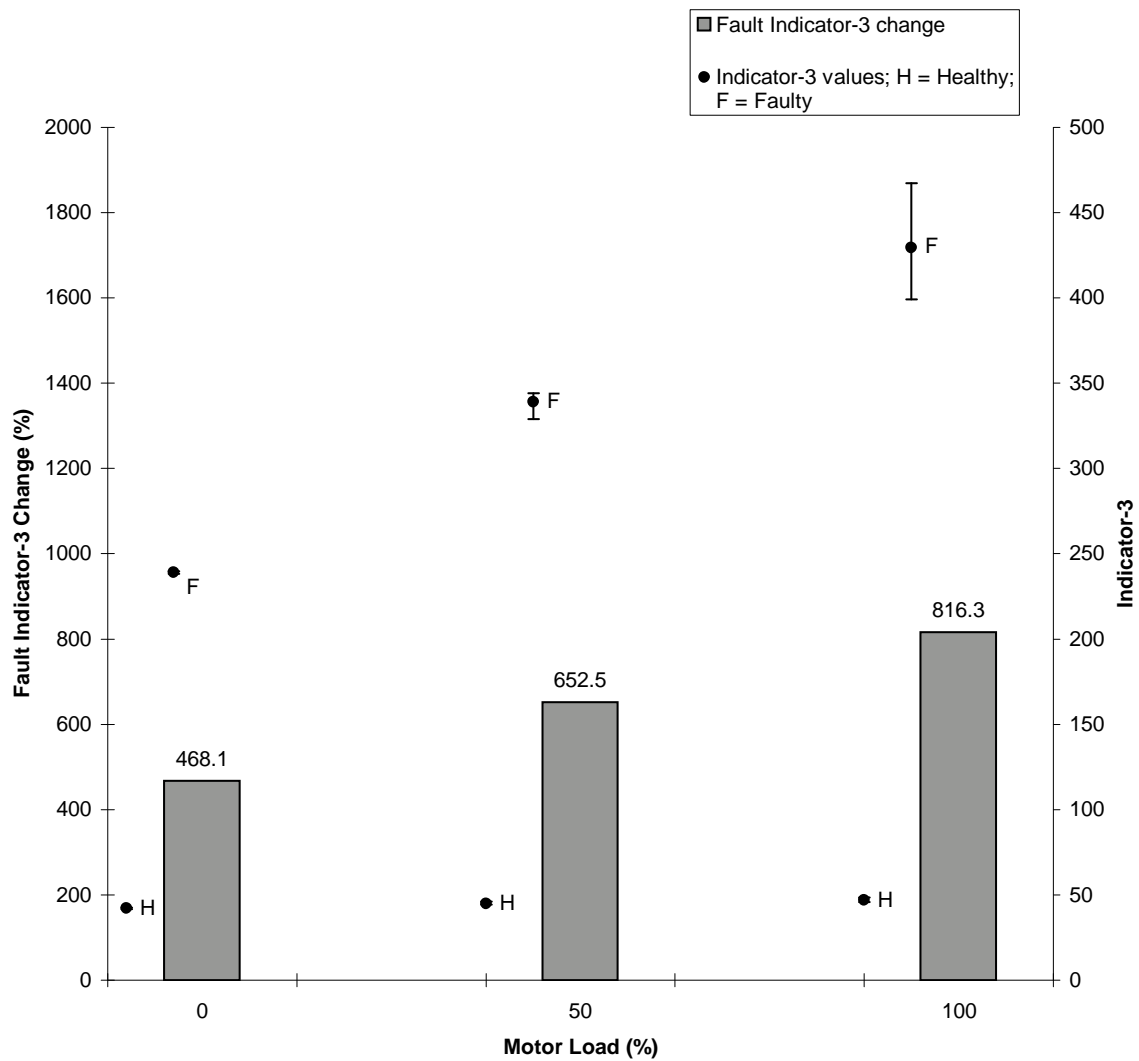


Fig. 22. Load dependence of Indicator-3 and Fault Indicator-3 Change for 800 hp motor; stator imbalance - case B (2.7Ω resistor in phase A).

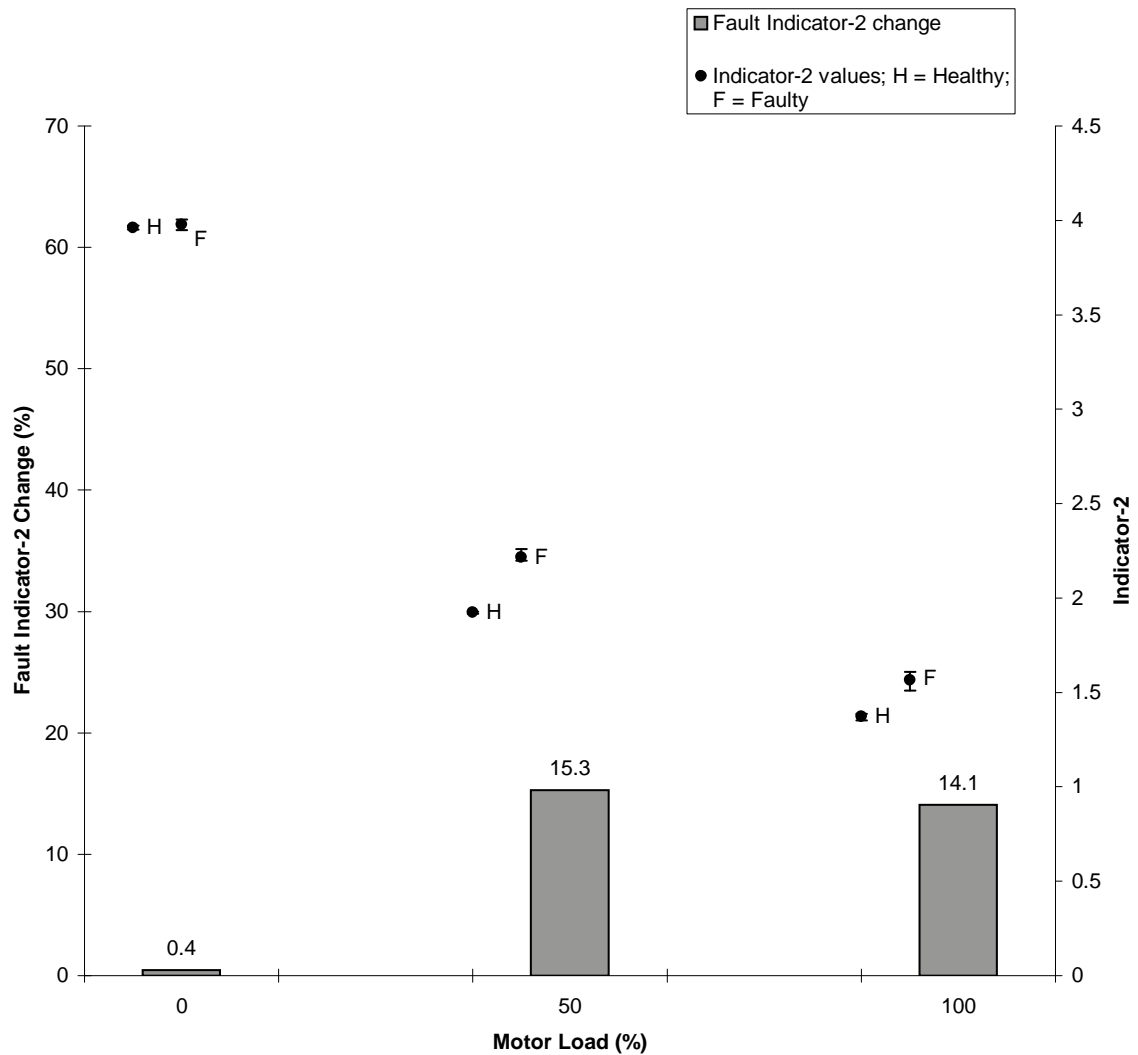


Fig. 23. Load dependence of Indicator-2 and Fault Indicator-2 Change for 500 hp motor; stator winding shorts - case 1 (2.7Ω turn-turn resistance in series with phase C).

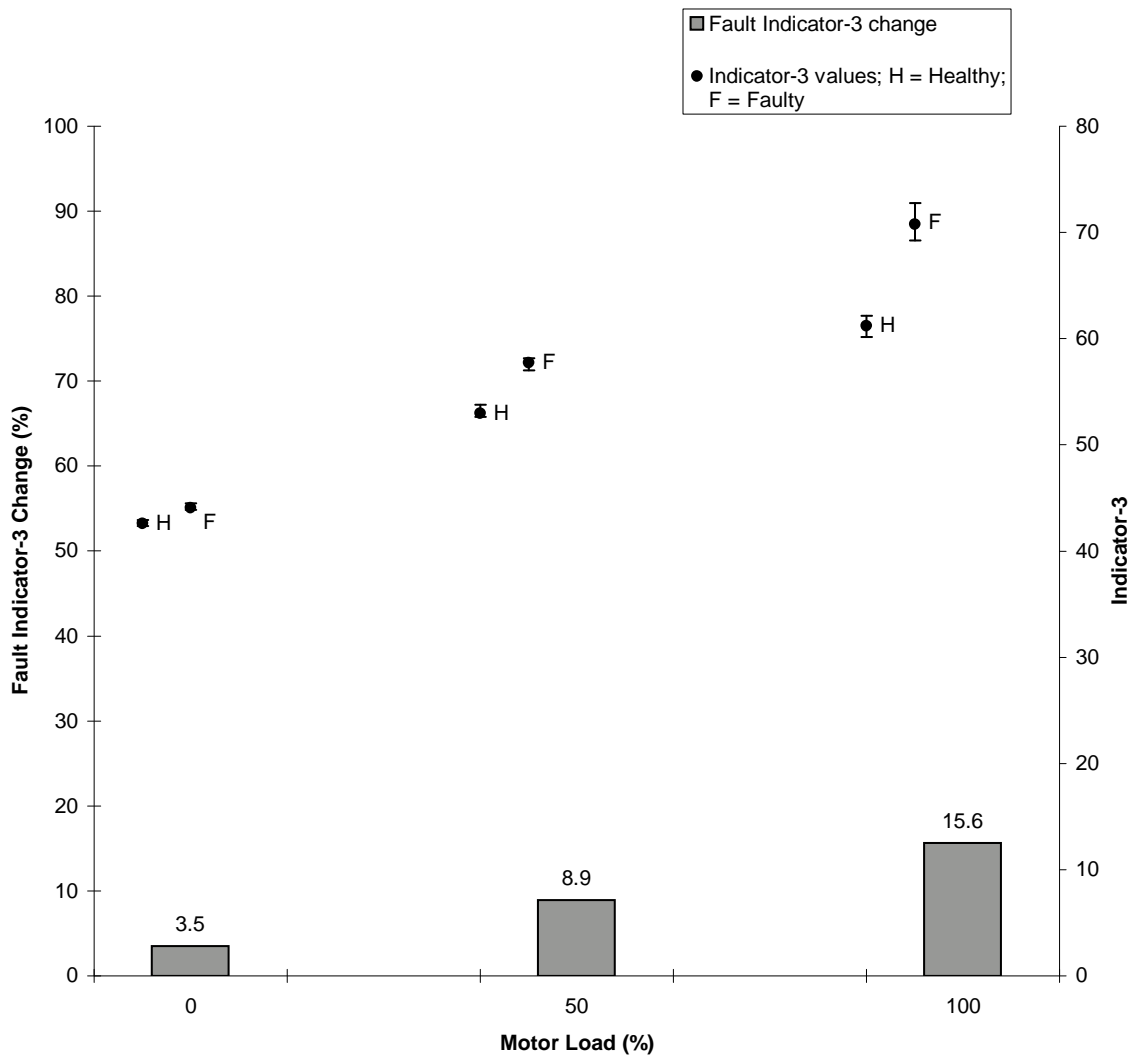


Fig. 24. Load dependence of Indicator-3 and Fault Indicator-3 Change for 500 hp motor; stator winding shorts - case 1 (2.7Ω turn-turn resistance in series with phase C).

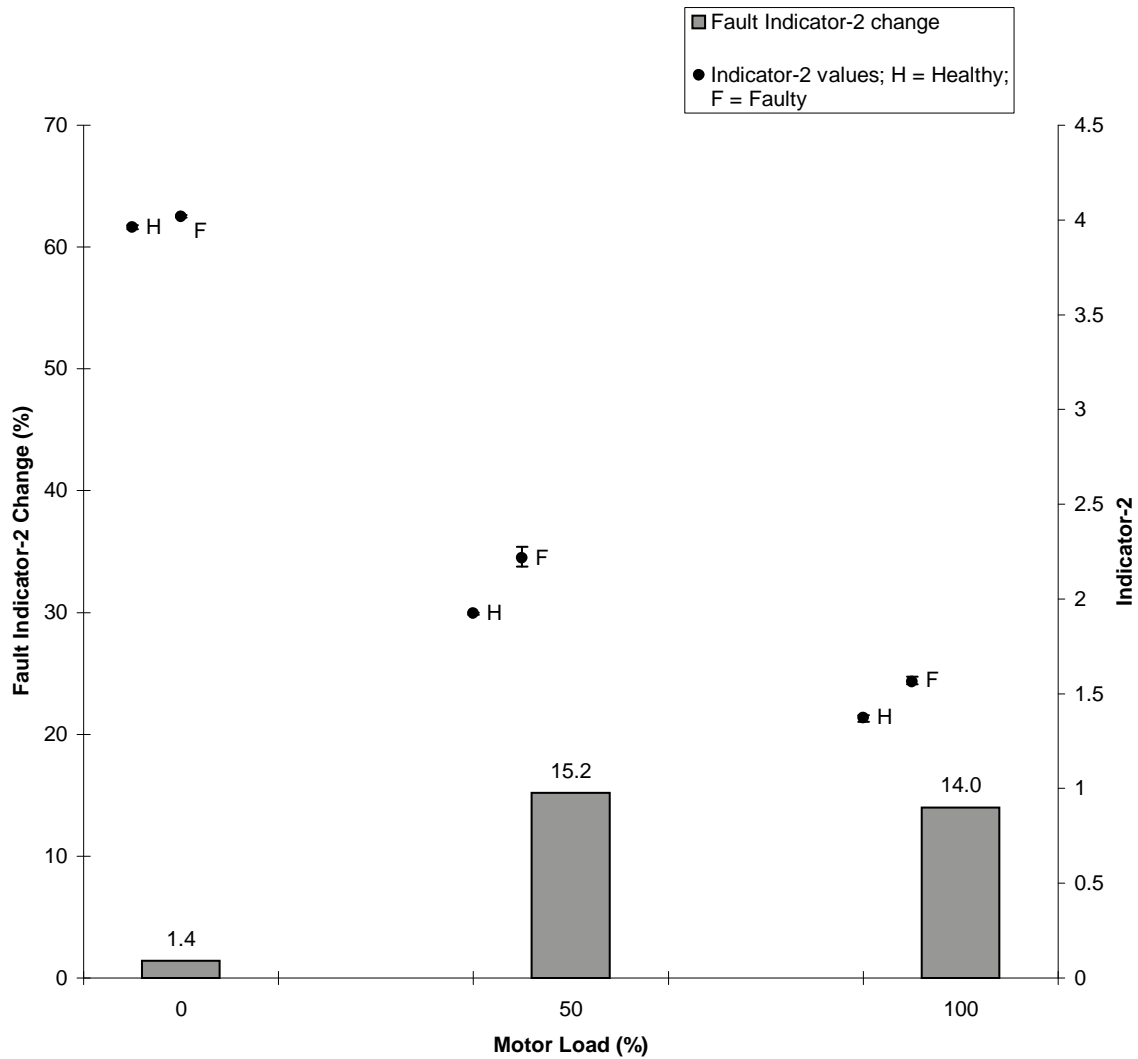


Fig. 25. Load dependence of Indicator-2 and Fault Indicator-2 Change for 500 hp motor; stator winding shorts - case 2 (1.35Ω turn-turn resistance in series with phase C).

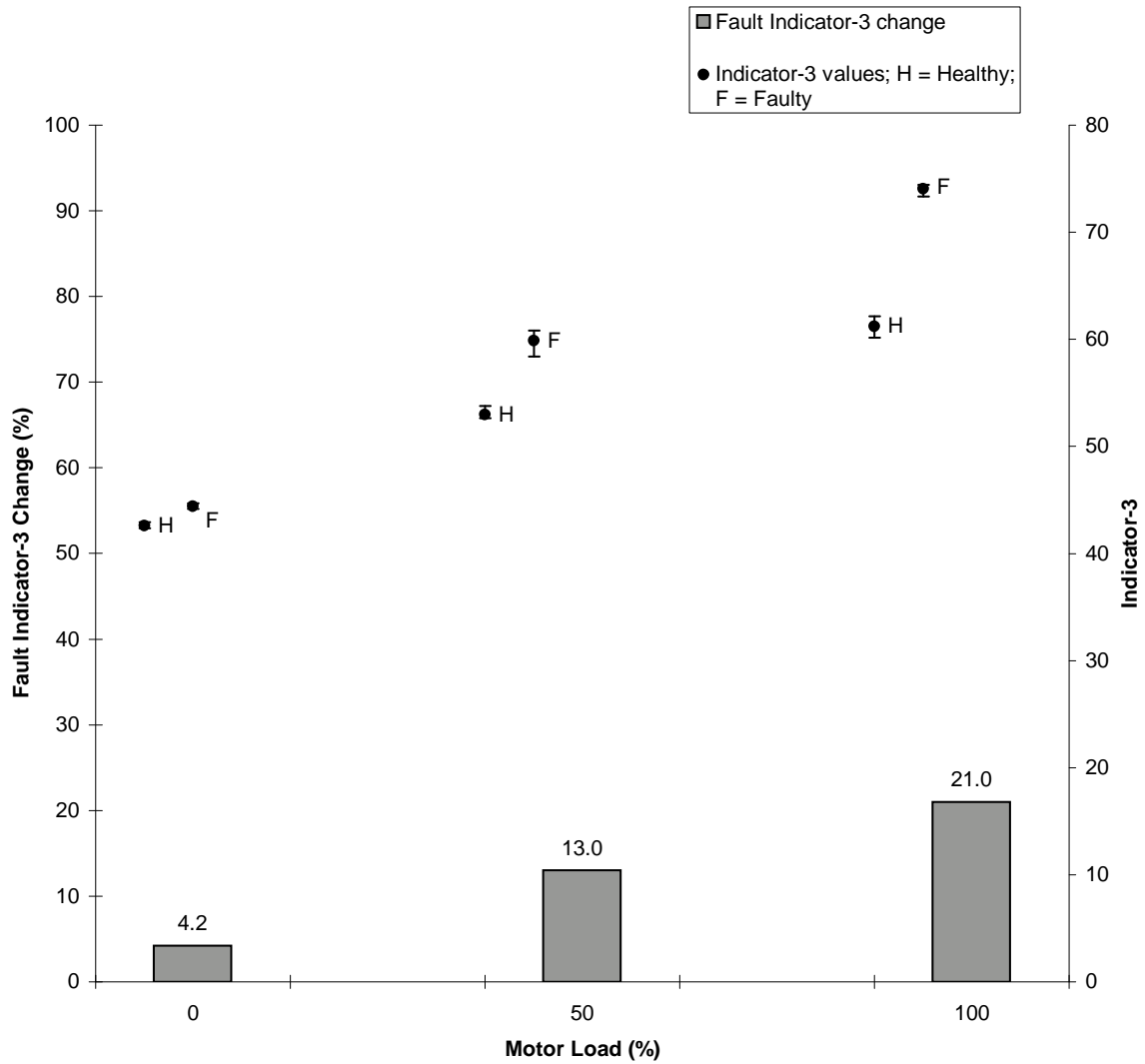


Fig. 26. Load dependence of Indicator-3 and Fault Indicator-3 Change for 500 hp motor; stator winding shorts - case 2 (1.35Ω turn-turn resistance in series with phase C).

hp motor, there is an resistance of $10\text{ M}\Omega$ in series with phase C. Figure 27 and Figure 28 show the load dependence of Indicator-2 and FIC-2 and Indicator-3 and FIC-3 for 500 hp motor with ground wall insulation. The FIC-2 and FIC-3 increases with increase in the motor load. At all loading conditions, both the indicators are indicative of the fault present and the indicator values for faulty case can be easily distinguished from the indicator values for healthy case.

Interlaminar insulation short experiments are also done on 500 hp motor by damaging the stator core (3 groups near iron edge and 1 group further inside). Figure 29 and Figure 30 show the load dependence of Indicator-2 and FIC-2 and Indicator-3 and FIC-3 for 500 hp motor with interlaminar insulation short. At 0% loading, both the indicators are non-indicative of the fault present. At 100% loading condition, both the indicators are indicative of the fault present and the FIC-2 and FIC-3 is same.

C. Chapter Summary

In this chapter, the results obtained for the various experiments are discussed. For every fault type being considered, the Fault Indicator Change (FIC) for each indicator is presented in the form of bar plot. The fault indicators computed from the electrical signatures are also presented by using error bar plot along with the bar plot. The error bar plot represents the variation of the value of fault indicators for healthy and faulty condition of motor. The patterns observed in these graphs are discussed, taking into consideration the effects of factors like loading.

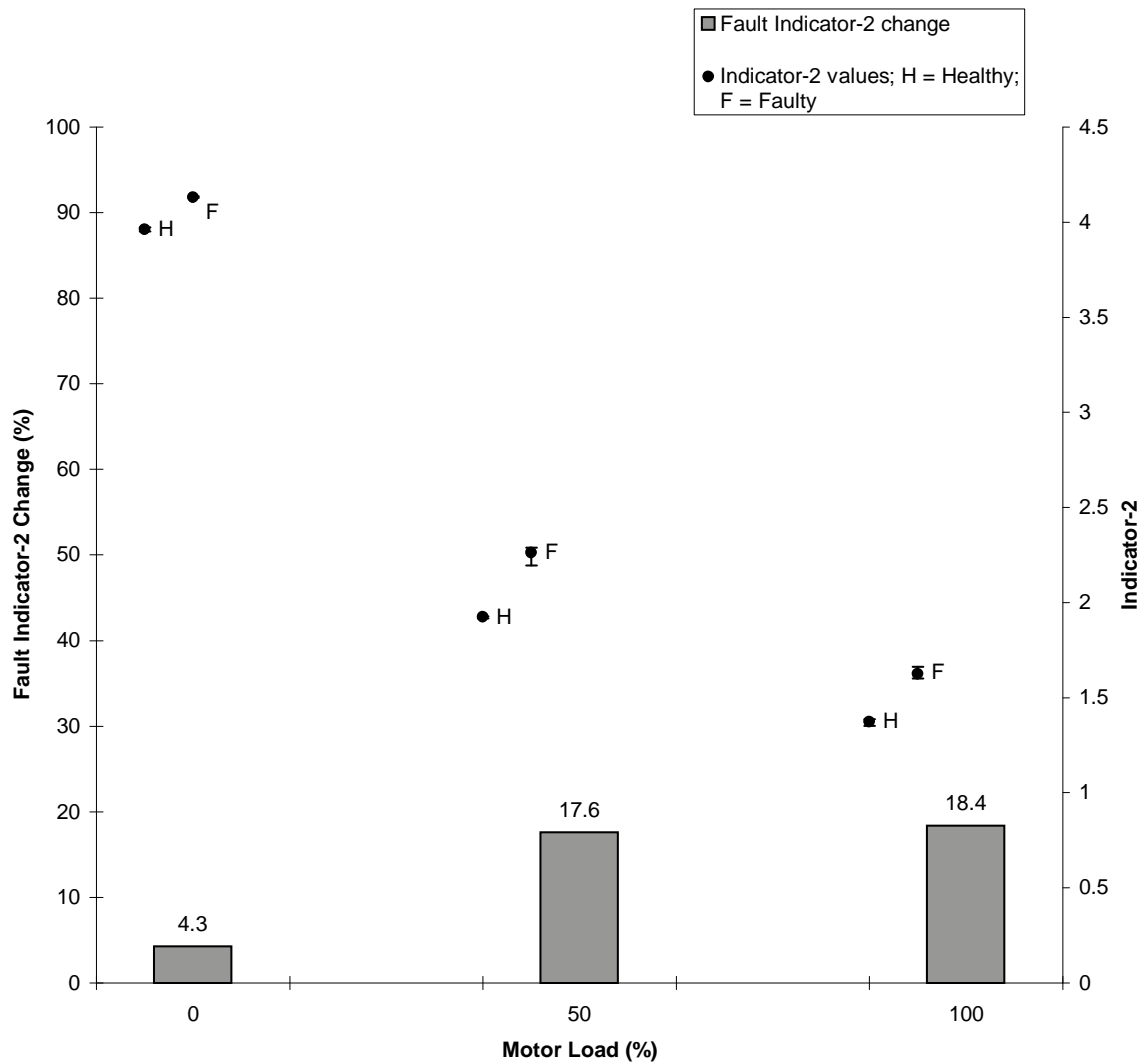


Fig. 27. Load dependence of Indicator-2 and Fault Indicator-2 Change for 500 hp motor; ground wall insulation ($10\text{ M}\Omega$ resistance in phase C).

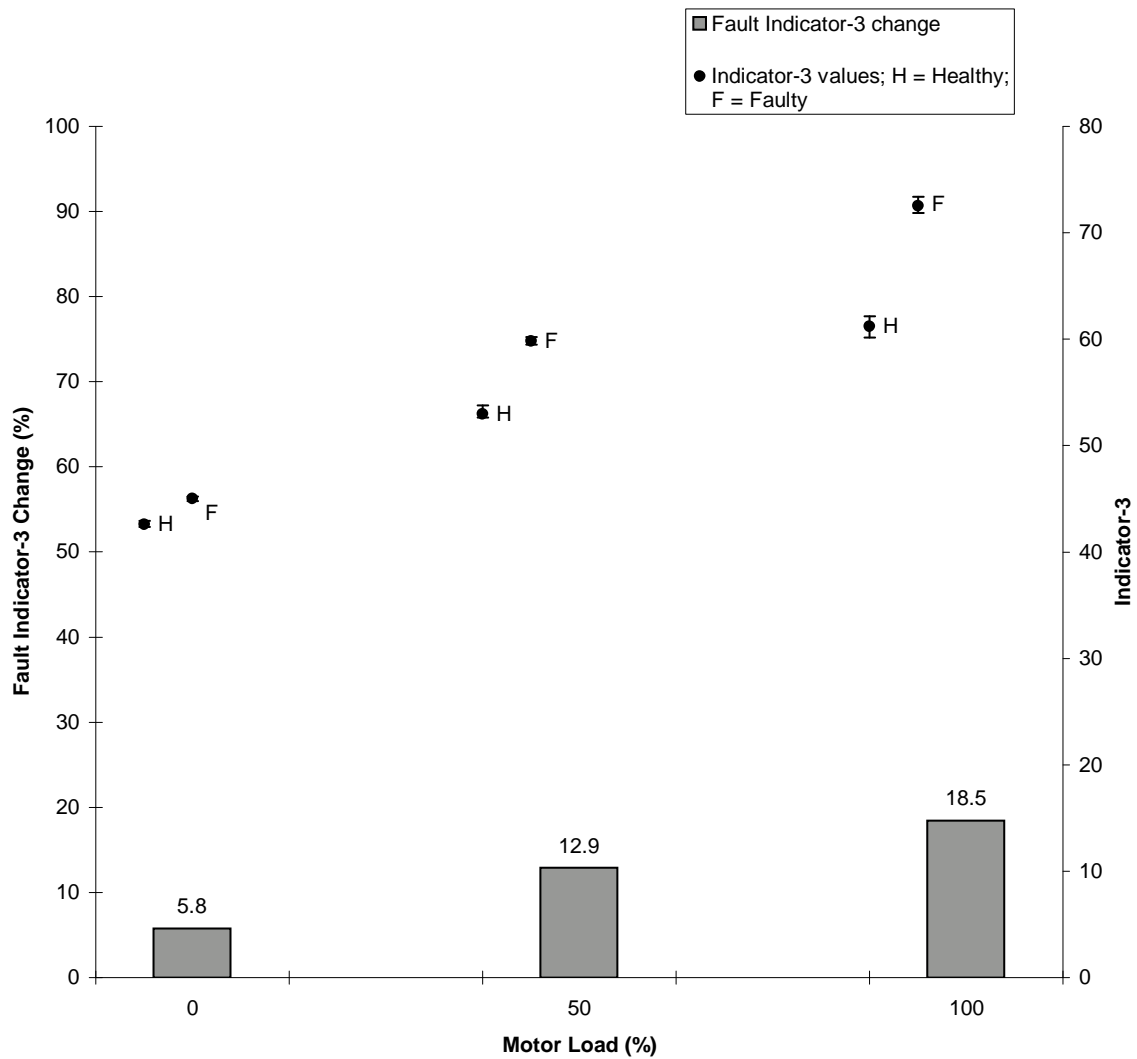


Fig. 28. Load dependence of Indicator-3 and Fault Indicator-3 Change for 500 hp motor; ground wall insulation (10 M Ω resistance in phase C).

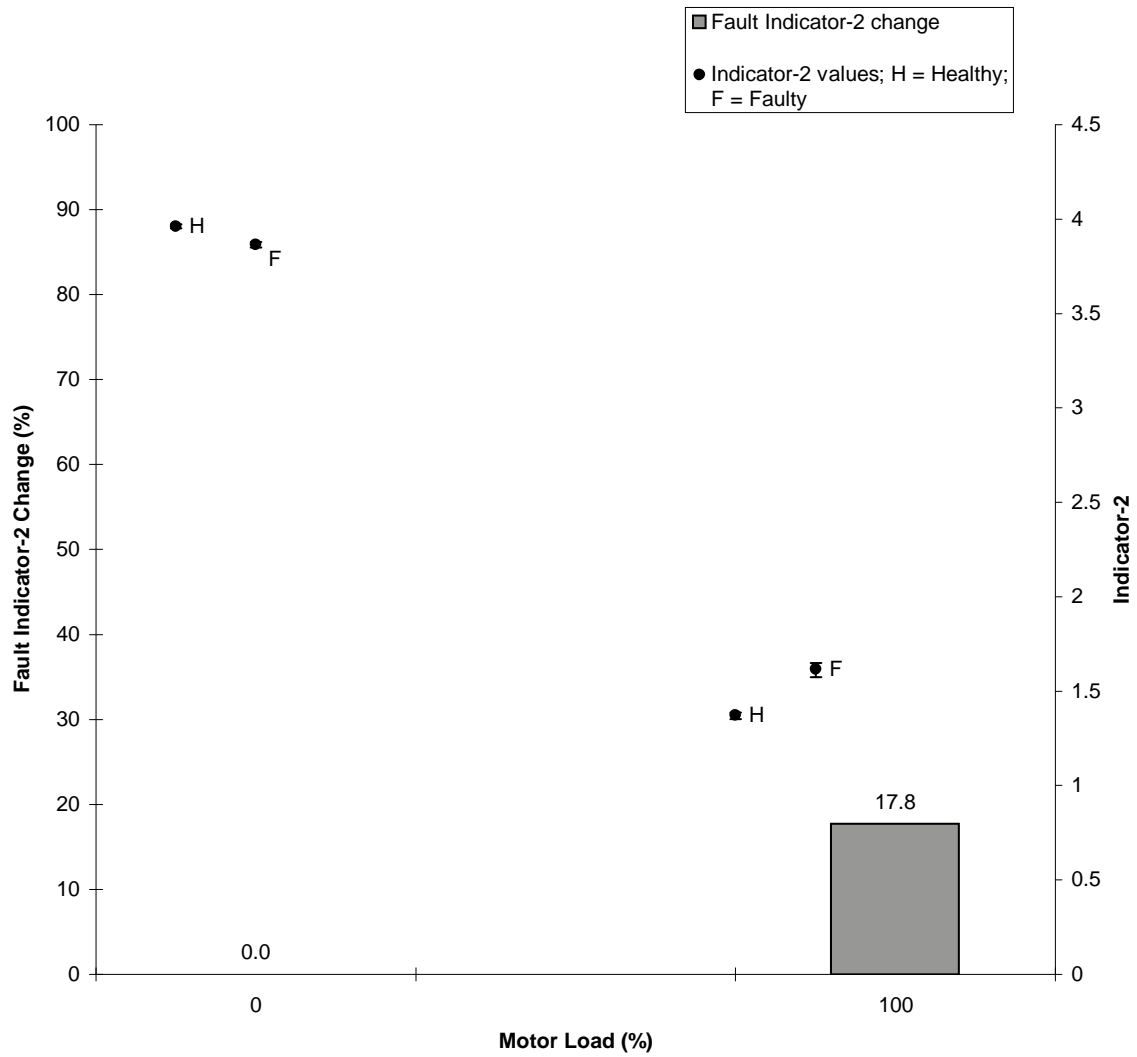


Fig. 29. Load dependence of Indicator-2 and Fault Indicator-2 Change for 500 hp motor; interlaminar insulation short (damaged stator core).

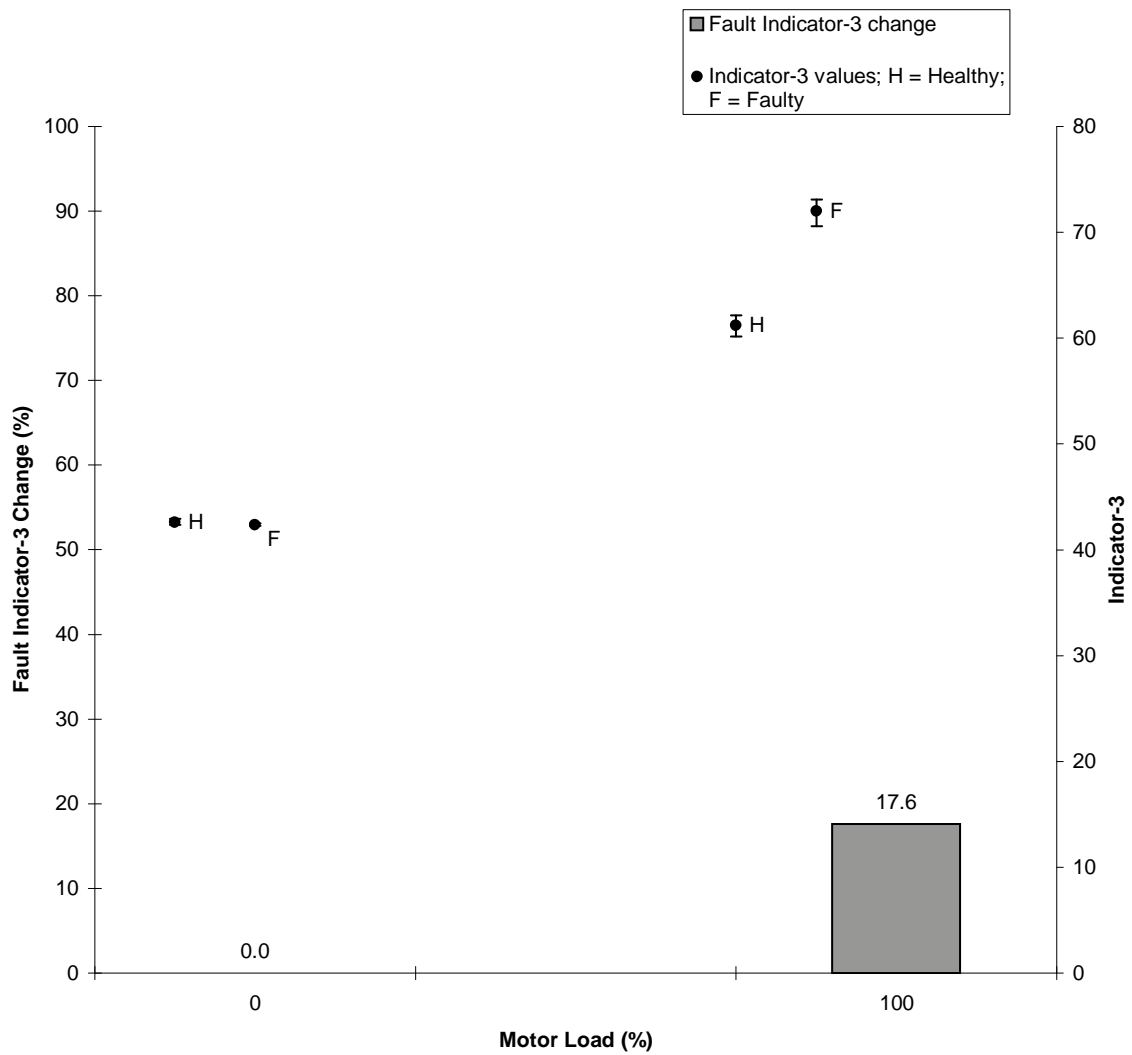


Fig. 30. Load dependence of Indicator-3 and Fault Indicator-3 Change for 500 hp motor; interlaminar insulation short (damaged stator core).

CHAPTER V

SUMMARY AND CONCLUSIONS

A. Summary of the Research

The purpose of this research is to develop a method for fault detection of induction motors using data-driven algorithms and to be able to distinguish actual faults from false alarms by investigating the variability of the fault indicators at a certain “healthy” condition of the motor.

In chapter II, different fault detection schemes are discussed, and the signal processing approach and development of fault indicators is further discussed. In signal processing, line voltages and phase currents measured using CT’s and PT’s are re-sampled and re-scaled. After re-sampling, the signal is passed through a signal segmentation routine that separates the quasi-stationary region of the signal from the non-stationary region and only the quasi-stationary signal is further processed to extract the fault features. After signal segmentation, the quasi-stationary signal is used to calculate five operating parameters of the motor and three fault indicators. The following operating parameters are developed to identify the operating condition of the motor:

- Moving window root mean square of all the three phases of voltages and currents
- Three-phase voltage imbalance
- Total harmonic distortion of the voltage signal
- Reciprocal of signal-to-noise ratio of the voltage signal

Once the quasi-stationary regions are acquired, the FFT-based method can be used for the processing of the signals to compute the fault indicators. Three fault

indicators are employed in this research, and they are:

- Reciprocal of signal-to-noise ratio of the current signal
- Three-phase current imbalance
- Negative-sequence component of the current signal

The former first indicator is used to detect the fault signature of mechanical failures, and the latter two represents the fault signature of electrical failures.

In chapter III, the experimental set-ups are explained and various fault cases are presented and discussed. It included discussions with specific details on the data acquisition hardware and description of experiments conducted. In this research, five distinct type of mechanical faults and four distinct type of electrical faults are considered. In mechanical faults, experiments for eccentric loading and single and double bearing faults are conducted on 1 hp and 3 hp motor while the other experiments are conducted with larger motors (Broken Rotor Bars and Air Gap Eccentricities with a 700 hp and 800 hp motor and Imbalance with a 500 hp motor). In electrical faults, experiments for multiple cases of stator imbalance are conducted with a 150 hp and 800 hp motor, stator winding shorts, ground wall insulation, and interlaminar insulation short with a 500 hp motor. This is done primarily to demonstrate the adaptability of the procedure to motors of different sizes and ratings. For all fault types, experiments are conducted at steady state operating conditions. But different levels of loading are separately considered for the analysis. This is done to study the effects of loading on the results.

For each case of the fault types, the computed values of operating parameters and fault indicators for healthy and faulty condition of the motor with the Fault Indicator Change (FIC) for all the three indicators are presented in a table format. All the

values of operating parameters and fault indicators for healthy and faulty condition are averaged over the respective number of data sets. The percentage increase of these mean fault indicators of faulty data from healthy data are then compared. It is followed by a discussion or an explanation of the observed behavior.

In chapter IV, the dependence of the indicator values and indicator change for mechanical and electrical faults on load level is summarized. Error bar plots of the indicator values for healthy and faulty condition of motor and bar plots of the indicator change(%) are presented and discussed for different motor loads. This was done to achieve the desired objective of distinguishing actual faults from false alarms by investigating the variability of the fault indicators.

B. Conclusions from the Research

Based on the discussions of the different results obtained, the conclusions drawn from this research can be summarized as follows:

- The developed fault detection system can distinguish mechanical faults from electrical faults. The indicator-1 is only affected by mechanical faults, whereas indicator-2 and indicator-3 are affected by electrical faults. Among the faults analyzed, only air-gap eccentricity is the type of mechanical fault which affects indicator-2 and indicator-3, so we can say it is an electro-mechanical fault. If a single fault occurs, regardless of whether it is mechanical or electrical, then the fault can be distinguished by observing the proposed indicators.
- From the results obtained, we can see the dependence of fault signatures on loading condition.
- The developed fault detection system is scalable to other size of machines. The relative behavior of the fault signatures is very similar for both small machines

as well as large machines, thus demonstrating the scalability of the proposed scheme. The property of scalability is a very attractive advantage, considering the number of motors installed in the same plant or process but have different ratings and manufacturers.

- The variability of the fault indicators is investigated by distinguishing the values of fault indicators for healthy from the values of fault indicators for faulty motor conditions.

C. Future Research Work

On the basis of the research reported in this thesis, some possible topics for future research work are as follows:

- The developed system has the capability of fault detection by classifying the detected faults into mechanical and electrical faults. Classifying the specific type of mechanical and electrical faults, and obtaining the information on the severity and the location of the faults would be the next step for a more comprehensive condition assessment system.
- The effects of dynamic loading can be studied and related experiments can be carried out. This can be especially helpful when dealing with the fault detection of system systems like pumps, compressors, etc. using the induction motor.
- Diagnostics of pumps driven by motors. Furthermore the developed system shows the flexibility of being applicable to other electrical machinery fault detection.
- Effects of closed-loop inverters on fault signatures. As the control loop modifies the behavior of the system, a more sophisticated procedure might be required.

REFERENCES

- [1] P. J. Tanver and J. Penman, *Condition Monitoring of Electrical Machines*, Letchworth, UK: Research Studies Press, 1987.
- [2] M. Benbouzid, "A Review of Induction Motors Signature Analysis as a Medium for Faults Detection," *IEEE Transactions on Industrial Electronics*, vol. 47, no. 5, pp. 984-993, October 2000.
- [3] P. Vas, *Parameter Estimation, Condition Monitoring, and Diagnosis of Electrical Machines*. Oxford, England: Clarendon Press, 1993.
- [4] A. Venugopal, "Comparative Analysis of Electrical and Mechanical Fault Signatures in Induction Motors," M.S. Thesis, Texas A&M University, College Station, Texas, 2003.
- [5] B. Liang, B. Payne, and A. Ball, "Detection and Diagnosis of Faults in Induction Motors Using Vibration and Phase Current Analysis," *Proceedings of the 1st International Conference on the Integration of Dynamics, Monitoring and Control (DYMAC 99)*, Manchester, UK, pp. 337-341, September 1999.
- [6] B. Payne, B. Liang, and A. Ball, "Modern Condition Monitoring Techniques for Electric Machines," *Proceedings of the 1st International Conference on the Integration of Dynamics, Monitoring and Control (DYMAC 99)*, Manchester, UK, pp. 325-330, September 1999.
- [7] R. R. Schoen, T. G. Habetler, F. Kamran, and R. G. Bartheld, "Motor Bearing Damage Detection Using Stator Current Monitoring," *IEEE Transactions on Industry Applications*, vol. 31, pp. 1274-1279, November/December 1995.

- [8] W. T. Thomson, D. Rankin, and D. G. Dorrell, "On-line Current Monitoring to Diagnose Airgap Eccentricity in Large Three-Phase Induction Motors-Industry Case Histories Verify the Predictions," *IEEE Transactions on Energy Conversions*, vol. 14, no. 4, pp. 1372-1378, December 1999.
- [9] J. R. Cameron, W. T. Thomson, and A. B. Dow, "On-Line Current Monitoring of Induction Motors- A Method for Calculating the Level of Air-Gap Eccentricity," in the *IEE 3rd International Conference on Electric Machines and Drives*, London, UK, pp. 173-177, IEE publication no. 282, November 1987.
- [10] N. M. Elkasabgy, A. R. Eastham, and G. E. Dawson, "Detection of Broken Bars in the Cage Rotor on an Induction Motor," *IEEE Transactions on Industry Applications*, vol. 28, pp. 165-171, January 1992.
- [11] S. Willianson and K. Mirzoian, "Analysis of Cage Induction Motors with Stator Winding Faults," *IEEE Transactions on Power Apparatus and Systems*, PAS-104, 1838-1842, 1985.
- [12] J. Sottile and J. L. Kohler, "An On-Line Method to Detect Incipient Failure of Turn Insulation in Random Wound Motors," *IEEE Transaction on Energy Conversion*, vol. 8, no. 4, pp. 762-768, December 1993.
- [13] G. B. Kliman, W. J. Premerlani, R. A. Koegl, and D. Hoeweler, "A New Approach to On-Line Turn Fault Detection in AC Motors," *Proceedings of the IEEE-IAS Annual Meeting*, San Diego, CA, pp. 687-693, 1996.
- [14] K. Kim, A. G. Parlos, and R. M. Bharadwaj, "Sensorless Fault Diagnosis of Induction Motors," *IEEE Transactions on Industrial Electronics*, vol. 50, no. 5, pp. 1038-1051, 2003.

- [15] A. G. Parlos, K. Kim and R. Bharadwaj, "Sensorless Detection of Mechanical Faults in Electromechanical Systems," *Mechatronics*, vol. 13, pp. 357-380, 2004.
- [16] M. Benbouzid, "Bibliography on Induction Motors Faults Detection and Diagnosis," *IEEE Transaction on Energy Conversion*, vol. 14, no. 4, pp. 1065–1074, December 1999.

VITA

The author, Shantur S. Tapar, was born on March 6, 1980 in Amravati, India. He received his Bachelor of Engineering degree in Mechanical Engineering from the College of Engineering, Amravati, India in May 2001. From Fall 2002 onwards he attended the Master of Science degree program in the Mechanical Engineering Department, Texas A&M University, College Station and received his degree in August 2005.

Permanent Address:

Shantur S. Tapar

15/2 "Shivarpan", Ganesh Colony,

Shilangan Road, Amravati, INDIA-444605

Phone: (091) 721-2578483

Email: shantur@gmail.com